UNIVERSITY OF OKLAHOMA

GRADUATE COLLEGE

THE INFLUENCE OF NITRATE ON THE SHORT-TERM CORROSION OF STEEL CATALYZED BY MARINE MICROORGANISMS

A DISSERTATION

SUBMITTED TO THE GRADUATE FACULTY

in partial fulfillment of the requirements for the

Degree of

DOCTOR OF PHILOSOPHY

BY

ANJUMALA HERATH
Norman, Oklahoma
2019

THE INFLUENCE OF NITRATE ON THE SHORT-TERM CORROSION OF STEEL CATALYZED BY MARINE MICROORGANISMS

A DISSERTATION APPROVED FOR THE
DEPARTMENT OF MICROBIOLOGY AND PLANT BIOLOGY

BY

Dr. Joseph M. Suflita, Chair

Dr. Kathleen E. Duncan, Co-chair

Dr. Mark A. Nanny

Dr. Ralph S. Tanner

Dr. Paul A. Lawson

Acknowledgements

A traditional acknowledgement would never be enough for my supervisors Dr. Joseph Suflita (Committee chair) and Dr. Kathleen Duncan (Co-chair) since they took me under their wing from a near ruinous situation and nurtured me back to who I am today, without which this would not be possible. Your motivation, guidance as well as patience encouraged me to continue to finish this work.

I also would like to express my sincere gratitude to my outstanding committee, Drs. Paul A. Lawson, Ralph S. Tanner and Mark A. Nanny. Without your insight, guidance and constructive criticism this would not be a success.

I am thankful to my former supervisor, Dr. Iwona Beech, for giving me the opportunity to join her lab and guiding me through the early stages of my Ph.D. studies. I would not have continued to pursue a doctoral degree if not for your encouragement. Your direction taught me to grow so much not only as a researcher but also as a person.

My sincere appreciation goes to the current and former members of Duncan, Suflita and McInerney laboratories. Special thanks to Dr. Irene Davidova, Dr. Athenia Oldham, Dr. Neil Wofford, Dr. Kimberly Thomas, Dr. Renxing Liang, Dr. Nathanial Losey, Annette De Capite, Katherine Sorrell, Meredith Thornton and Vince Sandifer.

I am grateful to members of Zhou lab including Dr. Aifen Zhou, Dr. Joy Van Nostrand, Dr. Yujia Qin and Dr. Jason Shi for their help in microarray analysis.

Dr. Joshua Cooper and James Floyd, thank you so much for your wonderful friendship. Your support immensely helped.

My heart-felt thanks to my parents and my brother for their continuous support, encouragement and unconditional love. To my darling son, your sweet smile was my inspiration. Finally, my husband, you were my strength throughout this process. Thank you for having faith in me.

Table of Contents

List of Tables

Chapter 1

Chapter 2

List of Figures

Chapter 1

Chapter 2

Abstract

Microbiologically influenced corrosion (MIC) is of global concern and a threat due to its economic, environmental as well as public health implications. Identifying the factors that govern or influence MIC is beneficial in predicting such effects and for taking early preventive measures. Although the basic process of MIC is electrochemical, when biotic components and environmental factors are included, MIC becomes a collection of complex interactions that requires individual components to be identified and studied in order to understand their effects. This dissertation focuses on the effect of elevated levels of nitrate on the MIC of steel exposed to seawater.

Metal exposed to seawater is known to be susceptible to MIC. Based on the analysis of field data of steel pilings exposed to coastal marine waters, Professor Robert Melchers put forward an empirical multi-phase phenomenological model of steel corrosion. The model proposes two periods where MIC occurs whereby the rate of corrosion depends on bacterial metabolic activity. The activity of the corrosive microbes is in turn thought to be largely a function of the nutrient supply. Oftentimes, the major nutrient limiting bacterial activity in seawater is dissolved inorganic nitrogen (DIN), most notably nitrate, ammonium and nitrite concentrations. The overall objective of my study was to investigate the effect of elevated levels of nitrate on marine biofilms that are associated with the corrosion of carbon steel. Based on the phenomenological model, the hypothesis was that nitrate enhances corrosion by general stimulation of microbial activity.

The first section of the dissertation interrogated the microbial communities of biofilms on carbon steel coupons exposed to shallow warm marine waters at four locations around the globe. Metagenomic analysis was performed with DNA extracted from the biofilms growing on coupons immersed at each location. Two of the locations (#5 and #7) had normal and relatively low levels of nitrate while the marine waters off the locations #4 and #6 had an unusually high level of dissolved inorganic nitrogen (DIN) (2.4 – 2.6 mg/L). However, the largest weight losses and rates of corrosion were independent of the DIN status of the ambient seawaters, thus the results did not support the hypothesis. Location #6 had the highest rate of general corrosion, as measured by weight loss by mild steel coupons, but both location #5 and #6 had more severe pitting corrosion, indicative of MIC. It was subsequently

hypothesized that the high DIN levels may have enriched for nitrate-reducing sulfate-reducing bacteria that led to relatively high sulfide-driven corrosion rates in location #6. Bacterial communities of both locations #4 and #6 had relatively high biomass based on DNA concentration as well as 16S qPCR. Moreover, they had higher frequencies of nitrate/nitrite reducing gene reads compared to the other two sites. The taxonomic analysis of nitrogen cycling genes revealed that high levels of nitrate was associated with the increase of nitrifying, facultative anaerobic as well as aerobic Alphaproteobacteria. The biofilms from location # 6 had a higher relative abundance of Deltaproteobacteria (majority were *Desulfovibrio*) and sulfur-oxidizing bacteria that is at least consistent with the higher corrosion rate compared to the other locations, but few of the sulfate-reducing bacteria also had nitrate reduction genes. Therefore, the second hypothesis was also disproven. Additionally, the relative frequency of *ccoN* genes (an indicator of aerobic respiration potential) was relatively high in the location #4 compared to the samples of other locations.

The effect of elevated levels of nitrate on carbon steel corrosion was also tested with the common marine organism *Marinobacter hydrocarbonoclasticus* SP17 as the biotic component. In light of unpublished observations we hypothesized that *Marinobacter* biofilms protect 1018 carbon steel under aerobic conditions. Furthermore, it was hypothesized that the biofilm cells inhibit or reduce corrosion specifically by the removal of oxygen. Carbon steel coupons were exposed to *Marinobacter* cells that were amended with nitrate or ammonium as the nitrogen source and incubated under aerated (unsealed) or oxygen limited (sealed) conditions. The weight loss of coupons with biofilm was significantly lower than that without a biofilm regardless of the nitrogen source or oxygen supply status. The coupon weight loss difference was significant between the sealed (oxygen-limited) and unsealed (oxygen-unlimited) incubations, with less weight lost from coupons incubated under oxygen-limited conditions. Dissolved ferrous iron measurements as an indicator of corrosion showed the same trends as measurements of weight loss with less corrosion associated with coupons with biofilms compared to biofilm-free coupons, regardless of the oxygen and nitrogen status, i.e., dissolved iron measurements were lower with coupons in sealed (limited-oxygen) treatments compared to unsealed treatments with or without a biofilm. The coupon weight loss and the dissolved ferrous iron measurements did not exhibit significant differences between abiotic treatments with nitrate, ammonium or no nitrogen source added. The observations

supported the hypothesis that *Marinobacter* biofilm protects 1018 carbon steel under aerobic conditions. The most likely mechanism for corrosion inhibition by the organism appeared to be oxygen respiration thereby limiting the ability of this gas to reach and interact with the coupon surface. In any event, the study did not support the hypothesis of enhanced corrosion in the presence of elevated levels of DIN, either nitrate or ammonium.

This dissertation relied on both field and laboratory experiments to interrogate the impact of elevated levels of nitrate in seawater on carbon steel corrosion. The observations did not support the contention that elevated levels of nitrate were associated with higher corrosion. Further, high levels of nitrate compared to ammonium as a DIN source were also not associated with significantly more corrosion in the presence of a common marine heterotrophic bacterium. The metagenomic analyses of biofilms from the field support the hypothesis of a generic stimulation of microbial proliferation. However, since both locations with high DIN did not experience same amount of corrosion and microbial activity was not tested, it does not explain increases in corrosion as proposed by Melchers. Admittedly, the examination of only four marine coastal areas can hardly be considered exhaustive. Similarly, the impact of a pure culture heterotrophic bacterium that is capable of utilizing nitrogen under both aerobic and anaerobic conditions can only partially reflect the many intricacies of entire marine microbial communities. However, the observations described herein suggest that the presence of high DIN or nitrate in local marine environment cannot be used as the reliable indicator of high corrosion rates as selection for nitrate-reducing microbes can include those that enhance MIC and those that do not. Additionally, the use of nitrate/nitrite reducing gene frequency and/or nitrogen cycling genes as a marker for corrosion should be reconsidered.

Preface

Microbiologically influenced corrosion (MIC), as a research topic, is receiving significant attention since it poses a threat to human safety, the environment as well as the economy. Metal infrastructure such as bridges, ships and their ballast tanks, oil and gas pipelines, offshore mooring systems and other carbon steel components that have been researched over the past few decades has provided ample evidence of the influence of microbes on corrosion. Developing tools or models for predicting corrosion loss are important as they will help to avoid huge economic losses. One influential model of marine corrosion is the phenomenological model by Dr. R.E. Melchers. Melcher's model describes five phases of long-term corrosion for steel in marine waters. Although the model is mainly focused on accelerated low water corrosion (ALWC: unusually high levels of corrosion observed on steel structures located just below the usual low tide level in natural sea waters), it still can be applied with appropriate caveats to corrosion of steel in tropical shallow waters. A number of studies by Melchers and his group have also shown correlation between higher levels of dissolved inorganic nitrogen (DIN) in seawater and higher levels of ALWC. The objective of this dissertation was to examine the influence of biological activity/metabolism on the corrosion of steel in seawater with special regard to Dr. Melcher's phenomenological model. My study focused specifically on the influence of nitrate on bacterial activity/metabolism and carbon steel corrosion. Chapter 1 is a field study designed to examine the impact of elevated nitrate levels in marine waters on corrosion and the resulting influence on the diversity of the attached microbial community. The effect of nitrate on metal corrosion was examined at the level of single species in Chapter 2 while the appendix documented the impact of this anion at the level of the transcriptome of a single species growing as a biofilm vs. planktonic phase.

Chapter 1 extended the analysis of already existing data obtained by the collaborative work of University of Oklahoma (OU), Department of Microbiology personnel in conjunction with the AMOG Consulting, Inc. The AMOG Consulting Inc. received corroded coupon samples as part of an investigation into the role of MIC on the rapid corrosion of mooring chains from Deepstar®, an engineering company involved in marine technology development, with Chevron Energy Technology Company as the lead sponsor. The coupons, manufactured from mooring chain steel, were immersed in seawater at four different locations for several months

prior to retrieval and analysis. Two of the locations (#4 and #6) had elevated levels of nitrate, while the other two (#5 and #7) had lower and more typical seawater concentrations of this anion. The samples were analyzed in the Department of Microbiology and Plant Biology at OU. Although the project produced corrosion analysis, metagenomic as well as metabolomic data, the current chapter analyzed only the metagenomic data to evaluate the phenomenological model by Dr. Melchers. The corrosion analysis through weight loss, light microscopy and scanning electron microscopy (SEM) was performed by Dr. Iwona Beech and Dr. Zakari Makama (Department of Microbiology and Plant Biology, OU). The major findings of the coupon surface analysis are reported in Chapter 1 as they relate to the metagenomic analysis. The DNA was extracted from the biofilms and preparation of the samples for illumina MiSeq Next Generation Sequencing (NGS) was done by Dr. Kathleen Duncan and myself. The initial taxonomic analysis using 16S rRNA gene sequences and functional gene analysis was also performed by Dr. Duncan using the MGMIC pipeline constructed by Dr. Boris Wawrik (University of Oklahoma). My objective was to obtain deeper insight on the microbial community composition and potential function at each of the four marine sampling stations by further interrogation of the taxonomic as well as functional gene data. More specifically, I sought to address, i) What are the major bacterial groups in each location potentially capable of causing corrosion? ii) What are the major pathways that can enhance/inhibit corrosion present in each location? Special emphasis was placed on the aerobic respiration, nitrogen and sulfate reducing as well as sulfur oxidation pathways. Nitrate reducing, sulfate reducing, and sulfur oxidizing genes were interrogated for their taxonomic identities. The unusually high levels of nitrate resulted in an increase in nitrate/nitrite reducing gene frequencies at two of the sites. The bacteria responded to high nitrate levels in both sites were mainly aerobic and nitrate reducing Alphaproteobacteria. Corrosion rates all depicted severe general corrosion attack in all four sites with one site (#6) having slightly higher corrosion rate and two of the locations (#5 and #6) having higher rates of pitting corrosion. The data suggested that the activity of sulfate reducing bacteria as well as sulfur oxidizing bacteria in biofilms may have resulted in the relatively high corrosion rate of the coupons of location #6. Additionally, coupons of location #4 likely experienced higher oxygen levels as a greater proportion of the sequences were affiliated with aerobic or facultatively anaerobic taxa and there was a higher relative abundance of genes coding for enzymes essential for oxygen respiration. The severe pitting rate of coupons in location #5 appears to be associated with the activity of sulfate

reducing bacteria, as the DNA extracted from those coupons contain a high number of sulfate reducing genes as well as a high relative abundance sulfate reducers such as *Desulfovibrio*. In location #7, the corrosion of one coupon was associated with a high relative abundance of sulfate reducers while sulfur oxidizers were more prevalent in the other replicate coupon. These observations suggest that high DIN levels in the environment is likely a poor indicator of MIC and should not be used as the primary indicator of associated problems.

Chapter 2 examined the effect of elevated levels of nitrate in seawater on corrosion of carbon steel employing *Marinobacter hydrocarbonoclasticus* SP17 as the biotic component. A single species was used to lower the complexity of the experiments and thereby allow for clearer interpretation of the results. Treatment variables included presence/absence of *Marinobacter*, nitrate versus ammonium as the nitrogen source, and sealed (e.g. limited oxygen) versus aerated (e.g. unlimited oxygen) incubation systems. The experiments revealed that *Marinobacter* indeed formed a biofilm on the coupons and that the weight loss of coupons with cells was always lower than without cells regardless of the nitrogen source. However, weight loss was less in the sealed bottles than the aerated bottles, and least in the sealed incubation systems containing *Marinobacter*. The weight loss reflected the concentration of oxygen in the bottles, with least weight loss and lowest oxygen levels in the sealed bottles with *Marinobacter.* Therefore, it was hypothesized that consumption of oxygen by the biofilm and planktonic cells reduced aerobic corrosion of coupons and that *Marinobacter* exercised a protective effect under these conditions.

The goal of Appendix 1 was to better understand the effect of elevated levels of nitrate on bacterial activity/metabolism when a biofilm forms on a suitable surface. Transcriptomic analysis (microarray) was planned for *Marinobacter hydrocarbonoclasticus* SP17 biofilm 1) when it occupied an inert surface (glass) and 2) when it grew on carbon steel. This research was performed under the direction of Dr. Iwona Beech. However, only part 1 (biofilm on glass surface) was completed and is reported as Appendix 1. Contrary to expectations, genes in the dissimilatory and assimilatory nitrate reduction pathways were downregulated in the presence of nitrate. Cytochrome oxidase genes (essential for oxygen respiration) were also downregulated, suggesting that the elevated levels of nitrate may be associated with a shift from aerobic to anaerobic respiration.

Chapter 1

Short-term deterioration of steel by microbiologically influenced corrosion (MIC) in marine waters with varying nitrate content: Metagenomic analysis of biofilms on corroded mooring chain coupons

Abstract

The accelerated corrosion observed in steel mooring systems of sea-going vessels has been attributed to microbiologically influenced corrosion. The present study was done in response to general as well as pitting corrosion observed in mooring systems by DeepStar®, a joint industry technology development consortium. Metal coupons cut from steel mooring chains were exposed in four different offshore locations. The locations #4 and #6 had similar levels of relatively high dissolved inorganic nitrogen (DIN 2.4 – 2.6 mg/L) while two other locations had undetectable levels of DIN. In light of a phenomenological model for metal corrosion in seawater put forward by Dr. R.E. Melchers and colleagues, it was hypothesized that DIN enhanced corrosion through the stimulation of microbial activity. However, coupons recovered from location #6 experienced a somewhat higher rate of general corrosion compared to locations #4, #5 and #7, and coupons from locations # 5 and #6 had more pitting corrosion. Alternatively, it was hypothesized that the high levels of nitrate (the major component of DIN at the study locations) was associated with an increase in nitrate-reducing sulfate-reducing bacteria (SRB), which might then lead to high rates of sulfide-driven pitting corrosion. Biofilms on two coupons from each location were recovered, DNA extracted and metagenomic analysis was conducted to characterize the microbial community structure and infer the metabolic potential of the biofilm communities at each location. Communities at the elevated nitrate locations (#4 and #6) had higher bacterial numbers (based on qPCR of 16S rRNA genes) than the low nitrate areas (#5 and #7), as well as a relatively higher frequency of nitrate/nitrite reducing gene reads. High numbers of SRB, based on qPCR of *dsrA* (essential gene for sulfate reduction) were found on both coupons from locations #5 and #6, and on one coupon from location #4. Based on analysis of the relative abundance of representative functional genes involved in major electron acceptor pathways, oxygen respiration appeared to be dominant in locations #4, #6, and #7, whereas sulfate reduction, as indicated by the relative abundance of *dsrA*, prevailed in location #5. The taxonomic analysis of nitrogen cycling genes revealed that high levels of nitrate were associated with a higher relative abundance of denitrifying, facultatively anaerobic and aerobic Alphaproteobacteria. Additionally, sulfur-oxidizing Epsilonproteobacteria responded to the high nitrate levels in location #4 but not in location #6. Collectively, the relatively high general and pitting corrosion in location #6 may be due to the combined effect of high numbers of bacteria, stimulated by nitrate, and in particular by high

numbers of sulfate reducing bacteria. Similarly, coupons from location #5 also had a high number and relative abundance of sulfate reducing bacteria as well as larger and deeper pits.

Thus high DIN is associated with higher numbers of biofilm bacteria but different groups of denitrifying bacteria can be enriched, possibly depending on the ambient oxygen levels. The availability of oxygen is expected to decrease as the biofilm matures, as in Melcher's model, and the degree of carbon steel pitting should increase as the number of anoxic regions multiply. The differences in biofilm community composition among coupons suggests that the coupons may have experienced different levels of oxygen availability when they were sampled. While only four sampling sites are evaluated, the results are inconsistent with the prediction of increased corrosion being differentially associated with high DIN in marine waters. As a corollary, the nitrate concentration as well as the frequency of nitrate/nitrite reducing and/or nitrogen cycling genes may not be useful as early warning signs of carbon steel corrosion and should be used with caution.

Introduction

Professor Robert Melchers put forward an empirical multi-phase phenomenological model for carbon steel corrosion in seawater (Melchers, 2003). The model is based on the analysis of steel pilings exposed over long periods of time to coastal waters from around the globe. The model has five phases (Figure 1A) and two periods of biological activity (Melchers, 2010; Melchers and Jeffrey, 2011). In phase 0, the metal surface is initially colonized with marine organisms (i.e. prokaryotes and microeukaryotes). The corrosion in phase 0 is an aerobic process that exhibits non-linear kinetics, influenced by both the chemical and bacterial environment (particularly if the bacterial nutrient supply is unlimited). Phase 1 is governed mainly by the diffusion of oxygen through the developing biofilm to the metal surface. With rust layer build up, localized anoxic/suboxic microenvironments get created in the biofilm. At this phase of development, the first stage of biological activity essentially ends. During Phase 3 and 4, the corrosion mechanisms change to largely anaerobic processes, mainly catalyzed by bacterial activity. The rate of corrosion during Phase 3 and 4 depends on bacterial metabolism and is a function of the nutrient supply. The nutrient most often limiting bacterial activity in seawater is dissolved inorganic nitrogen (DIN), including nitrate, ammonium and nitrite (Melchers, 2014). The role of bacterial activity on carbon steel corrosion (microbiologically influenced corrosion - MIC) during 0-1 phases have been confirmed with field-collected data as well as laboratory experimentation (Melchers, R. E. 2007; Melchers and Jeffrey, 2011).

Accelerated general and pitting corrosion observed in mooring systems has been previously attributed to MIC (Rosen *et al.,* 2014; Witt *et al.,* 2016). The SCORCH JIP (Seawater Corrosion of Ropes & Chain - Joint Industry Project) was developed to address multiple cases of severe pitting and localized corrosion of chains and wire ropes of mooring systems in tropical waters. The SCORCH JIP examined mooring chain links recovered from floating production units based in West Africa and Indonesia (Rosen *et al.,* 2014). These were in service only for seven years and had experienced severe general corrosion in the splash zone and mega-pitting in the submerged near-surface zone. Although not based on adherent microbial community analysis, the element composition of the rust from the recovered chain links suggested that pitting was the result of MIC (Rosen *et al.,* 2014). Furthermore, a strong correlation was observed between the pitting and the nutrient concentration of the environment. Nitrate concentration (as N) in particular was unusually high in both locations (West Africa – 12.08 mg/L and Indonesia – 1 mg/L), thus the study suggested the further investigation of the association between MIC and nutrient concentration (Rosen *et al.,* 2014).

Since 2010, mooring systems in facilities off coast of Nigeria, Angola and Equatorial Guinea have received replacements as corrosion was suspected to be associated with MIC (Witt *et al.,* 2016).

In 2014, a field study was conducted by the project comparing two sites of the coast of West Africa (Witt *et al.,* 2016). Coupons at one site experienced comparatively higher corrosion including the formation of mega-pits. The DNA profile on coupons of the two sites were different with sequences representing sulfate reducing bacteria (SRBs) in the biofilm of the high corrosive site. However, the relative abundance of OTUs representing SRBs was low compared to other major bacterial groups. Although the findings were consistent with MIC in the high corrosive site, the ability of SRBs to produce severe general and pitting corrosion when in such low abundance was not verified (Witt *et al.,* 2016).

The present study was designed as a continuation of the SCORCH JIP to better understand MIC associated with mooring systems and to evaluate MIC mitigation strategies. A molecular analysis of the microbial communities on coupons was performed to gain insight on the adherent biofilms associated with MIC that may lead to the initial phases of general corrosion and the formation of macroscopic pits in mooring chains. To that end, metal coupons cut from steel mooring chains were exposed to four offshore locations in parts of the world that experienced different rates of corrosion. Biofilms on the coupons were recovered and metagenomic analysis was conducted to compare the microbial community structure and to infer the metabolic potential of the adherent populations. In light of the model put forward by Melchers and colleagues (Melchers, R. E, 2003; Melchers, R. E. 2007; Melchers, R. E, 2010; Melchers and Jeffrey, 2011), and previous observations of pitting corrosion of mooring chain links associated with high DIN levels (Rosen *et al.,* 2014), it was hypothesized that DIN enhances corrosion by the general stimulation of microbial activity. If true, high rates of corrosion should be more evident in samples recovered from high DIN locations relative to low DIN areas. Alternatively, it might be that the high levels of nitrate (a component of DIN) in marine environments are associated with the differential increase in nitrate reducing sulfate reducing bacteria (Marietou, 2016). When aerobic conditions prevail in marine waters, sulfate reduction is typically negligible and the ability utilize nitrate as terminal electron acceptor might allow this type of SRBs to remain viable. When microbial biofilm development on coupon surfaces restrict oxygen penetration, the activity of this group of organisms would lead to an increase in corrosion through the production of high levels of sulfide that subsequently react with iron leading to formation of Fe (II) sulfide. Such an association would lead to relatively high sulfide-driven corrosion rate in coupons recovered from high nitrate locations.

Materials and Methods

Metal coupon samples /Field sampling kit

Metal samples were manufactured from offshore mooring chain links donated by Vicinay Marine and Asian Star Anchor Chain. The rectangular coupons (85 mm X 30 mm X 6mm) were taken near the surface of mooring chain links (Figure 2) and had a slight curvature on one side. Each coupon had two holes (8mm diameter) 12 mm and 26 mm away from the short edge of the coupon.

The coupons were connected together to make a field exposure kit called the "microbiological fishing kit" (MFK) as described elsewhere (Witt *et al*., 2016). The MFK used in this study was slightly modified from that previously described in that the coupons were attached to plastic rods by one hole with a non-conductive bolt and spacer, and by the other hole with a plastic cable tie (Figure 3). The candidate locations selected to conduct the study are shown in figure 4 and were labeled as location #4, #5, #6 and #7 (Figure 4). The duration of exposure and depth of exposure of each MFK are given in Table 1. From the recovered MFKs, coupons C1, C2, C5, C8 and C10 were used for various analyses. All coupons Except C1 were treated with DNAzol (MRC, Inc. Cincinnati, OH, a reagent used to preserve DNA) prior to shipping.

Metal coupon cleaning

Coupons were shipped to the University of Oklahoma laboratory in individual transparent plastic bags. The surface of coupons C2 and C5 were scraped using a sterile spatula to remove the outer biofilm for subsequent DNA extraction. The coupons were then stored at -20^{o}C until surface analysis. Coupons C1, C5, C8 and C10 were cleaned following an ASTM standard protocol (ASTM G1-03, 2011). Briefly, coupons were dipped in a cleaning solution (3.5 g/l of hexamethylenetetramine (Sigma-Aldrich, St. Louis, MO) in 6M HCl) followed by brief immersions in acetone and methanol. The coupons were subsequently dried using N_2 gas and used for weight loss analysis to estimate rates of general corrosion. Coupon pit depth was evaluated by light microscopy using an SEM/SEM stereo pair analysis.

Water sampling

Water samples were collected from each exposure location at a depth of 2-5m below the water surface and were put on ice for preservation. The samples were analyzed for chemical composition in a laboratory close to the sampling locations (conducted by collaborators) and the reports were made available to the authors by DeepStar®.

Biofilm collection and DNA extraction

Coupons C2 and C5 of each location were used for biofilm collection and DNA extraction for metagenome analysis. The outer biofilm of each coupon was scraped using a sterile Teflon spatula and 0.25g of the scrapings were added to sterile 2 ml screw cap tubes. DNAzol (50 µl, MRC, Inc. Cincinnati, OH) was added to the biofilm material and mixed by vortexing. The tubes were stored at 20°C until DNA could be extracted as described elsewhere (Cellikol-Aydin *et al.,* 2016). This procedure is a combination of the Power Soil DNA extraction method (MO-BIO Laboratories, Carlsbad, CA) and the Maxwell® 16 Tissue LEV (Low Elution Volume) Total RNA purification kit AS1220 with the Maxwell® 16 instrument (Promega Corp, Madison, WI). A tube of beads from Power soil extraction kit was added to each screw cap tube containing biofilm. The solution C1 from the same kit (60 µl) was added next and mixed by vortexing for few seconds. Three heat/thaw cycles were performed next as follows: 5 minutes at 70°C and 5 minutes at -80°C. Proteinase K (10 µl, Quigen, Valencia, CA) was added to each sample and incubated at 45°C for 1 h. After that, the tubes were bead-beaten for 2 minutes. The samples were centrifuged at 10,000 x g for 30 seconds at room temperature and the supernatant was transferred to a new tube. After adding 250 µl of solution C2 of Power soil extraction kit and vortexing, the samples were incubated at 40°C for 5 minutes. Then, the samples were centrifuged at 10,000 x g for 1 minute at roome temperature and the supernatant was transferred to a clean tube. The solution C3 (200 µl) of Power soil extraction kit was added next, vortexed and incubated for 5 minutes at 4°C. The samples were then centrifuged at 10,000 x g for 1 minute at room temperature and the supernatant was transferred to a clean tube. Afterwards, 500 µl of RLA (RNA lysis buffer) and 500 µl RDB (RNA dilution buffer) were added and the samples and mixed well. The DNA was extracted from this mixture using the FFPE (formalin-fixed, paraffin-embedded)/Cells program of the Maxwell® 16 instrument. The DNA was eluted in 100 µl of nuclease-free water and DNA quantified using a Qubit® 2.0 Fluorometer and the Qubit® dS DNA HS assay (Life Technologies, Grand Island, NY) according to manufacturer's instructions. The DNA samples were sequenced on an Illumina MiSeq instrument in the Next Generation Sequencing Facility at Oklahoma Medical Research Foundation, Oklahoma City, OK.

qPCR

Number of copies of bacterial 16S/archaeal rRNA gene and *dsrA* gene (dissimilatory sulfate reductase catalytic subunit, used to estimate #s of sulfate-reducing bacteria) was determined using qPCR. For bacterial/archaeal 16S, each qPCR reaction was performed in triplicate with a final volume of 15 µl containing 3 µl of biofilm DNA, 0.04 µl of forward primer (519F: 5' CAGCMGCCGCGGTAA 3', 100 µl stock, Klindworth *et al*., 2013), 0.08 µl of reverse primer (Bac_785R: 5' TACNVGGGTATCTAATCC 3',

100 µl stock, Klindworth *et al*., 2013), 7.5 µl of 2X Power SYBR green qPCR mix (Life Technologies, Grand Island, NY) with the balance provided by RT-PCR grade water. The real-time PCR reaction was run in a StepOnePlusTM Real-Time PCR System (Applied Biosystems, Carlsbad, CA, StepOneSoftware v2.1) at 95°C for 10 minutes followed by forty cycles of 95°C for 30 s, 52°C for 45 seconds and 72°C for 45 seconds with data collection at 72°C. For *dsrA*, the primers DSR1F and RH3-dsrR were used (Ben-Dov *et al.,* 2007). Samples were run in triplicate and each reaction mixture contained 3 µl of biofilm DNA 1:10 or 1:100 dilution, 0.1 µl of each primer (100 µl stock), 1.5 µl of 5M Betaine, 7.5 µl of 2X Power SYBR green qPCR mix with the balance provided by RT-PCR grade water. Thermal cycling was carried out in the same RT-PCR system as above with the following cycling conditions: initial denaturation at 95°C for 10 minutes was followed by forty cycles of 95°C for 15 seconds, 60°C for 30 seconds and 72°C for 20 seconds and 79°C for 10 seconds. Standard curves were developed by utilizing a plasmid containing one copy of either 16S or *dsrA* gene sequence.

Metagenomic analysis

The raw sequences were processed using the MGMIC pipeline application. The quality of sequences were assessed by FastQC (Andrews, 2010). Primer/Illumina adapter/barcode sequences were detected and trimmed using a combination of custom scripts integrated with TrimGalore (Babraham Bioinformatics) and Cutadapt (Martin, 2011). Reads were trimmed to a Phred quality score of 30 and poly-AAA tails and artifacts were eliminated using HomerTools (Heinz *et. al.,* 2010). The read processing tool Trimmomatic (Bolger *et al.,* 2014) was applied to screen sequences for a minimum length of 100 bp and to remove any homopolymers (>6bp). Unpaired reads were removed and sequences were converted to fasta format via Biopieces (http://www.biopieces.org). Finally, the success of quality screening was assessed by rerunning FastQC (Andrews, 2010).

16S rRNA gene based microbial community analysis

Using the MGMIC pipeline application, the 16S rRNA gene sequences were extracted from the metagenome by USEARCH (Edgar, 2010) against the SILVA 111 reference alignment database (Quast *et al.,* 2013). All reads with >70% identity over a 100 bp fragment to the Silva database were extracted and assigned taxonomy via closed reference picking in relation to the Silva 118 reference alignment via QIIME pipeline (Caporaso *et al.,* 2010).

Functional gene analysis

Functional gene prediction was performed by searches of functional gene databases via USEARCH (Edgar 2010) by setting a minimum overlap of 50 columns at a 70% identity. Frequencies were calculated as RPKM (reads per kbp per megabase) and RPKM was calculated as = (reads / exon length) * (1,000,000 / mapped reads). The gene frequency for each gene was then normalized against the number of *rpoB* genes per sample and multiplied by 1000. Only one copy of *rpoB* is found per bacterial genome and therefore the number of *rpoB* genes is equivalent to the number of cells. Thus, the final calculated gene frequency gives the number of copies of a certain gene per 1000 cells. The reads of nitrogen and sulfur cycling genes were extracted from functional gene analysis and used the BLASTN function against NCBI nucleotide database (Altschul *et al*., 1990) to gain phylogenetic identification.

Results

Location parameters

The coupons in all four locations were exposed to subtropical seawater in the euphotic zone although the four environments differed in several important parameters (Figure 4, Table 1). In locations #4 and #5, the coupons were exposed 20 meters below the sea surface whereas coupons were exposed 3 meters below the surface for locations #6 and #7. The water temperature was slightly higher at location #6 (28^{o}C) whereas it was 26^{o}C at the other three sampling areas. The length of exposure of the coupons in seawater varied from 74 d (location #7) to 116 d (location #5), with location #4 at 95 d and location #6 at 92 d.

The dissolved inorganic nitrogen (DIN) content in particular, was very high (> 2 mg/L) at locations #4 and #6 compared to the other two locations. Nitrate was the dominant form of DIN at both #4 and #6. Dissolved oxygen was not recorded for locations #4 and #7.

Corrosion analysis

Corrosion analyses were conducted by collaborating colleagues (Drs. Iwona Beech and Zakari Makama) and shown here to illustrate differences in coupon damage from the four locations and the variation in damage among the coupons in the same location (Figure 5). The rates were determined based on weight loss of each coupon but are not further described due to confidentiality agreements. The highest corrosion rate was observed with the coupons recovered from location #6 followed by locations #5, #7 and the lowest in #4. According to the NACE International Standards of corrosion rate

interpretation (NACE Standard, 2005), the damage in all four locations fall into the category of severe. The average rate at location #4 was just above the lower limit of severe corrosion rate while the others had values above the limit.

Statistically, there was a significant difference between the groups as determined by one-way ANOVA ($F(3,12) = 3.538$, $P = 0.048$). A Tukey HSD test further indicated that the corrosion rates of location #4 were statistically significantly lower than that of location #6. Based on light microscopy and SEM, more aggressive pitting was observed on coupons exposed to locations #5 and # 6 compared to the other two locations (data not shown due to confidentiality agreements). While coupons of all locations experienced pitting, the pits of locations #5 and #6 were much deeper and wider compared to same measures at the other locations.

Biofilm community analysis

The DNA concentration from 500 mg of biofilm samples of two coupons from each location was used as a surrogate to estimate relative biomass quantities (Table 2). The highest biomass was found in the biofilms recovered from coupons of location #4. Coupons #6-C5 and #7-C2 had total biomass higher than 1000 ng followed by coupon #6-C2 with 968 ng. Coupon #7-C5 had only half of biomass compared to the other coupon (#7-C2) recovered from the same location. The lowest biomass based on DNA concentration was found in the biofilms recovered from location #5 (Table 2).

With reference to qPCR data, the number of bacterial and archaeal 16S rRNA gene copies of biofilms from locations #4 and #6 was 10 times higher than the biofilms of other two locations (Table 2). When number of copies of *dsrA* sequences is considered, biofilms of locations #5 and #6 contained more copies in general except for the high number of copies from coupon C5 of location #4 (Table 2, Figure 8). The qPCR for *dsrA* copy number of coupon C2 of location #5 was repeated several times but always resulted with an average higher than the 16S copy number.

Based on the analysis of 16S rRNA gene sequences extracted from metagenomes, C2 and C5 of location #4 and C2 of location #7 had >50% relative abundance of eukaryotes (Figure 6, Table S1). In biofilms of coupons #7-C5, #5-C2 and #5-C5, the relative proportion of 16S rRNA reads representing eukaryotes were 43%, 44% and 27%, respectively, with the lowest relative proportion of eukaryotes occurring in the biofilms of coupons from location #6. There also appears to be an effect of coupon position, with coupon C5 in each location having a lower relative abundance of eukaryotes than coupon C2. The eukaryotic sequences represented cnidarians, marine arthropods, bryozoans and radiolarians.

The great majority of the remaining 16S rRNA gene sequences were those of bacteria rather than archaea. The number of archaeal *rpoB* sequences was less than 1% that of bacterial *rpoB* sequences except for location #7 (approximately 1%). Around 90% of 16S rRNA gene reads in biofilms of location #6 were bacterial sequence reads (Figure 6). In the biofilm community of coupons C2 and C5 of location #6, Alphaproteobacteria made up 31.68% and 21.26% of the total reads with 79% and 67% of them representing family Rhodobacteraceae, respectively. Deltaproteobacteria accounted for 13.2% and 42.32% of the total reads in C2 and C5 of the same location, respectively (Figure 6, Table S1) and the majority (95% and 80%, respectively) were of genus *Desulfovibrio*. The relative abundances of Gammaproteobacterial reads in the same biofilm samples were 11% and 29% (Figure 6, Table S1). The majority of Gammaproteobacterial reads in C2 were members of the Vibrionaceae, with *Thalassomonas* and *Vibrio* most abundant, while Campylobacteraceae dominated C5, including the sulfur oxidizing bacteria *Sulfurimonas* and *Arcobacter*.

In the biofilm communities C2 and C5 of location #5, Deltaproteobacteria was the dominant bacterial group with relative abundances of 23.5% and 38.7%, respectively (Figure 6, Table S1), with >80% of them represented by *Desulfovibrio.* Alpha- and Gammaproteobacteria were found in relatively smaller proportions (less than 10%) in the #5 samples (Figure 6, Table S1). The majority of the OTUs in the Alphaproteobacteria belonged to family Rhodobacteraceae. Epsilonproteobacteria made up 2.8 and 5.8%, respectively, of the total 16S reads in the same biofilm samples (C2 and C5), dominated by the sulfur oxidizer *Sulfurimonas* (Figure 6, Table S1).

The biofilms recovered from the location #4 had ~9% relative abundance of Alphaproteobacterial sequence reads (Figure 6, Table S1). Biofilm on coupon #4-C5 had 11.28% of total reads representing Deltaproteobacteria while the other coupon of the same location (#4-C2) had only 1.89% total reads belonging to the same bacterial taxon, with the majority represented by *Desulfovibrio*. Epsilonproteobacteria made up 7.5 and 3.2%, respectively, of the total 16S reads in the same biofilm samples, dominated by the sulfur oxidizers *Sulfurimonas* together with *Arcobacter* (Figure 6, Table S1) About 4.59% and 5.64%, respectively, of the total 16S reads of #4-C2 and #4-C5 biofilms accounted for Zetaproteobacteria with iron-oxidizing genus *Mariprofundus* accounting for all of them.

With respect to 16S rRNA sequence analysis of the two biofilm samples of location #7, bacterial community composition of the two coupons were quite different in terms of relative abundances of major bacterial groups as well as the relative proportion of eukaryotes (Figure 6, Table S1). Particularly, relative abundance of Deltaproteobacteria in #7-C5 was 22.2% while in #7-C2, the value was only 3.1%, with the majority in each case was *Desulfobacter* (Figure 6, Table S1). Moreover,

Alphaproteobacteria accounted for 13.1% of total reads in #7-C5 when the same group accounted for 4.8% of total reads in #7-C2.

Functional gene analysis

To gain some insight on the potential major respiration pathways present, the metagenome of each biofilm was interrogated for the frequency of gene copies involved in in oxygen respiration (*ccoN*), nitrate/nitrite reduction (*napA, napB, narG, narH, narI, narJ and nirK*), sulfate reduction (*aprA, aprB, dsrA,* dsrB) and sulfur/sulfide oxidation (*soxA, soxB, soxC, soxX, soxY, soxZ*). The normalized gene frequencies were summed based on the pathway.

Based on functional gene analyses, the biofilm bacterial community from all four locations had the potential for oxygen respiration, sulfur/sulfide oxidation (Figure 8, Table S2), sulfate reduction and nitrate/nitrite reduction (Figure 9, Tables S3 and S4). The ability of the microbial community to catalyze aerobic respiration is indicated by the frequency of the *ccoN* gene (cbb3-type cytochrome C oxidase catalytic subunit). Coupons of location #4 had the highest frequency of these genes (217.4 and 220.4 reads, Figure 8, Table S2) and location #5 the lowest frequency. Further, biofilms of location #4 had the highest proportion of sulfur oxidation genes with normalized frequencies higher than 300 (Figure 8, Table S2). The lowest representation of sulfur/sulfide oxidation genes was by biofilms of location #5 with frequencies of 116 and 158 and coupon C2 of location #7 with a frequency of 161 (Figure 8).

As far as the functional genes involved in anaerobic pathways are concerned, the biofilms from high nitrate locations #4 and #6 samples had higher frequencies of nitrate/nitrite reduction genes compared to the other two locations (Figure 9, Tables S3 and S4). Coupons #4-C2 and #4-C5 had normalized frequencies of 450.1 and 431.9 while the coupons #6-C2 and #6-C5 had 352 and 345.6 frequencies (Table S3). In contrast, the highest number of reads for sulfate reduction genes were found in the #5 biofilms (554.8 and 668.2,) followed by coupons #6-C5 (544.3) and #7-C5 (457.1, Figure 9, Table S4).

In order to rank the potential of the aerobic and anaerobic pathways of each biofilm, the frequency of a single representative gene of each pathway was compared (Table 3). Location #4 biofilms each had the highest potential for oxygen respiration as represented by relative abundance of *ccoN* genes, with less potential for dissimilatory sulfate reduction. For location #5, sulfate reduction and oxygen respiration both had fairly high potential but there was little potential for sulfur oxidation or dissimilatory nitrate reduction. Considering location #6, biofilm of C2 had highest potential for aerobic respiration followed by dissimilatory nitrate reduction and low potential for sulfur oxidation

and sulfate reduction (Table 3). In contrast, dissimilatory sulfate reduction had a much higher potential in biofilm of C5 of the same location. With respect to location #7, potential for oxygen respiration was the highest for C2 while in C5, potential for oxygen respiration was highest but the dissimilatory sulfate reduction appeared to have a very high potential as well, as shown by frequency of *dsrA* gene (Table 3). In locations #5, #6 and #7, potential for oxygen respiration was lower (as depicted by relative abundance of *ccoN* gene copies) and potential for dissimilatory sulfate reduction was higher in C5 coupons compared to C2 coupons (Table 3). Additionally, the potential for nitrate reduction was relatively higher in coupons of locations #4 and #6 (Table 3).

Taxonomic identification/grouping of reads associated with nitrogen and sulfur cycling

In order to identify the dominant organisms involved in nitrogen and sulfur cycling in biofilms of each coupon, the sequences of nitrate reduction (*napA, napB, narG, narH, narI, narJ and nirK*), sulfate reduction (*aprA, aprB, dsrA,* dsrB) and sulfur oxidation (*soxA, soxB, soxC, soxX, soxY, soxZ*) were interrogated for taxonomic identification. The organisms associated with more than 10 copies of a certain gene were identified thorough BLASTN searches of the sequences against NCBI nucleotide database (Altschul *et al*., 1990). The resulting organisms were binned into major proteobacterial groups. The number of reads observed for each gene and, the full list of organisms associated with these processes is shown in Tables S5 and S6.

Based on the taxonomic analysis of each location, the majority of the nitrate/nitrite reducing genes in the high nitrate locations #4 and #6 were associated with Alphaproteobacteria (Figure 10). The #4 samples had 59.9 and 83.4 reads related to Alphaproteobacteria whereas the #6 samples had 130.3 and 145.7 of such reads. Some Alphaproteobacteria were common to both locations #4 and #6 and included both aerobes (*Brucella melitensis*, *Ochrobactrum anthropi*) and denitrifiers (*Roseobacter denitrificans*, *Paracoccus denitrificans*, *Pseudovibrio* sp., Table S5). Location #4 also had 40.7 and 57.7 reads reflecting the presence of nitrate/nitrite reducing genes in the Epsilonproteobacteria (Figure 10). Members of Epsilonproteobacteria found in #4 samples included the sulfur-oxidizer *Sulfurimonas autotrophica* as well as the sulfur-oxidizing denitrifiers*, Sulfurimonas denitrificans* and *Sulfurimonas gotlandica* (Table S5). While the biofilm of C2 of location #7 had no dominant organism with nitrate/nitrite reducing genes (no organism had gene copy numbers higher than 10), coupon C5 had around 17.2 reads representing Epsilonproteobacteria (Figure 10). The sulfur-oxidizing denitrifier *Sulfurimonas gotlandica* was the dominating Epsilonproteobacterium on this coupon (Table S5). Considering Gammaproteobacteria, the members of the group identified in #4 samples included *Shewanella sediminis, Shewanella halifaxensis* and *Pseudomonas entomophila* (Table S5). Of these organisms, *Shewanella halifaxensis* is known to denitrify. Reads identified as Gammaproteobacteria

in location #6 include those of *Saccharophagus degradans* (an aerobic cellulose metabolizing organism), *Alteromonas macleodii*, *Hahella chejuensis* (obligate aerobes) and *Simiduia agarivorans* (nitrate reducer, Table S5). Nitrate/nitrite gene harboring Gammaproteobacteria were dominant only in biofilms of locations #4 and #6 (Table S7). Deltaproteobacteria associated with nitrate/nitrite reduction genes were highest in coupon #6-C5 (61.1 reads), followed by #7-C5 (32.1 reads), #5-C2 (24.6 reads), #6-C2 (11.1 reads) and the lowest in #4-C5 (5.8 reads, Figure 10, Table S5). No bacteria in coupon #7-C2 had nitrate/nitrite reduction gene reads higher than 10. The Deltaproteobacteria identified in these samples include the sulfate-reducing bacteria, *Desulfocapsa sulfexigens*, *Desulfovibrio alaskensis G20*, *Desulfovibrio desulfuricans*, *Desulfovibrio vulgaris* Hildenborough and *Desulfovibrio gigas* (Table S5). Of these Deltaproteobacteria, *Desulfovibrio desulfuricans* is known to reduce nitrate (Marietou *et al*., 2005).

The majority of the organisms harboring sulfate reduction genes in all coupons except #4-C2 were Deltaproteobacteria (Figure 11, Table S6). Highest sulfate reduction gene frequency associated with Deltaproteobacteria was found in #5-C2 (554.7 reads, Figure 11). Additionally, biofilms of coupons #6-C5 (460.6 reads) and #7-C5 (394.3) had comparatively higher frequencies for sulfate reduction genes associated with Deltaproteobacteria. The detected Deltaproteobacteria in locations #4, #5 and #6 were several *Desulfovibrio* spp., and in location #7 were *Desulfotignum phosphitoxidans*, *Desulfobacterium autotrophicum* and *Desulfohalobium retbaense* (Table S6).

With respect to dominant organisms associated with sulfur/sulfide oxidation genes, Alphaproteobacteria harboring this group of genes were found in all coupons (Figure 12). Biofilms from locations #4 and #6 had relatively higher frequencies of sulfur/sulfide oxidation genes associated with Alphaproteobacteria. In biofilms of location #6, the frequencies observed were 84.6 and 106.2 and the identified organisms included facultative anaerobes *Polymorphum gilvum*, *Roseobacter denitrificans* and *Pseudovibrio sp.* (Table S6). The two biofilms of location #4 had gene frequencies of 41.4 and 61.8 representing Alphaproteobacteria and among the organisms were the obligate aerobes *Leisingera methylohalidivorans, Ruegeria pomeroyi* and facultative anaerobes *Polymorphum gilvum, Pseudovibrio sp., Roseobacter denitrificans* (Table S6). Additionally, biofilms from location #4 had a substantial number of sulfur/sulfide oxidation genes associated with Epsilonproteobacteria (46.6 and 80.2, Figure 12) and the group was dominated by sulfur oxidizing genus *Sulfurimonas* (Table S6) which was noted above as possessing denitrification genes (Table S5).

Discussion

The current investigation was conducted to better understand MIC associated with mooring systems and to develop mitigation strategies for MIC. Metal coupons cut from mooring chain links were exposed to four marine environments from across the globe. The locations were generally comparable in most physical and chemical attributes, but two of the locations had high DIN concentrations. The extent of corrosion was assessed by weight loss of metal coupons and the determination of pitting corrosion by light microscopy. In addition, DNA was extracted from the adherent biofilms on the coupons and a metagenomics analysis was performed in an attempt to deduce if MIC could be associated with particular types of microorganisms.

Corrosion rates

Based on the corrosion rates, it is clear that coupons exposed to location #6 experienced higher rates of general corrosion compared to those of other three locations (Figure 5). The general corrosion rates seems to be in the same range for the locations #4, #5 and #7, although the average corrosion rate of location #4 was significantly lower than the rest due to the gain in weight of one coupon (coupon #4-C8). Overall, the average corrosion rates (based on NACE standards, 2005) depict severe corrosion attack on coupons exposed in all four locations. However, according to light microscopy, locations # 5 and 6 experienced more pitting corrosion. These observations imply that, the environment and the biofilm communities present in all four locations contributed to severe corrosion in mooring chain coupons. Moreover, the differences in community composition and potential pathways that contributed towards corrosion might have led to the variability in corrosion rates and especially might have accounted for the higher pitting in locations #5 and #6.

Biofilm community structure and possible corrosion mechanisms

The information extracted from 16S rRNA gene identification of microbial community members as well as functional gene analyses of metagenomic data shows differences in terms of species composition and dominant electron acceptor pathways among the four locations as well as among individual coupons. Owing to the presence of a variety of microhabitats, a diverse microbial community with different physiologies can reside in the same biofilm (Leewandowski, 2000). Thus, the corrosion of the coupons attributed to MIC can be a collective result of the activities of corrosion enhancing as well as inhibiting microbes (Vigneron *et al.,* 2018).

Based on functional gene analysis (Table 3, Figure 8), coupons from location #4 are likely to have more oxygenated biofilms in comparison to other locations. Oxygen respiration is clearly the dominant energy utilizing pathway followed by sulfur oxidation. Carbon steel corrosion processes

therefore would most likely be governed by oxygen diffusion (0-1 phase of Melchers' model, Figure 1A) to the coupon surfaces. The oxidation of reduced forms of sulfur are also likely given the presence and presumed activity of *Sulfurimonas* spp. (Figure 12, Table S6) in these biofilms. The products of sulfur oxidation lead to iron corrosion as a well-documented MIC process (as reviewed in Little *et al*., 2000, Lahme et al. 2019). Sulfides formed through the action of SRB activity can be oxidized to acidic end products in the presence of oxygen and lead to severe corrosion (reviewed in Little *et al*., 2000).

As far as location #5 is considered, it can be inferred that the biofilms were in a more anaerobic state with a high potential for sulfate reduction as evident by the high sulfate reduction gene frequency (Table 3, Figure 9). The majority of these genes were harbored by the genus *Desulfovibrio* (Figure 11, Table S6). The SRBs are considered to be one of the major taxonomic groups contributing to anaerobic corrosion (Beech and Sunner, 2004; Dall'Agnol and Moura, 2014) as they produce hydrogen sulfide that reacts with the metal surface to form metal sulfide (Little *et al.,* 2000). The same activity could be attributed to higher pit depth and pit diameter observed in coupons recovered from location #5.

With reference to location #6, the biofilms of the two coupons analyzed showed rather different types of microbial physiology/metabolism associated with the surfaces based on functional gene analysis (Table 3, Figure 6 and Figure 11). Sulfate reduction is likely to be the dominant electron acceptor utilizing pathway in Coupon #6-C5 with the highest abundance of sulfate reducing genes harbored by *Desulfovibrio* spp. (Figure 11, Table S6). It appears that the biofilm in coupon C5 was experiencing more anaerobic activity but also had some aerobic niches for aerobes to exist (1-2 phase of Melchers' model, Figure 1). Thus, it is likely that the acid from oxidized sulfur compounds produced by *Sulfurimonas* spp. and Gammaproteobacteria *Thioalkalivibrio* sp. added to the overall MIC resulting in a comparatively higher corrosion rate in C5 (Figure 5). On the other hand, Coupon C2 of location #6 likely had a more oxygenated environment facilitating aerobic metabolism (Table 3). The oxidation of iron (abiotic) can be suggested as contributing to corrosion as well as the activity of sulfur oxidizers *Thioalkalivibrio* spp. and *Allochromatium vinosum* (Table S6), resulting in pitting corrosion as well as increasing the general corrosion rate (Figure 3).

In location #7, coupon C2 appeared to reresent a relatively aerobic environment as implied by the relative frequency of *ccoN* (Table 3). Based on the relatively high potential of sulfur oxidation, it is likely the sulfur oxidation that led to the observed corrosion rate in coupon C2. On the other hand, the sulfate reducing community (relatively high in abundance) may have helped account for the corrosion of coupon C5 of location #7 (Figures 9 and 11). Based the observations of functional gene analysis of coupons of locations #5, #6 and #7, it appears that the coupon in a more interior position

(C5) experienced a more anoxic state than the other replicate (C2) at the time of sampling (Table 3, Figures3, 6 and 9).

Effect of elevated nitrate

High nitrate levels were measured at both the #4 and #6 field locations (2.4 – 2.6 mg/L). Increased levels of general nutrient levels in marine environments, and in particular DIN (including nitrate), would be expected to facilitate severe pitting as well as uniform corrosion catalyzed by the attached microflora (Melchers and Jefferey 2012, 2013; Melchers 2014). Indeed, the absolute size of the bacterial population, according to 16S copy numbers determined by qPCR, was one order of magnitude higher in locations #4 and # 6 compared to the other two locations (Table 2, Figure 8). Thus, the higher DIN, particularly nitrate, in the environment likely stimulated the proliferation of resident microbes. However, there were very different rates of corrosion encountered at the two high nitrate locations with the higher corrosion rate in location #6 and variability within that location. This observation indicates higher bacterial populations in #4 and #6 but not necessarily greater biocorrosive activity in both locations.

Biofilms of locations #4 and #6 had relatively high frequencies of nitrate/nitrite reduction gene sequences (Figure 9) that could have been a result of high levels of nitrate in seawater. The organisms responded to high levels of nitrate in both locations were mainly members of the group Alphaproteobacteria (Figure 10 and Table S5) with some aerobes (*Brucella melitensis*, *Ochrobactrum anthropi*), denitrifiers (*Paracoccus denitrificans*) as well as sulfur-oxidizing, nitrate-reducers (*Roseobacter denitrificans* and members of the genus *Pseudovibrio*, Tables S5 and S6). Some Gammaproteobacteria (e.g. denitrifying thiosulfate/sulfite/sulfur reducers such as *Shewanella* spp.) were also among the dominant nitrate/nitrite gene harboring organisms that were associated with high levels of nitrate (Figure 10). *Shewanella* spp. are also noted as metal-reducers (Vigneron *et al.,* 2018). Interestingly, no Gammaproteobacteria were found dominant at locations #5 and #7 (Figure 10). At location #4, a high relative abundance of Epsilonproteobacteria (*Sulfurimonas* spp.) were found harboring nitrate/nitrite reduction genes (Figure 10 and Table 5). These are denitrifying sulfur oxidizers and noted for their ability to promote MIC (reviewed in Vigneron et al., 2018, Lahme et al. 2019). The increase of sulfur-oxidizing nitrate reducing Epsilonproteobacteria has been previously observed in oil production facilities in response to nitrate injection (reviewed in Vigneron et al., 2018; Lahme et al., 2019; Lahme and Hurburt, 2017). The stimulation of sulfate-reducing nitrate-reducing Deltaproteobacteria by nitrate injection has also been reported (Vigneron *et al.,* 2017) but not observed in locations #4 or #6. The Deltaproteobacteria in the high corrosion location #6 were primarily sulfate-reducers rather than sulfate-reducing nitrate-reducing organisms, although some

harbored nitrogen cycling genes (Figure 10, Table S5). The ability of SRBs to utilize nitrate as a terminal electron acceptor is almost certainly underappreciated. Marietou (2016) points out that culture-dependent attempts to characterize SRBs capable of this activity might have been predisposed to false negative results due to the use of media with reductants that inhibit nitrate reduction.

Application of Melchers' model

The coupons from all four locations were exposed to seawater for less than a year. Therefore, it is reasonable to assume that the coupons were in the early stages (phase 0-2) of corrosion as determined by Melchers' phenomenological model (Melchers, 2003; Melchers, 2010; Melchers and Jeffrey, 2011). The model was very useful in explaining the development of the biofilm on coupon surfaces as well as the corrosion attack in different phases. The model was used in this discussion (early paragraphs) in explaining the possible factors governing the corrosion of coupons extracted from the four different locations.

As Melchers' model proposes (Melchers, 2003; Melchers, 2010; Melchers and Jeffrey, 2011;Melchers, 2014), the high nitrate content in #6 and #4 locations is indeed associated with higher bacterial populations as well as an increase in nitrate-reducing organisms (Figures 9, 10 and Table S5). However, the corrosion rates were dissimilar in the two high nitrate locations. Such an observation is inconsistent with Melchers' proposed model and the presumed impact of DIN on MIC. Melchers' model was originally developed based on observations from steel pilings exposed to sea water for long periods of time (≥ 12 mo, Melchers, 2014) and was proposed to predict long-term corrosion (Melchers, 2014) behavior. The SCORCH JIP project also investigated the MIC of mooring chain links with the hypothesis that the phenomenological model would explain the unusual corrosion rates. Since mooring systems are built to last decades and the corroded mooring links observed by SCORCH JIP (Rosen *et al.,* 2014) were in service for seven years, Melchers' model may indeed provide an explanation for the high rate observed of general as well as pitting corrosion. Given the constraints of time and budget, the coupons of current study were exposed to marine waters for less than a year and may therefore only provide only a limited early view of the salient corrosion processes.

The DIN (specifically nitrate in this study) led to general stimulation of microbial biomass but not necessarily MIC. The hypothesis that DIN enhances corrosion by general stimulation of microbial activity cannot be supported by the existing data. Alternatively, it was hypothesized that the high nitrate content might differentially enrich for nitrate reducing sulfate reducing bacteria. This prospect would lead to relatively high sulfide-driven corrosion rate in samples from locations #4 and #6. The relatively high corrosion rate of coupons recovered from the high nitrate seawater in #6 could not be attributed to known nitrate-reducing sulfate reducers. However, it is very clear that far more needs to

learned about the ability of SRB to utilize nitrate in oxygen-poor but nitrate-rich environments (Marietou, 2016). Rather, the increased corrosion in these waters appears to be the combined effect of sulfate reducing bacteria in conjunction with nitrate-reducing sulfur oxidizing bacteria. The high level of pitting corrosion in coupons from location #5 however, are associated with high numbers of sulfate reducing bacteria but not with nitrate-reducing sulfur oxidizing bacteria. Melchers' phenomenological model, although mainly applied to long-term marine corrosion, has also been used in MIC in a marine setting despite the time of exposure. While hardly an exhaustive test of the model implications, the failure to support the role of DIN on the degree of MIC would seem to warrant caution in future applications of the model. Additionally, the use of nitrate/nitrite reducing gene frequency and/or nitrogen cycling genes as a marker for corrosion needs to be reconsidered.

Acknowledgements

This work makes use of field data that was funded and collected for DeepStar® Phase 12 CTR 12402 by AMOG Consulting, Inc. The author would like to acknowledge technical guidance and contributions of DeepStar® Floating Systems committee and thank DeepStar® for access to the field data.

Table 1. Summary of water quality, depth and time of exposure.

Location	DIN (mg/L)	Dissolved Oxygen (mg/l)	Nitrate (mg/L)	Ammonia (mg/l)	Conductivity (Salinity) µS/cm	Temperature* (℃)	pH	Depth of exposure (m)	Duration of exposure (days)
#4	2.6	-	2.49	0.093	55,000	26	7.9	20	95
#5	<0.01	7.27	<0.01	-	52,380	28	7.3	20	116
#6	2.4	6	2.33	0.11	49,463	26	8.3	3	92
#7	<0.7	-	<0.6	-	18,200	26	7	3	74

Table 2. The total mass of DNA extracted from 500 mg of biofilm, the number of eubacterial 16S and dsrA (dissimilatory sulfate reductase catalytic subunit) gene copies/g of each biofilm (determined by qPCR).

Location	Coupon	total DNA (ng)	number of 16S copies		number of dsr copies	
			Average	SD	Average	SD
#4	C2	2320	2.20E+09	1.57E+08	1.28E+07	3.65E+06
	C5	2200	3.67E+09	1.51E+08	1.14E+09	3.47E+07
#5	C2	424	3.49E+08	9.57E+07	1.72E+09	7.55E+07
	C5	208	1.95E+08	1.02E+06	1.65E+08	1.83E+07
#6	C2	968	1.44E+09	9.14E+07	1.50E+08	2.17E+07
	C5	1040	2.11E+09	7.40E+07	2.43E+08	4.11E+07
#7	C2	1024	3.28E+08	1.13E+08	4.47E+06	7.35E+04
	C5	512	5.10E+08	1.52E+07	1.18E+07	2.43E+06

Table 3. Analysis of representative functional genes involved in major electron acceptor pathways.

Colors are based on the frequencies that were normalized to the copy number of *rpoB* gene and multiplied by 1000. Oxygen respiration: *ccoN* (cbb3-type cytochrome C oxidase catalytic subunit); Dissimilatory nitrate reduction: *narG* (respiratory nitrate reductase alpha/catalytic subunit); Dissimilatory sulfate reduction: *dsrA* (dissimilatory sulfite reductase catalytic/alpha subunit); Sulfur oxidation: *soxB* (S-sulfosulfanyl-L-cysteine sulfohydrolase).

Location / Coupon	*ccoN*	*soxB*	*narG*	*dsrA*
#4-C2	217.477	124.2	125.5	15.8
#4-C5	220.469	121.3	124.0	65.8
#5-C2	133.078	42.2	24.6	142.9
#5-C5	105.245	46.6	31.9	181.7
#6-C2	202.288	59.5	106.5	48.7
#6-C5	160.937	67.8	115.6	135.1
#7-C2	173.913	49.9	69.2	33.8
#7-C5	132.935	68.7	39.6	110.5

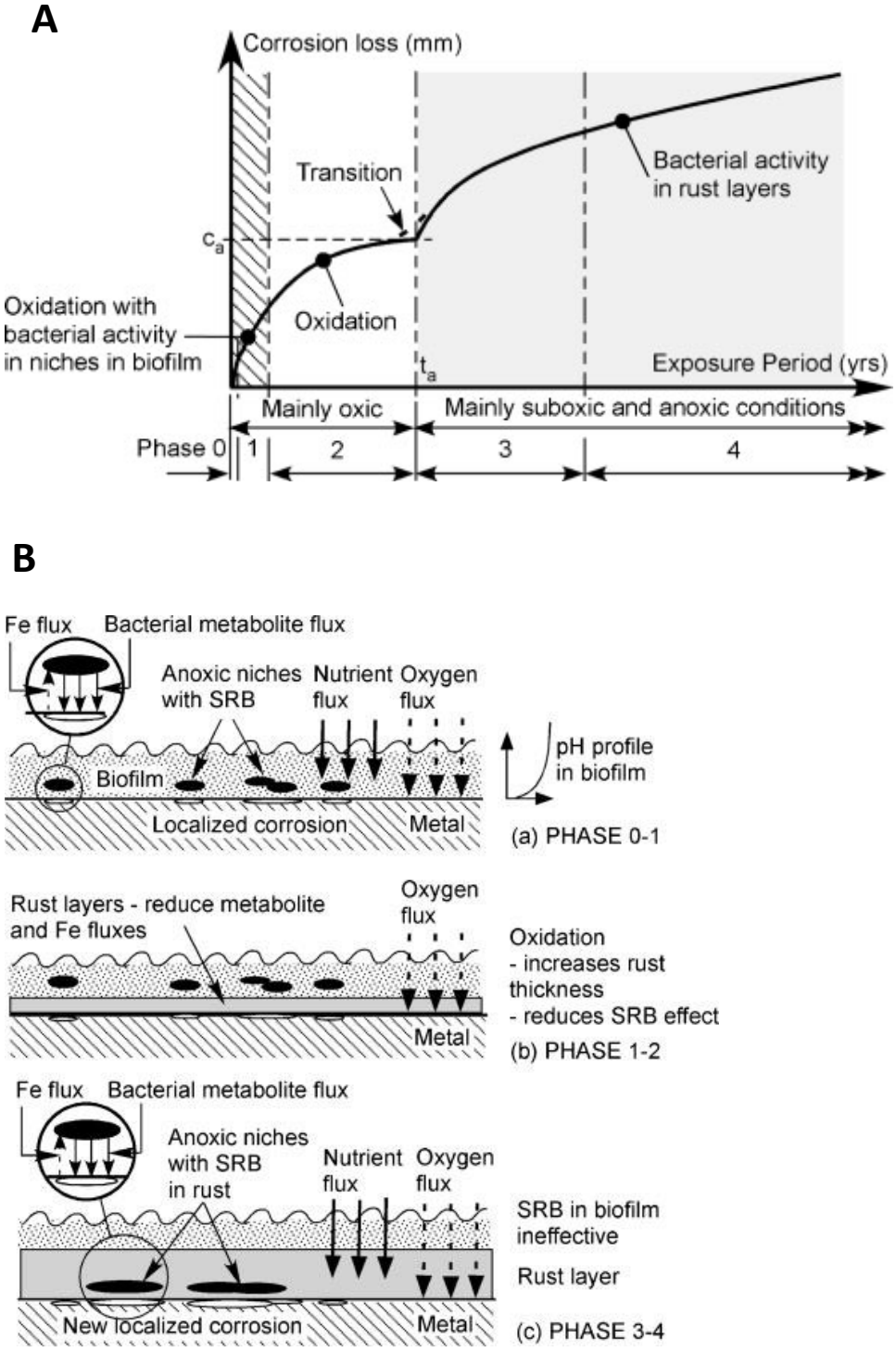

Figure 1. (A) Phenomenological model for corrosion loss as a function of time (B) Schematic of development of bacterial activity with time (Melchers, 2010).

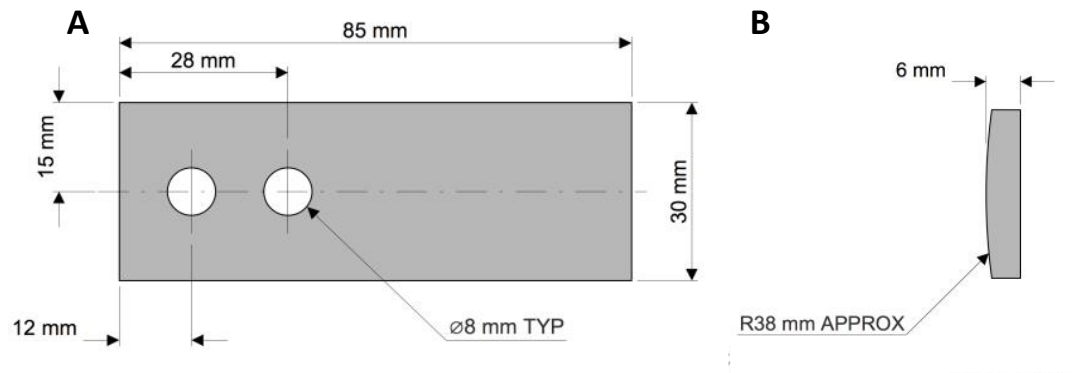

Figure 2. **Dimensions of the chain link samples**. (**A**) Top view. (**B**) Side view (Image supplied by AMOG Consulting, Inc.)

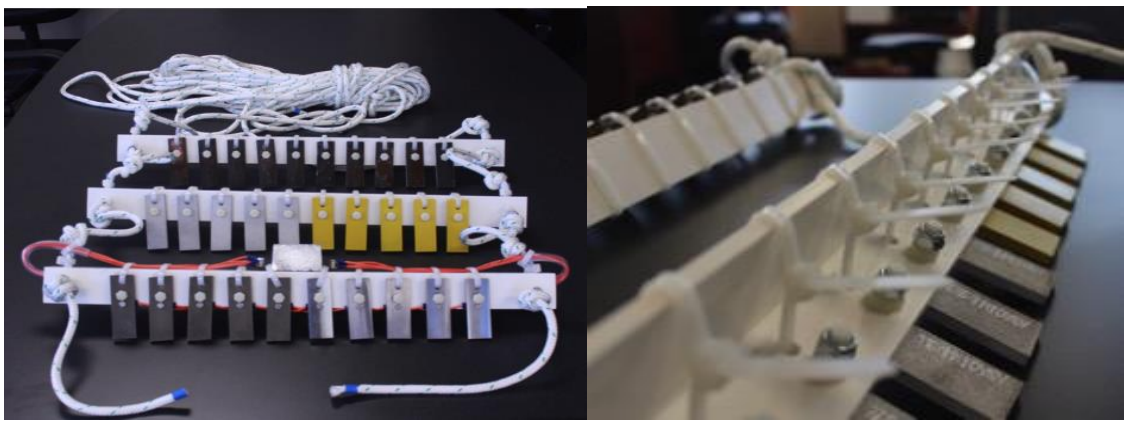

Figure 3. Assembly of Microbiological fishing kit (MFK) (Image supplied by AMOG Consulting, Inc.).

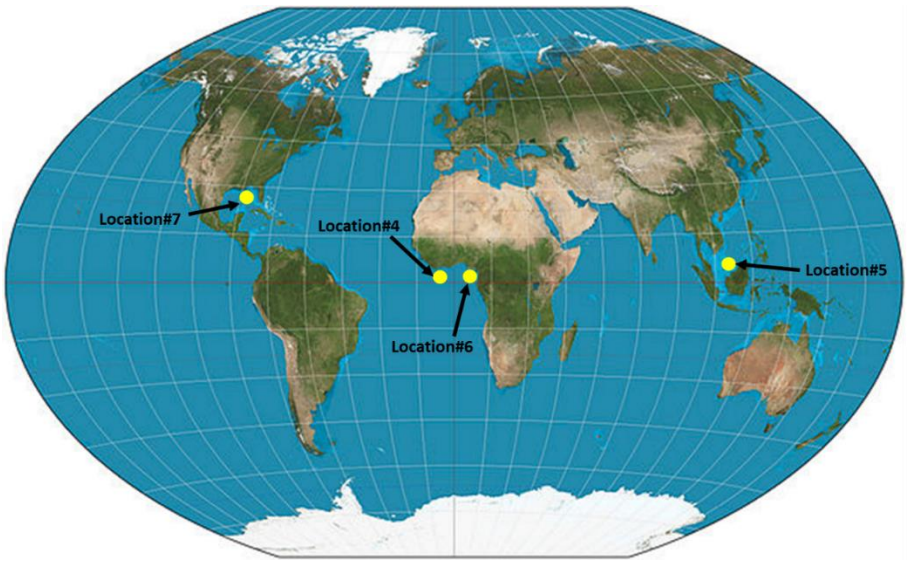

Figure 4. Location of the four sample sites. (https://en.wikipedia.org/wiki/World_map).

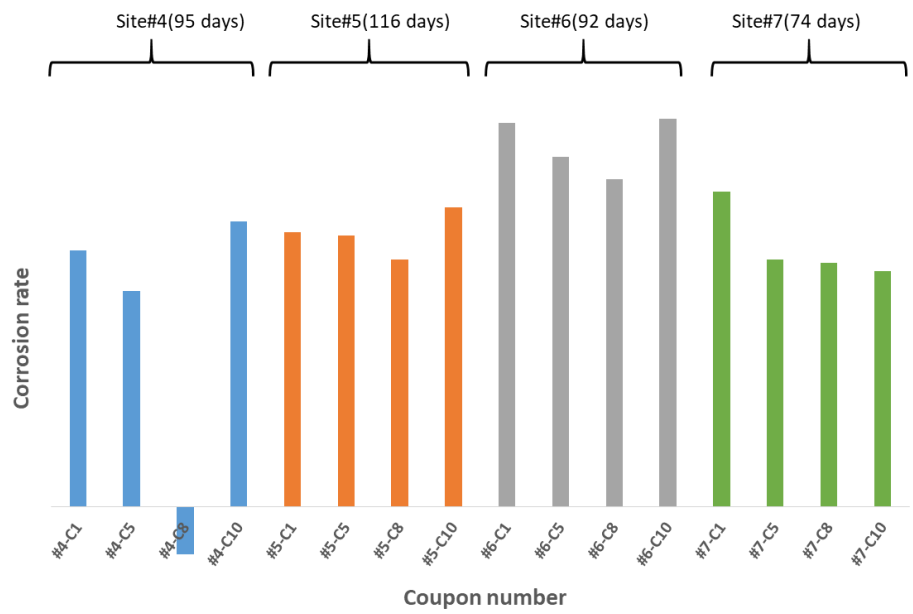

Figure 5. Corrosion rates of each coupon determined by weight loss (corrosion loss analysis was performed by Dr. Zakari Makama). Actual corrosion rate cannot be displayed due to confidentiality agreements.

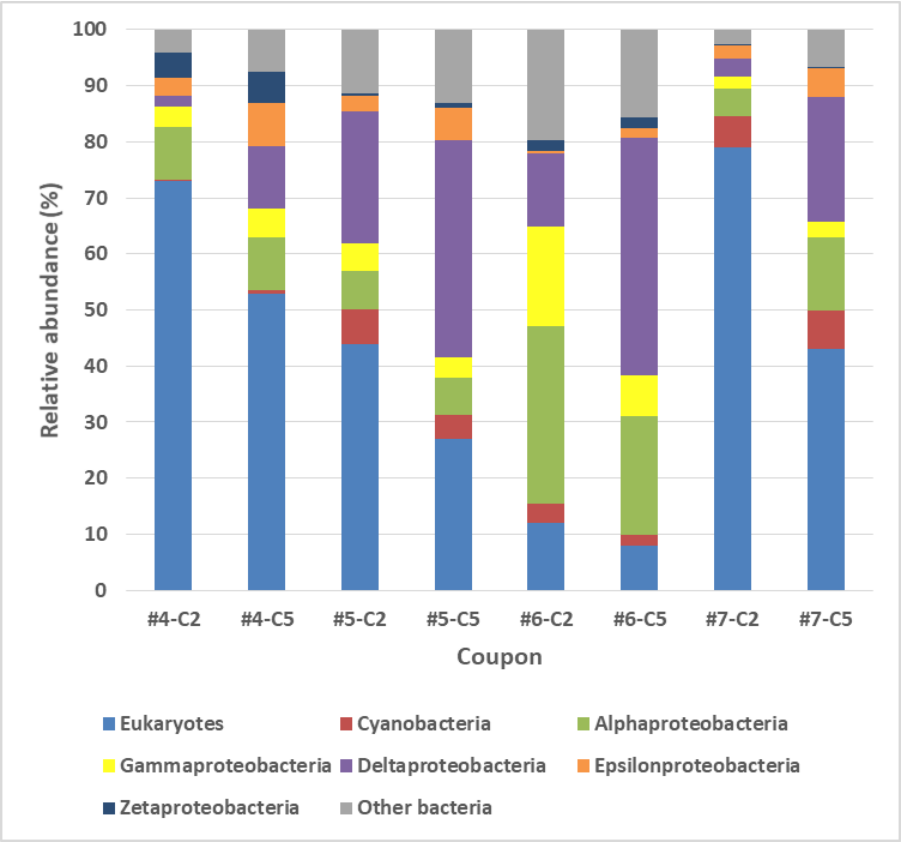

Figure 6. Microbial community composition (with bacteria at class level) of the biofilms formed on the coupons of the four different sites. 16S rRNA gene sequences were extracted from the metagenome and were analyzed using Qiime (Version 1.8.0).

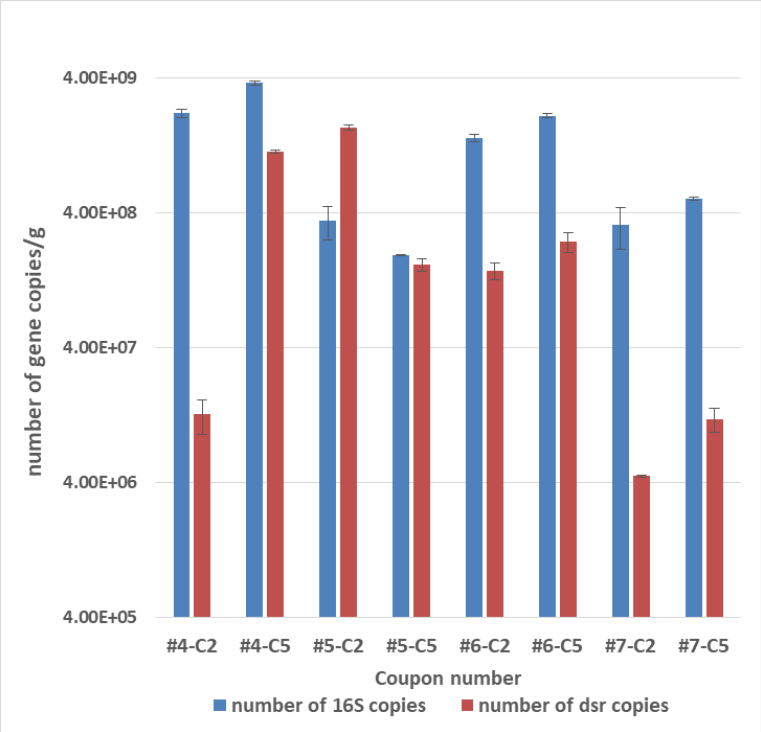

Figure 7. The number of copies of 16S and *dsrA* (dissimilatory sulfate reduction catalytic subunit) of each biofilm determined by quantitative real time-qPCR (n = 3). Average value and error bars (+/- 1 STD) are shown.

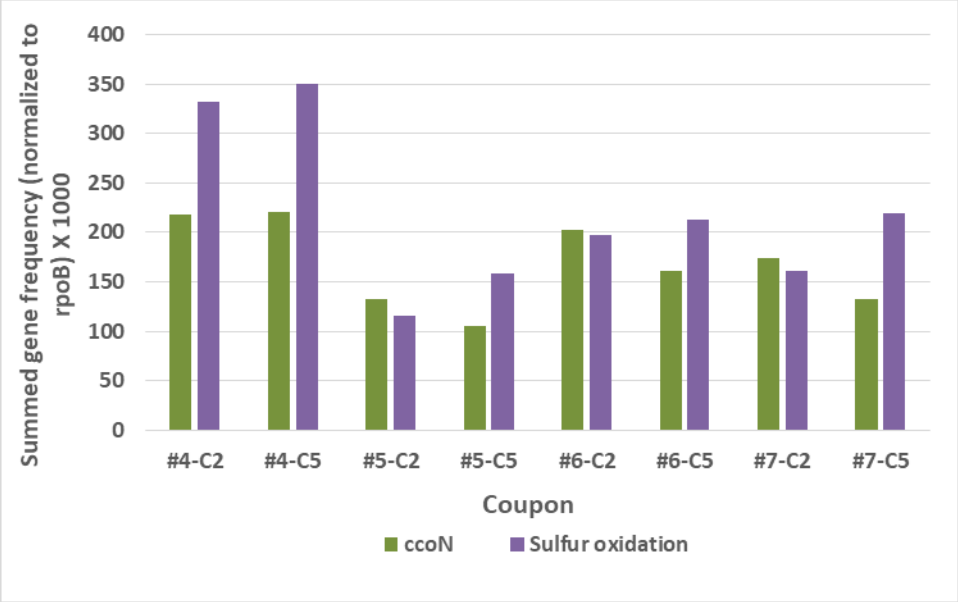

Figure 8. Summed frequencies of genes involved in sulfur oxidation (*soxA, soxB, soxC, soxX, soxY* and *soxZ*) and the frequency of gene *ccoN*. Gene ccoN codes for cbb3-type cytochrome C oxidase catalytic subunit that is indicative of aerobic respiration. The frequencies were normalized to the copy number of *rpoB* gene and multiplied by 1000. One copy of *rpoB* is found per cell and therefore the number of *rpoB* genes is equivalent to the number of cells. The value presented by the bars is the number of the summed copies of the particular group of genes per 1000 cells. (See Table S2).

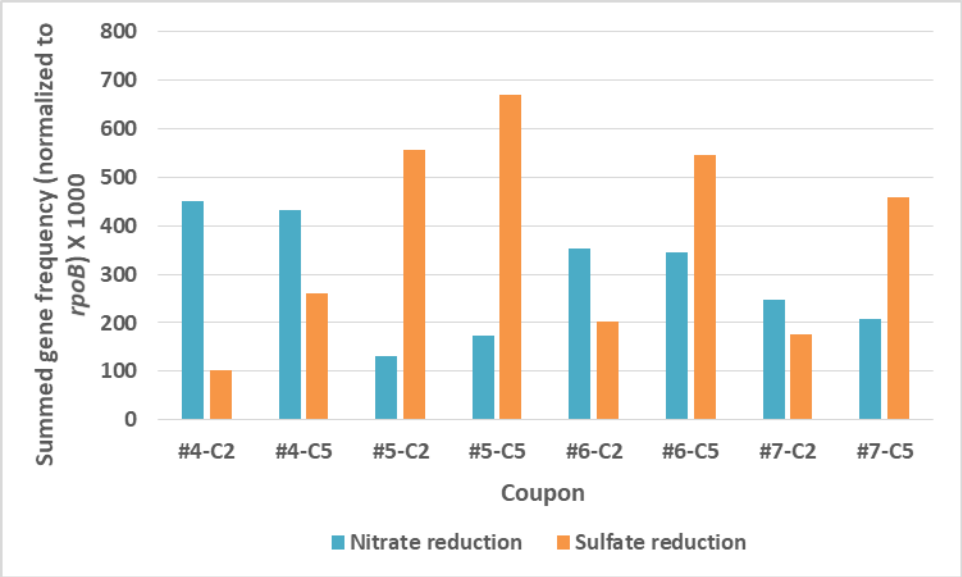

Figure 9. Summed frequencies of genes involved in nitrate/nitrite (*napA, napB, narG, narH, narI, narJ* and *nirK*) and sulfate reduction (*aprA, aprB, dsrA* and *dsrB*). The frequencies were normalized to the copy number of *rpoB* gene and multiplied by 1000. One copy of *rpoB* is found per cell and therefore the number of *rpoB* genes is equivalent to the number of cells. The value presented by the bars is the number of the summed copies of the particular group of genes per 1000 cells. (See Tables S3 and S4).

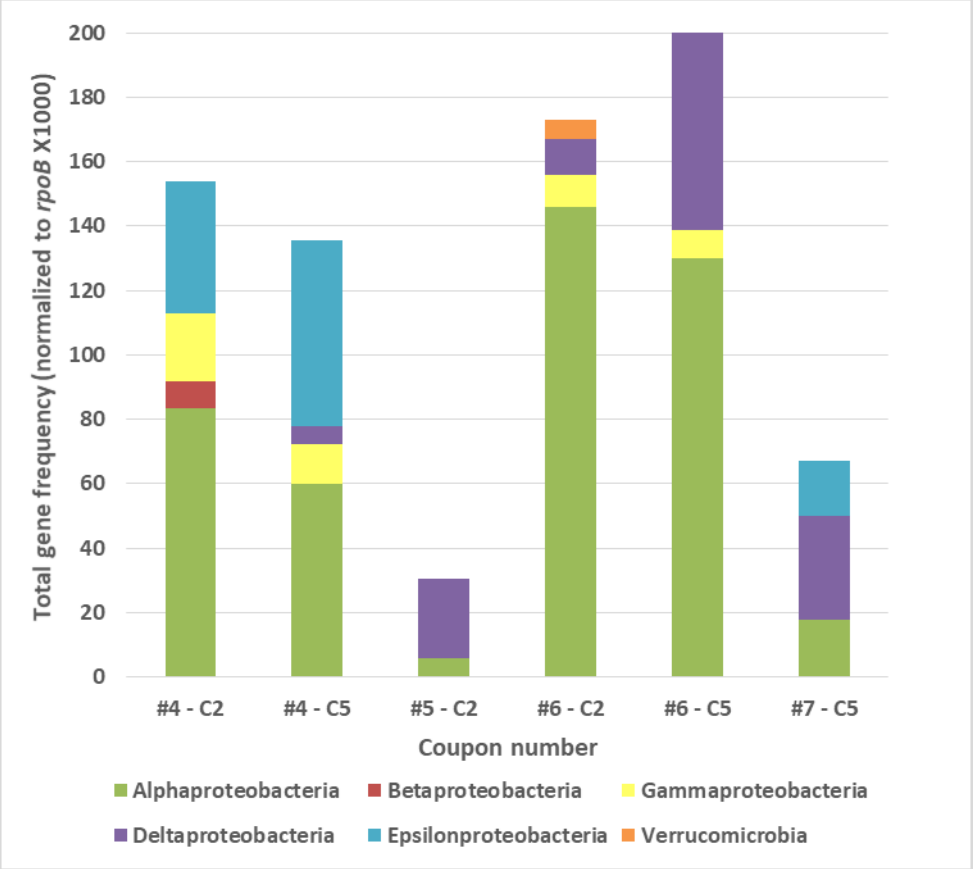

Figure 10. Taxonomic analysis of nitrate/nitrite reduction genes (*napA, napB, narG, narH, narI, narJ and nirK*) in metagenomic data of biofilm samples and the amounts of gene frequencies belonging to the dominant bacterial groups. Genes with copy numbers higher than ten of a particular organism ID were compared to NCBI database and the identities of the best matches were obtained. The frequencies of each gene found in the identified dominant organisms (with copy number higher than 10) were normalized to the copy number of *rpoB* gene and multiplied by 1000. The normalized values were summed to obtain the total copy number belonging to dominant organisms for each bacterial group. The value presented by the bars is the number of copies of the particular group of genes per 1000 cells. Analysis of coupon #5-C5 could not be completed due to issues with metagenomic analysis pipeline. There were no organisms with more than 10 copy numbers of the analyzed genes for coupon #7-C2. (See Table S5).

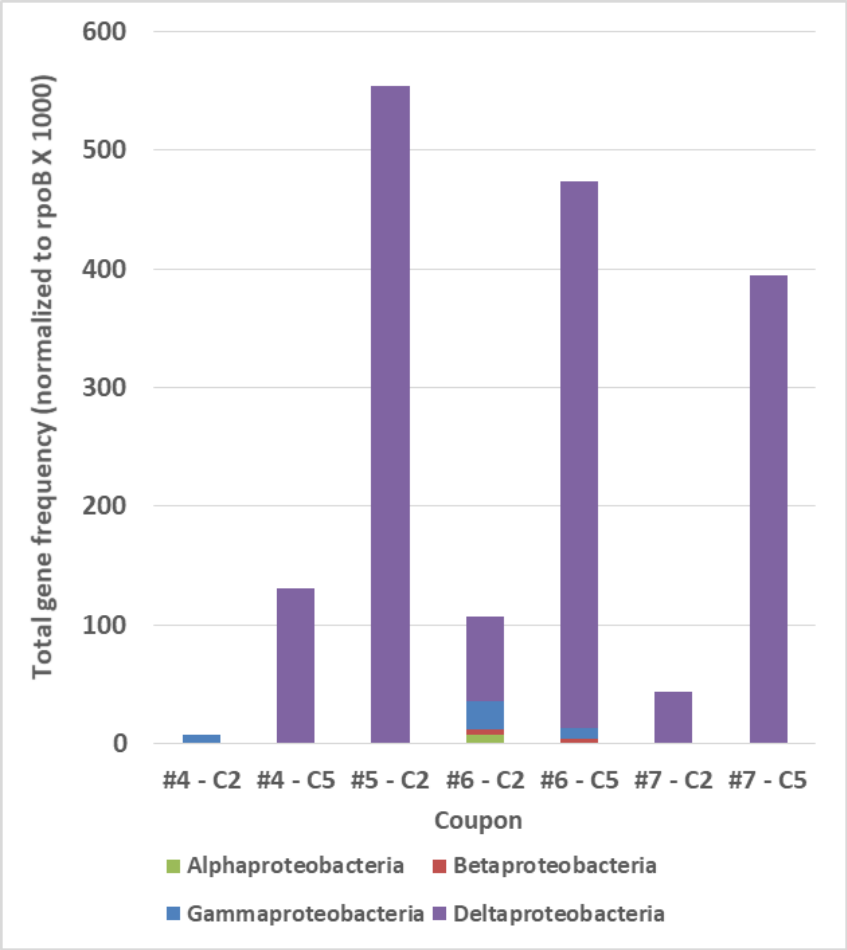

Figure 11. Taxonomic analysis of sulfate reduction genes (*aprA, aprB, dsrA,* dsrB) in metagenomic data of biofilm samples and the amounts of gene frequencies belonging to the dominant bacterial groups. Genes with copy numbers higher than ten of a particular organism ID were compared to NCBI database and the identities of the best matches were obtained. The frequencies of each gene found in the identified dominant organisms (with copy number higher than 10) were normalized to the copy number of *rpoB* gene and multiplied by 1000. The normalized values were summed to obtain the total copy number belonging to dominant organisms for each bacterial group. The value presented by the bars is the number of copies of the particular group of genes per 1000 cells. Analysis of coupon #5-C5 could not be completed due to issues with metagenomic analysis pipeline. (See Table S6)

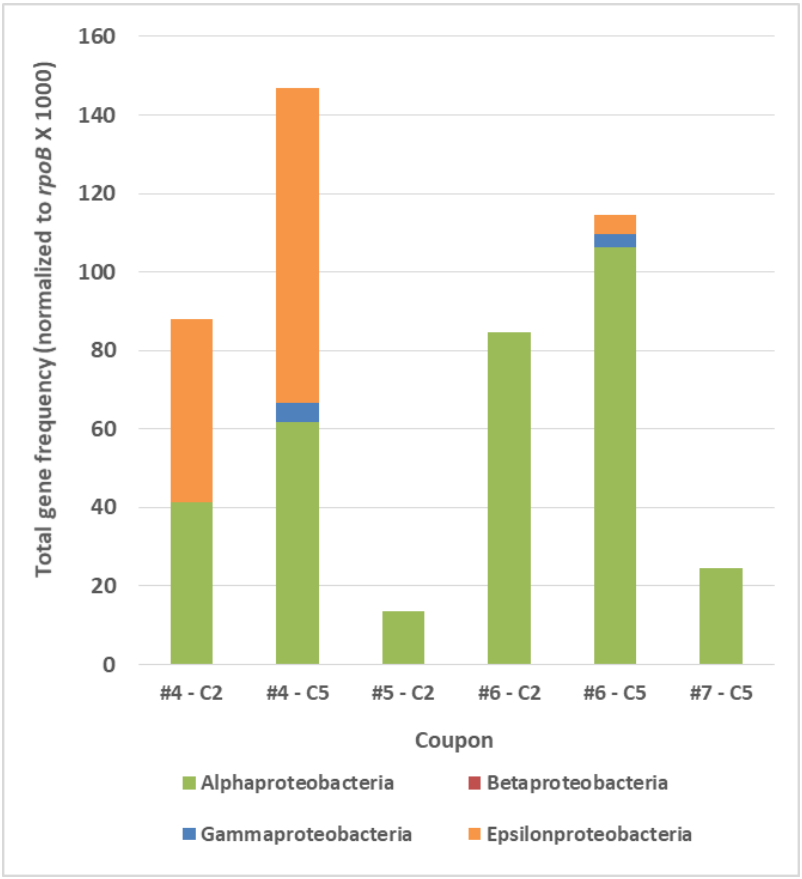

Figure 12. Taxonomic analysis of sulfur/sulfide oxidation genes (*soxA, soxB, soxC, soxX, soxY* and *soxZ*) in metagenomic data of biofilm samples and the amounts of gene frequencies belonging to the dominant bacterial groups. Genes with copy numbers higher than ten of a particular organism ID were compared to NCBI database and the identities of the best matches were obtained. The frequencies of each gene found in the identified dominant organisms (with copy number higher than 10) were normalized to the copy number of *rpoB* gene and multiplied by 1000. The normalized values were summed to obtain the total copy number belonging to dominant organisms for each bacterial group. The value presented by the bars is the number of copies of the particular group of genes per 1000 cells. Analysis of coupon #5-C5 could not be completed due to issues with metagenomic analysis pipeline. There were no organisms with more than 10 copy numbers of the analyzed genes for coupon #7-C2. (See Table S6).

Supplementary tables and figures

Table S1. Taxonomic summary of the four sites. The taxonomic analysis was based on the 16S reads extracted from metagenomes and analyzing using Qiime (version 1.8.0). The abundance of each group is given relative to the total number of reads.

Coupon	#4-C2	#4-C5	#5-C2	#5-C5	#6-C2	#6-C5	#7-C2	#7-C5
All Eukaryotes (%)	73.0	53.0	44.0	27.0	12.0	8.0	79.0	43.0
All bacteria (%)	27.0	47.0	56.0	73.0	88.0	92.0	21.0	57.0
Cyanobacteria (%)	0.3	0.5	6.2	4.4	3.5	1.8	5.7	6.8
Proteobacteria (%)	22.7	39.5	39.2	56.2	65.1	75.4	12.8	43.3
Alphaproteobacteria (%)	9.5	9.4	6.7	6.6	31.7	21.2	4.8	13.1
Gammaproteobacteria (%)	3.5	5.2	5.0	3.7	17.6	7.4	2.1	2.9
Deltaproteobacteria (%)	1.9	11.3	23.5	38.7	13.2	42.3	3.2	22.2
Epsilonproteobacteria (%)	3.2	7.5	2.8	5.8	0.4	1.8	2.5	5.1
Zetaproteobacteria (%)	4.6	5.6	0.5	0.7	1.8	1.8	0.1	0.1

Table S2. Frequency of sulfur oxidizing genes (normalized to rpoB gene frequency x 1000). The genes interrogated were L-cysteine S-thiosulfotransferase - soxAX complex (soxA,soxX), S-sulfosulfanyl-L-cysteine sulfohydrolase (soxB), sulfane dehydrogenase subunit (soxC) and sulfur oxidizing complex (soxY, soxZ).

COUPON	*SOXA*	*SOXB*	*SOXC*	*SOXX*	*SOXY*	*SOXZ*	TOTAL
#4-C2	38.1	124.2	79.5	19.7	42.0	28.9	332.5
#4-C5	37.4	121.3	87.0	16.2	63.1	25.2	350.3
#5-C2	14.8	42.2	25.7	1.6	21.9	9.9	116.1
#5-C5	18.5	46.6	36.3	6.2	34.3	16.1	158.0
#6-C2	24.2	59.5	48.4	10.5	40.2	14.1	196.7
#6-C5	28.3	67.8	53.8	9.4	37.7	16.1	213.3
#7-C2	20.9	49.9	48.3	14.5	17.7	9.7	161.0
#7-C5	23.2	68.7	56.0	17.2	40.3	14.2	219.6

Table S3. **Frequency of nitrate/nitrite reducing genes** (normalized to *rpoB* gene frequency x 1000). The genes interrogated were periplasmic nitrate reductase catalytic subunit (*napA*), beta subunit (*napB*), respiratory nitrate reductase alpha/catalytic subunit (*narG*), beta subunit (*narH*), gamma subunit (*narI*), delta subunit (*narJ*), nitrite reductase (*nirK*).

COUPON	*NAPA*	*NAPB*	*NARG*	*NARH*	*NARI*	*NARJ*	*NIRK*	TOTAL
#4-C2	160.3	13.1	125.5	48.6	26.9	11.2	64.4	450.1
#4-C5	138.9	26.6	124.0	43.3	31.6	14.9	52.8	431.9
#5-C2	30.7	4.9	24.6	20.8	41.1	2.7	5.5	130.3
#5-C5	50.1	8.6	31.9	17.1	51.8	4.8	9.3	173.5
#6-C2	115.7	7.2	106.5	48.0	34.3	10.8	29.4	352.0
#6-C5	88.2	4.9	115.6	59.9	48.7	15.8	12.5	345.6
#7-C2	61.2	9.7	69.2	38.6	30.6	6.4	30.6	246.4
#7-C5	65.7	6.0	39.6	21.7	59.0	6.0	9.7	207.6

Table S4. Frequency of sulfate reducing genes (normalized to *rpoB* gene frequency x 1000). The genes interrogated were adenylylsulfate reductase catalytic subunit (*aprA*), beta subunit (*aprB*), dissimilatory sulfite reductase catalytic/alpha subunit (*dsrA*) and beta subunit (*dsrB*).

COUPON	*APRA*	*APRB*	*DSRA*	*DSRB*	TOTAL
#4-C2	42.7	17.7	15.8	26.9	103.2
#4-C5	117.2	29.8	65.8	48.7	261.5
#5-C2	233.8	49.8	142.9	128.1	554.8
#5-C5	262.9	60.3	181.7	163.2	668.2
#6-C2	85.3	21.6	48.7	47.7	203.3
#6-C5	212.4	68.1	135.1	128.7	544.3
#7-C2	87.0	19.3	33.8	37.0	177.1
#7-C5	194.9	39.6	110.5	112.0	457.1

Table S5. Taxonomic analysis of nitrogen cycling gene hits (*napA, napB, narG,narH, narI, narJ and nirK*) in metagenomic data biofilm samples. Genes with hits higher than ten were compared to NCBI database and the identities of the best matches were classified to their major groups. Oxygen tolerance group: (A) Aerobic (FA) facultative anaerobic (AN) obligate anaerobic.

coupon		Taxonomic identity	gene frequency normalized to *rpoB* x 1000						
			napA	***napB***	***narG***	***narH***	***narI***	***narJ***	***nirK***
#4 - C2	Alphaproteobacteria	*Leisingera methylohalidivorans* (A)	7.9						
		Paracoccus denitrificans (FA)			15.1				
		Roseobacter denitrificans (FA)			36.1	24.3			
	Betaproteobacteria	*Nitrosomonas sp.* (A)							8.5
	Gammaproteobacteria	*Pseudomonas entomophila* (A)							11.2
		Shewanella sediminis (FA)			9.9				
	Epsilonproteobacteria	*Sulfurimonas autotrophica* (FA)	7.2						
		Sulfurimonas denitrificans (FA)	7.9						
		Sulfurimonas gotlandica (FA)	25.6						
#4 - C5	Alphaproteobacteria	*Brucella melitensis* (A)			5.0				
		Ochrobactrum anthropi (A)			8.6				
		Paracoccus denitrificans (FA)			5.4				
		Pseudovibrio sp. (FA)			7.7				
		Roseobacter denitrificans (FA)			26.6	6.8			
	Gammaproteobacteria	*Shewanella halifaxensis* (FA)			5.4				
		Shewanella sediminis (FA)			6.8				
	Deltaproteobacteria	*Desulfovibrio alaskensis G20* (AN)					5.9		
	Epsilonproteobacteria	*Arcobacter sp.* (FA)	6.8						
		Sulfurimonas denitrificans (FA)	6.8						
		Sulfurimonas gotlandica (FA)	31.1	13.1					
#5 - C2	Alphaproteobacteria	*Ochrobactrum anthropi* (A)			6.0				
	Deltaproteobacteria	*Desulfovibrio vulgaris Hildenborough* (AN)					15.9		
		Desulfovibrio vulgaris Miyazaki F (AN)					8.8		
#6 - C2	Alphaproteobacteria	*Azorhizobium caulinodans* (A)			3.6				
		Brucella melitensis (A)			12.1	4.6			
		Dinoroseobacter shibae (FA)	19.9						
		Hyphomonas neptunium (A)			3.6	4.9			
		Methylobacterium radiotolerans (A)			4.2				
		Ochrobactrum anthropi (A)			17.6	9.2		4.2	
		Paracoccus denitrificans (FA)			5.9	3.6			
		Pseudovibrio sp. (FA)			9.2				
		Rhodobacter sphaeroides (FA)	5.9						
		Roseobacter denitrificans (FA)			11.8	7.5	3.6		
		Ruegeria pomeroyi (A)							8.5
		Tistrella mobilis (A)			5.9				
	Gammaproteobacteria	*Saccharophagus degradans* (A)	4.2						
		Simiduia agarivorans (FA)	5.9						
	Deltaproteobacteria	*Desulfocapsa sulfexigens* (AN)	3.9						
		Sorangium cellulosum (AN)	7.2						
	Verrucomicrobia	*Coraliomargarita akajimensis* (A)	5.9						
#6 - C5	Alphaproteobacteria	*Brucella melitensis* (A)			15.5	12.2			
		Dinoroseobacter shibae (FA)	5.2						
		Hyphomonas neptunium (A)			7.6	4.6			
		Maricaulis maris (A)					3.7		
		Ochrobactrum anthropi (A)			27.4	11.0		8.5	
		Paracoccus denitrificans (FA)			4.0				
		Pseudovibrio sp. (FA)			9.4				
		Roseobacter denitrificans (FA)			12.2				
		Tistrella mobilis (A)			5.2	4.0			
	Gammaproteobacteria	*Alteromonas macleodii* (A)			4.9				
		Hahella chejuensis (A)			3.7				
	Deltaproteobacteria	*Desulfovibrio alaskensis G20* (AN)					10.3		
		Desulfovibrio desulfuricans (AN)	19.8						
		Desulfovibrio gigas (AN)					9.7		
		Desulfovibrio vulgaris Hildenborough (AN)					8.5		
		Anaeromyxobacter dehalogenans (FA)	3.3						
		Sorangium cellulosum (AN)	5.2						
		Thermodesulfatator indicus (AN)	4.3						
#7 - C5	Alphaproteobacteria	*Dinoroseobacter shibae* (FA)	9.0						
		Roseobacter denitrificans (FA)			8.2				
	Deltaproteobacteria	*Desulfovibrio alaskensis G20* (AN)					17.2		
		Desulfovibrio vulgaris Miyazaki F (AN)					14.9		
	Epsilonproteobacteria	*Sulfurimonas gotlandica* (FA)	17.2						

Table S6. Taxonomic analysis of sulfur cycling gene hits (*aprA, aprB, dsrA, dsrB, soxA, soxB, soxC, soxX, soxY and soxZ*) in metagenomic data of biofilm samples. Genes with hits higher than ten were compared to NCBI database and the identities of the best matches were classified to their major groups. Oxygen tolerance group: (A) Aerobic (FA) facultative anaerobic (AN) obligate anaerobic.

Coupon		Taxonomic identity	gene frequency normalized to rpoB x 1000									
			aprA	*aprB*	*dsrA*	*dsrB*	*soxA*	*soxB*	*soxC*	*soxX*	*soxY*	*soxZ*
#4 - C2	Alphaproteobacteria	*Leisingera methylohalidivorans* (A)						11.2				
		Phaeobacter gallaeciensis (FA)						7.9				
		Roseobacter denitrificans (FA)						12.5				
		Ruegeria pomeroyi (A)							9.9			
	Gammaproteobacteria	*Thioalkalivibrio sp.* (FA)	7.2									
	Epsilonproteobacteria	*Sulfurimonas autotrophica* (FA)						8.5				
		Sulfurimonas gotlandica (FA)					8.5	17.7	11.8			
#4 - C5	Alphaproteobacteria	*Leisingera methylohalidivorans* (A)						6.8				
		Polymorphum gilvum (FA)						12.2				
		Pseudovibrio sp. (FA)					7.7		5.9			
		Roseobacter denitrificans (FA)						11.7			5.4	
		Ruegeria pomeroyi (A)						5.0	7.2			
	Gammaproteobacteria	*Thiomicrospira crunogena* (A)							5.0			
	Deltaproteobacteria	*Desulfobacterium autotrophicum* (AN)	5.4									
		Desulfohalobium retbaense (AN)	5.0									
		Desulfovibrio aespoeensis (AN)	6.8		5.0	15.3						
		Desulfovibrio alaskensis G2(AN)	15.3									
		Desulfovibrio piezophilus (AN)	22.1		17.6	6.3						
		Desulfovibrio salexigens (AN)			5.4							
		Desulfovibrio sp. (AN)	14.9		5.9							
		Desulfovibrio vulgaris Hildenborough (AN)			6.3							
	Epsilonproteobacteria	*Sulfurimonas autotrophica* (FA)						5.0				
		Sulfurimonas gotlandica (FA)					5.0	36.5	15.8		12.2	
		Sulfurovum sp. (FA)							5.9			
#5 - C2	Alphaproteobacteria	*Polymorphum gilvum* (FA)						13.7				
	Deltaproteobacteria	*Desulfovibrio vulgaris Hildenborough* (AN)	14.2									
		Desulfovibrio alaskensis G2 (AN)	7.7		9.4							
		Desulfovibrio salexigens (AN)	18.6									
		Desulfovibrio aespoeensis (AN)	22.5		22.5	32.3						
		Desulfovibrio sp. (AN)	98.6	3.1	69.6	4.5						
		Desulfotignum phosphitoxidans (AN)	6.6		12.6	14.8						
		Desulfobacula toluolica (AN)	6.6									
		Desulfovibrio gigas (AN)	1.5									
		Desulfovibrio piezophilus (AN)			7.1							
		Desulfomicrobium baculatum (AN)				2.8						
#6 - C2	Alphaproteobacteria	*Dinoroseobacter shibae* (FA)									3.6	
		Ensifer meliloti (A)									6.2	
		Leisingera methylohalidivorans (A)							4.9			
		Planktomarina temperata (FA)					4.9			4.2		
		Polymorphum gilvum (FA)						15.7	7.2			
		Pseudovibrio sp. (FA)					4.2		9.2			3.9
		Rhodomicrobium vannielii (AN)			3.6	4.2						
		Roseobacter denitrificans (FA)						4.9			5.9	
		Ruegeria pomeroyi (A)						5.6				
		Xanthobacter autotrophicus (A)							4.2			
	Betaproteobacteria	*Thiobacillus denitrificans* (FA)	4.6									
	Gammaproteobacteria	*Allochromatium vinosum* (AN)	9.2									
		Marichromatium purpuratum (AN)			3.9							
		Thioalkalivibrio sp. (FA)	6.2									
		Thioalkalivibrio sulfidophilus (FA)	4.2									
	Deltaproteobacteria	*Desulfovibrio piezophilus* (AN)	16.0	5.2	18.6	7.8						
		Desulfovibrio sp. (AN)	16.0		3.6	3.6						
#6 - C5	Alphaproteobacteria	*Bradyrhizobium japonicum* (FA)						3.3			4.3	
		Ensifer meliloti (A)									4.9	
		Hyphomonas neptunium (A)					5.5				3.3	
		Phaeobacter gallaeciensis (FA)					4.0					
		Planktomarina temperata (FA)					4.6		3.7			
		Polymorphum gilvum (FA)						24.9	4.6		3.3	
		Pseudovibrio sp. (FA)					7.0		7.9			6.1
		Roseobacter denitrificans (FA)									9.7	
		Ruegeria pomeroyi (A)						4.0				
		Xanthobacter autotrophicus (A)							5.2			
	Betaproteobacteria	*Thiobacillus denitrificans* (FA)	4.3									
	Gammaproteobacteria	*Allochromatium vinosum* (AN)	4.6								3.3	
		Thioalkalivibrio sulfidophilus (FA)	4.0									
	Deltaproteobacteria	*Desulfohalobium retbaense* (AN)	5.2									
		Desulfovibrio aespoeensis (AN)	22.2	23.7	15.8	56.3						
		Desulfovibrio piezophilus (AN)	84.9	28.0	87.9	39.9						
		Desulfovibrio salexigens (AN)	7.3									
		Desulfovibrio sp. (AN)	57.5	7.9	12.8	11.3						
	Epsilonproteobacteria	*Sulfurimonas autotrophica* (FA)							4.9			
#7 - C2	Deltaproteobacteria	*Desulfotignum phosphitoxidans* (AN)	25.8			17.7						
#7 - C5	Alphaproteobacteria	*Polymorphum gilvum* (FA)						11.9	12.7			
	Deltaproteobacteria	*Desulfobacterium autotrophicum* (AN)	38.8	2.2	1.5	23.2						
		Desulfotignum phosphitoxidans (AN)	96.3	11.2	65.0	52.3						
		Desulfobacula toluolica (AN)	29.1		16.4	21.7						
		Desulfohalobium retbaense (AN)				9.8						

Table S7. Phylogenetic analysis of nitrogen cycling genes (*napA, napB, narG, narH, narI, narJ and nirK*) in metagenomic data of biofilm samples extracted from each coupon. Identities of the best matches were classified to their major groups and dominant organisms were identified.

	Alpha-proteobacteria	Beta-proteobacteria	Gamma-proteobacteria	Delta-proteobacteria	Epsilon-proteobacteria	Verrucomicrobia
#4 - C2	*Leisingera methylohalidivorans*	*Nitrosomonas sp.*	*Pseudomonas entomophila*		*Sulfurimonas autotrophica*	
	Paracoccus denitrificans		*Shewanella sediminis*		*Sulfurimonas denitrificans*	
	Roseobacter denitrificans				*Sulfurimonas gotlandica*	
#4 - C5	*Brucella melitensis*		*Shewanella halifaxensis*	*Desulfovibrio alaskensis G20*	*Arcobacter sp.*	
	Ochrobactrum anthropi		*Shewanella sediminis*		*Sulfurimonas denitrificans*	
	Paracoccus denitrificans				*Sulfurimonas gotlandica*	
	Pseudovibrio sp.					
	Roseobacter denitrificans					
#5 - C2	*Ochrobactrum anthropi*			*Desulfovibrio vulgaris Hildenborough*		
				Desulfovibrio vulgaris Miyazaki F		
#6 - C2	*Azorhizobium caulinodans*		*Saccharophagus degradans*	*Desulfocapsa sulfexigens*		*Coraliomargarita akajimensis*
	Brucella melitensis		*Simiduia agarivorans*	*Sorangium cellulosum*		
	Dinoroseobacter shibae					
	Hyphomonas neptunium					
	Methylobacterium radiotolerans					
	Ochrobactrum anthropi					
	Paracoccus denitrificans					
	Pseudovibrio sp.					
	Rhodobacter sphaeroides					
	Roseobacter denitrificans					
	Ruegeria pomeroyi					
	Tistrella mobilis					
#6 - C5	*Brucella melitensis*		*Alteromonas macleodii*	*Anaeromyxobacter dehalogenans*		
	Dinoroseobacter shibae		*Hahella chejuensis*	*Desulfovibrio alaskensis G20*		
	Hyphomonas neptunium			*Desulfovibrio desulfuricans*		
	Maricaulis maris			*Desulfovibrio gigas*		
	Ochrobactrum anthropi			*Desulfovibrio vulgaris Hildenborough*		
	Paracoccus denitrificans			*Sorangium cellulosum*		
	Pseudovibrio sp.			*Thermodesulfatator indicus*		
	Roseobacter denitrificans					
	Tistrella mobilis					
#7 - C5	*Dinoroseobacter shibae*			*Desulfovibrio alaskensis G20*	*Sulfurimonas gotlandica*	
	Roseobacter denitrificans			*Desulfovibrio vulgaris Miyazaki F*		

Table S8. Phylogenetic analysis of sulfur cycling genes (*aprA, aprB, dsrA, dsrB, soxA, soxB, soxC, soxX, soxY* and *soxZ*) in metagenomic data of biofilm samples extracted from each coupon. Identities of the best matches were classified to their major groups and dominant organisms were identified. The name of organisms with sox genes is underlined.

	Alpha-proteobacteria	Beta-proteobacteria	Gamma-proteobacteria	Delta-proteobacteria	Epsilon-proteobacteria
#4 - C2	*Leisingera methylohalidivorans*	*Thioalkalivibrio sp.*			*Sulfurimonas autotrophica*
	Roseobacter denitrificans				*Sulfurimonas gotlandica*
	Ruegeria pomeroyi				
#4 - C5	*Leisingera methylohalidivorans*		*Thiomicrospira crunogena*	*Desulfovibrio aespoeensis*	*Sulfurimonas autotrophica*
	Polymorphum gilvum			*Desulfovibrio alaskensis G20*	*Sulfurimonas gotlandica*
	Pseudovibrio sp.			*Desulfovibrio piezophilus*	
	Roseobacter denitrificans			*Desulfovibrio sp.*	
	Ruegeria pomeroyi			*Desulfovibrio vulgaris Hildenborough*	
#5 - C2	*Polymorphum gilvum*			*Desulfovibrio vulgaris Hildenborough*	
				Desulfovibrio alaskensis G20	
				Desulfovibrio salexigens	
				Desulfovibrio aespoeensis Aspo-2	
				Desulfovibrio sp. ND132	
				Desulfotignum phosphitoxidans	
				Desulfobacula toluolica	
				Desulfovibrio gigas	
				Desulfovibrio piezophilus	
				Desulfomicrobium baculatum	
#6 - C2	*Leisingera methylohalidivorans*	*Thiobacillus denitrificans*	*Allochromatium vinosum*	*Desulfovibrio aespoeensis*	
	Ensifer meliloti		*Marichromatium purpuratum*	*Desulfovibrio piezophilus*	
	Planktomarina temperata		*Thioalkalivibrio sp.*	*Desulfovibrio sp.*	
	Polymorphum gilvum		*Thioalkalivibrio sulfidophilus*		
	Pseudovibrio sp.				
	Rhodomicrobium vannielii				
	Roseobacter denitrificans				
	Ruegeria pomeroyi				
#6 - C5	*Allochromatium vinosum*	*Thiobacillus denitrificans*	*Thioalkalivibrio sulfidophilus*	*Desulfovibrio aespoeensis*	*Sulfurimonas autotrophica*
	Bradyrhizobium japonicum			*Desulfovibrio piezophilus*	
	Ensifer meliloti			*Desulfovibrio salexigens*	
	Hyphomonas neptunium			*Desulfovibrio sp.*	
	Polymorphum gilvum				
	Pseudovibrio sp.				
	Roseobacter denitrificans				
	Ruegeria pomeroyi				
#7 - C2				*Desulfotignum phosphitoxidans*	
#7 - C5	*Polymorphum gilvum*			*Desulfobacterium autotrophicum*	
				Desulfotignum phosphitoxidans	
				Desulfobacula toluolica	
				Desulfohalobium retbaense	

References

Andrews, S. (2010). FastQC: a quality control tool for high throughput sequence data. Available online at: http://www.bioinformatics.babraham.ac.uk/projects/fastqc

Beech, I. B., and Sunner, J. (2004). Biocorrosion: towards understanding interactions between biofilms and metals. *Current Opinion in Biotechnology*, *15*(3), 181-186.

Ben-Dov, E., Brenner, A., Kushmaro, A. (2007). Quantification of sulfate-reducing bacteria in industrial wastewater, by real-time polymerase chain reaction (PCR) using dsrA and apsA genes. *Microbial ecology*, *54*(3), 439-451.

Boisvert, S., Laviolette, F., and Corbeil, J. (2010). Ray: simultaneous assembly of reads from a mix of high-throughput sequencing technologies. *Journal of Computational Biology*, *17*(11), 1519-1533.

Boisvert, S., Raymond, F., Godzaridis, É., Laviolette, F., and Corbeil, J. (2012). Ray Meta: scalable de novo metagenome assembly and profiling. *Genome Biology*, *13*(12), R122.

Bolger, A. M., Lohse, M., and Usadel, B. (2014). Trimmomatic: a flexible trimmer for Illumina sequence data. *Bioinformatics*, *30*(15), 2114-2120.

Caporaso, J. G., Bittinger, K., Bushman, F. D., DeSantis, T. Z., Andersen, G. L., and Knight, R. (2010). PyNAST: a flexible tool for aligning sequences to a template alignment. *Bioinformatics*, *26*(2), 266-267.

Celikkol-Aydin, S., Gaylarde, C. C., Lee, T., Melchers, R. E., Witt, D. L., and Beech, I. B. (2016). 16S rRNA gene profiling of planktonic and biofilm microbial populations in the Gulf of Guinea using Illumina NGS. *Marine Environmental Research*, *122*, 105-112.

Dall'Agnol, L. T., and Moura, J. J. G. (2014). Sulphate-reducing bacteria (SRB) and biocorrosion. *Understanding Biocorrosion: Fundamentals and Applications*, 77.

Edgar, R. C. (2010). Search and clustering orders of magnitude faster than BLAST. *Bioinformatics*, *26*(19), 2460-2461.

Fontaine, E., Rosen, J., Potts, A., Ma, K. T., and Melchers, R. (2014, May). SCORCH JIP-Feedback on MIC and Pitting Corrosion from Field Recovered Mooring Chain Links. In *Offshore Technology Conference*. Offshore Technology Conference.

Garcia, H. E., R. A. Locarnini, T. P. Boyer, J. I. Antonov, O.K. Baranova, M.M. Zweng, J.R. Reagan, D.R. Johnson, 2014. World Ocean Atlas 2013, Volume 3*: Dissolved Oxygen, Apparent Oxygen Utilization, and Oxygen Saturation.* S. Levitus, Ed., A. Mishonov Technical Ed.; NOAA Atlas NESDIS 75, 27 pp.

Haveman, S. A., Greene, E. A., Stilwell, C. P., Voordouw, J. K., and Voordouw, G. (2004). Physiological and gene expression analysis of inhibition of *Desulfovibrio vulgaris Hildenborough* by nitrite. *Journal of Bacteriology*, *186*(23), 7944-7950.

Heinz, S., Benner, C., Spann, N., Bertolino, E., Lin, Y. C., Laslo, P., ... & Glass, C. K. (2010). Simple combinations of lineage-determining transcription factors prime cis-regulatory elements required for macrophage and B cell identities. *Molecular cell*, *38*(4), 576-589.

http://www.bioinformatics.babraham.ac.uk/projects/trim_galore/

Hyatt, D., LoCascio, P. F., Hauser, L. J., and Uberbacher, E. C. (2012). Gene and translation initiation location prediction in metagenomic sequences. *Bioinformatics*, *28*(17), 2223-2230.

Lahme, A., & Hubert, C. (2017). Corrosion risks associated with (bio) chemical processes in sour systems due to nitrate injection or oxygen ingress. *Microbiologically Influenced Corrosion in the Upstream Oil and Gas Industry*.

Lahme, S., Enning, D., Callbeck, C. M., Vega, D. M., Curtis, T. P., Head, I. M., & Hubert, C. R. (2019). Metabolites of an oil field sulfide-oxidizing, nitrate-reducing Sulfurimonas sp. cause severe corrosion. *Appl. Environ. Microbiol.*, *85*(3), e01891-18.

Lee, T. and and Kilner, A (2016). CTR 12402: Integrity Management of Mooring Systems against Corrosion Working Committee Technical Discussion [*PowerPoint Presentation*].

Lewandowski, Z. (2000). MIC and biofilm heterogeneity. *Proceedings of Corrosion*, *400*, 1-7.

Little, B. J., Ray, R. I., and Pope, R. K. (2000). Relationship between corrosion and the biological sulfur cycle: a review. *Corrosion*, *56*(4), 433-443.

Locarnini, R. A., A. V. Mishonov, J. I. Antonov, T. P. Boyer, H. E. Garcia, O. K. Baranova, M. M. Zweng, C. R. Paver, J. R. Reagan, D. R. Johnson, M. Hamilton, and D. Seidov, 2013. World Ocean Atlas 2013, Volume 1: *Temperature*. S. Levitus, Ed., A. Mishonov Technical Ed.; NOAA Atlas NESDIS 73, 40 pp.

Marietou, A. (2016). Nitrate reduction in sulfate-reducing bacteria. *FEMS microbiology letters*, *363*(15), fnw155.

Marietou, A., Richardson, D., Cole, J., and Mohan, S. (2005). Nitrate reduction by *Desulfovibrio desulfuricans*: a periplasmic nitrate reductase system that lacks NapB, but includes a unique tetraheme c-type cytochrome, NapM. *FEMS Microbiology Letters*, *248*(2), 217-225.

Martin, M. (2011). Cutadapt removes adapter sequences from high-throughput sequencing reads. *EMBnet. Journal*, *17*(1), 10-12.

Melchers, R. E. (2003). Modeling of marine immersion corrosion for mild and low-alloy steels—Part 1: Phenomenological model. *Corrosion*, *59*(4), 319-334.

Melchers, R. E. (2007). Transition from marine immersion to coastal atmospheric corrosion for structural steels. *Corrosion*, *63*(6), 500-514.

Melchers, R. E. (2010). Transient early and longer term influence of bacteria on marine corrosion of steel. *Corrosion Engineering, Science and Technology*, *45*(4), 257-261.

Melchers, R. E. (2014). Long-term immersion corrosion of steels in seawaters with elevated nutrient concentration. *Corrosion Science*, *81*, 110-116.

Melchers, R. E., and Jeffrey, R. (2011). Bacteria have transient influences on marine corrosion of steel.

Melchers, R. E., and Jeffrey, R. (2012). Corrosion of long vertical steel strips in the marine tidal zone and implications for ALWC. *Corrosion Science*, *65*, 26-36.

Melchers, R. E., and Jeffrey, R. J. (2013). Accelerated low water corrosion of steel piling in harbours. *Corrosion Engineering, Science and Technology*, *48*(7), 496-505.

NOAA. How far does light travel in the ocean? National ocean service weblocation, https://oceanservice.noaa.gov/facts/light_travel.html, accessed on 4/21/2019.

Price, M. N., Dehal, P. S., and Arkin, A. P. (2010). FastTree 2–approximately maximum-likelihood trees for large alignments. *PloS One*, *5*(3), e9490.

Quast, C., Pruesse, E., Yilmaz, P., Gerken, J., Schweer, T., Yarza, P., ... and Glöckner, F. O. (2013). The SILVA ribosomal RNA gene database project: improved data processing and web-based tools. *Nucleic Acids Research*, *41*(D1), D590-D596.

Rosen, J., Potts, A. E., and Melchers, R. E. (2014, September). MIC and pitting corrosion on field recovered mooring chain links. In *Proceedings of the Corrosion and Prevention Conference, Australian Corrosion Association, Darwin* (pp. 21-24).

Standard, N. A. C. E. (2005). Preparation, Installation, Analysis, and Interpretation of Corrosion Coupons in Oilfield Operations. *Houston, TX: NACE (National Association of Corrosion Engineers) International*.

Vigneron, A., Alsop, E. B., Lomans, B. P., Kyrpides, N. C., Head, I. M., & Tsesmetzis, N. (2017). Succession in the petroleum reservoir microbiome through an oil field production lifecycle. *The ISME journal*, *11*(9), 2141.

Vigneron, A., Head, I. M., & Tsesmetzis, N. (2018). Damage to offshore production facilities by corrosive microbial biofilms. *Applied microbiology and biotechnology*, *102*(6), 2525-2533.

Witt, D., Ma, K.-T., Lee, T., Gaylarde, C., Celikkol, S., Makama, Z., & Beech, I. (2016, May 2). Field Studies of Microbiologically Influenced Corrosion of Mooring Chains. Offshore Technology Conference. doi:10.4043/27142-MS

Wu, Y. W., Tang, Y. H., Tringe, S. G., Simmons, B. A., and Singer, S. W. (2014). MaxBin: an automated binning method to recover individual genomes from metagenomes using an expectation-maximization algorithm. *Microbiome*, *2*(1), 26.

Chapter 2

Effect of *Marinobacter hydrocarbonoclasticus* SP17 biofilms on corrosion of 1018 carbon steel in the presence of nitrate

Abstract

Microbiologically influenced corrosion (MIC) is of global concern due to its economic, social as well as human health consequences. Pollution of coastal waters from land-based sources, mainly agricultural runoff, can lead to increase of nutrients, particularly nitrate. The effect of nutrient availability on MIC has been studied extensively but conclusions from different studies are contradictory; e.g. some research show nutrients increase MIC while the others conclude increased nutrient levels lessen MIC. The current study investigated the effect of *Marinobacter hydrocarbonoclasticus* SP17 cells on the corrosion of 1018 carbon steel. Carbon steel coupons were exposed to medium containing *Marinobacter* cells that was amended with nitrate or ammonium as the nitrogen source and incubated under aerated (unsealed) or oxygen limited (sealed) conditions for 6 weeks. *Marinobacter* formed a biofilm on the coupons, as shown by recovery of viable cells from the coupons. The weight loss of coupons with biofilm was significantly lower than the abiotic controls regardless of the nitrogen source or oxygen supply status. The coupon weight loss difference was significantly less in sealed (oxygen-restricted) incubation systems compared to unsealed irrespective of presence of biofilm cover. The amount of ferrous iron dissolution from the coupons was also lower in the presence of biofilm compared to the abiotic control treatment regardless of the nitrogen source or oxygen supply. The observations are consistent with the hypothesis that *Marinobacter* biofilm protects 1018 carbon steel under aerobic conditions by reducing the amount of oxygen that would otherwise interact with the coupon surface. Further, these observations do not support previous observations of enhanced corrosion in the presence of elevated levels of nitrate compared to ammonium.

Introduction

The consequences of metal corrosion are a global issue and include major economic, environmental and human health implications (Kilbane and Lamb, 2005; Videla and Herera, 2005). Currently, methods for controlling MIC are costly and are not efficient in controlling and/or inhibiting the growth of microbes. Hence, attempts have been targeted towards environment-friendly, effective and yet much more specific MIC control measures.

Microbiologically influenced corrosion or MIC has been defined as the deterioration of metal caused by the presence or the activities of microorganisms adhering to the surface (Beech *et al.,* 2000). Microbes can interact with the environment/metal surface in many different ways (Dall'Agnol and Moura, 2014) and therefore the mechanism of MIC cannot be linked to a single reaction, process or a species of microorganisms (Kip and van Veen, 2015). The microorganisms associated with MIC include sulfate reducing bacteria (SRBs), archaea, methanogens, acetogenic bacteria, nitrate reducing bacteria, metal oxidizing bacteria and metal reducing bacteria. Sulfate-reducing bacteria are considered to be the major causative group under anoxic conditions (i.e. pipelines, fuel storage facilities, ballast tanks etc.) and have been most extensively studied (Beech and Sunner, 2004; Dall'Agnol and Moura, 2014). Corrosion of steel in intermittently oxygenated marine waters (e.g. Accelerated Low Water Corrosion, ALWC) is also of great concern (Melchers, 2014b; Melchers and Jeffrey, 2012). Metal structures exposed to the euphotic zone of warm, oxygenated sea water experience a great deal of corrosion that becomes a threat to the stability of these structures (Melchers, 2019). Although sulfate reducing bacteria (SRBs) are traditionally considered a major culprit in MIC, anaerobic microorganisms are unlikely to be abundant initially in ALWC due to the oxygenated sea water environment.

Based on the analyses of steel pilings exposed for long periods to coastal waters, an empirical multi-phase phenomenological model of steel corrosion in sea water was formulated by Professor Robert Melchers (Melchers, 2003). The model has five phases with two periods of bacterial activity (Melchers, 2010; Melchers and Jeffrey, 2011). Once the metal is exposed to sea water, metal surface is colonized with marine organisms. The corrosion is aerobic with non-linear kinetics, influenced by a combination of chemical and bacterial activity. This first phase of bacterial activity can make a significant contribution to corrosion, especially if the nutrient supply is not limited. The model assumes that bacterial

activity/metabolism depends on the available nutrient supply, and in particular on the dissolved inorganic nitrogen (DIN) pool size (Melchers, 2014b). Influence during the first period of bacterial activity on corrosion mass loss has been implicated with field data (Melchers, 2007; Melchers and Jeffrey, 2011) as well as laboratory experiments (Lee *et al.,* 1995).

A number of studies provide evidence linking an increase in MIC to higher concentrations of nutrients such as DIN, but the relationship is not straightforward (Little and Lee, 2014 and references there in). Microorganisms need nutrients for growth and the uptake of nutrients can stimulate the rate of corrosion (Little, B.J. 2003; Rodin et al., 2000; Jigletsova *et al.,* 2004). Additionally, organic acids produced by fermentative bacteria can act as a nutrient for other microorganisms in the community, such as SRB, and lead to increased MIC (Mand et al., 2012). Rajasekar and Ting (2011) observed enhanced corrosion resistance in stainless steel 304 cultured together with *Bacillus megaterium* and *Pseudomonas* sp. in the presence of inorganic nitrates and phosphates. They proposed an acceleration of metabolite production in the presence of inorganic nutrients which led to the formation of a passive layer (Rajasekar and Ting, 2011). Pillay and Lin (2013) observed a reduced corrosion rate in mild steel in the presence of some bacterial isolates with 5 mM $NaNO_3$ or NH_4NO_3 under aerobic conditions compared to the bacterial isolates without addition of nitrate. Interestingly, the same study provided evidence for nitrate enhancing metal corrosion under abiotic conditions. The presence of 5 mM $NaNO_3$ or NH_4NO_3 resulted in increased corrosion rate of mild steel under aerobic conditions even in the absence of cells (Pillay and Lin, 2013).

Three mechanisms of metal corrosion inhibition by biofilms have been proposed (reviewed in Zuo, 2007; Kip and Veen, 2015) (1) removal of corrosive substances through bacterial activity/metabolism (e.g. removal of oxygen under aerobic conditions) (2) growth inhibition of corrosion-causing organisms by other organisms in the biofilm through production of antimicrobial agents and (3) formation of a protective layer (such as passivating metal oxides or extracellular polymeric substances (EPS)). A number of studies have investigated oxygen removal via respiration and/or metabolism as a possible cause of inhibition of corrosion (Pedersen and Hermansson, 1991; Jayraman *et al.,* 1997a; Jayraman *et al.,* 1999a; Ismail *et al*, 2002; Dubiel *et al.,* 2002). The observations by Dubiel and colleagues (2002) indicated microbial respiration (aerobic as well as iron respiration) as a possible key

factor reducing corrosion. Utilization of microbes secreting antimicrobial agents inhibiting the growth of corrosion-causing organisms is the second strategy (Jayraman et al., 1997a; Jayraman et al., 1997b; Jayraman et al., 1999b). Formation of a phosphate-containing protective layer was proposed as the possible mechanism of corrosion inhibition by some *Pseudomonas* spp. (Gunasekaran *et.al*., 2004; Chongdar *et.al.,* 2005) and *Shewanella oneidensis* strain MR-1 (Dubiel *et.al.,* 2002). Additionally, studies on sulfate reducing bacteria (SRBs) have shown corrosion inhibition under anaerobic conditions by EPS extracted from *Desulfovibrio alaskensis* (Stadler *et al.,* 2008; 2010).

According to Melchers' phenomenological model, the initial period of corrosion (phases 0 and 1) are governed by oxygen diffusion and bacterial activity, which in turn is a function of nutrient availability (Melchers R.E. 2010; Melchers R.E. 2014). Nitrate is one of the forms of DIN found in the marine environment and varies in concentration depending on location (Melchers, 2012; 2014). The level of nitrate in unpolluted seawater is below detection level (Garcia et al., 2014) while the locations with elevated levels of nitrate can be as high as 2 mM (Fontaine *et al.,* 2014). Pollution of coastal waters from land-based sources (mainly agricultural runoff) leads to significant increase of nutrients such as nitrate, ammonia, phosphate, sulfate as well as sulfite (Ngatia *et al.,* 2019).

As previously stated, Melchers' model was developed based largely from field data (Melchers, 2003, Melchers 2010) and the laboratory studies depicting the periods of bacterial influence (as a community) in the model (Melchers and Jeffrey, 2011; Lee *et al*., 1995). Although the bacterial influence in terms of corrosion is depicted, the mechanism behind the influence is yet to be elucidated and the presence of a bacterial community increases the complexity of the experiments and interpretation of results. To obtain a better understanding of the effect of elevated levels of nitrate on MIC and/or MIC inhibition, the behavior of a single species marine biofilm was studied. We employed *Marinobacter hydrocarbonoclasticus* SP17, a gram-negative, rod-shaped, non-spore forming bacterium (Gauthier *et.al*, 1992), as the model organism. It is a halotolerant (0.08 – 3.5mM NaCl) member of the Gammaproteobacteria and can utilize oxygen, nitrate and nitrite as electron accepters (Gauthier *et.al*, 1992). *Marinobacter* spp. are common and found in different marine habitats including coastal water, sediment, deep waters, hydrothermal vents as well as oil fields (reviewed in Handley and Lloyd, 2013).

The objective of this chapter was to investigate the effect of *Marinobacter* biofilm/activity on corrosion of 1018 carbon steel under elevated levels of nitrate. In light of the previous observations (unpublished data), we hypothesized that *Marinobacter* biofilm protects 1018 carbon steel exposed to elevated nitrate levels under aerobic conditions. Possible mechanisms inhibiting corrosion include removal of oxygen by microbial respiration/ activity, removal of products of microbial metabolism that act to corrode the metal surface.

Materials and Methods

Media and cultivation of *Marinobacter hydrocarbonoclasticus* SP17

A synthetic sea water medium modified after Widdel and Bak (1992) was used for culturing *Marinobacter hydrocarbonoclasticus* SP17 (Gauthier *et.al*, 1992). The medium contained the following components per liter: 100 ml of Widdel's 10X salt mix (NaCl, 60.0 g; $MgCl_2$, 3.0 g; $CaCl_2$, 0.5 g; Na_2SO_4, 3.0 g; KH_2PO_4, 0.2 g; KCl , 0.5 g and 10 ml of 100X RST trace metals (Tanner, 1989), 3.5g of Na_2SO_4 and 0.01 g/L of sodium lactate as the carbon source. The pH was adjusted to 7.2. The composition of trace metal solution is KOH, 2.0 g; and $MnSO_4$ .H_2O. 1.0 g; Fe $(NH_4)_2(SO_4)_2.H_2O$, 0.8 g; $CoCl_2$.$8H_2O$, 0.2g; $ZnSO_4$.$7H_2O$, 0.2 g; $CuCl_2$.$2H_2O$, 0.02 g; $NiCl_2$.$6H_2O$, 0.02 g; Na_2MoO_4 .$2H_2O$, 0.02 g; Na_2SeO_4, 0.02 g; Na_2WO_4, 0.02 g. For each 9 ml of the medium, 0.3 mL 10% $NaHCO_3$, and 1.0 mL 100x RST vitamins (Tanner 1989) were added.

The organism was streaked onto tryptic soy agar plates from -80℃ glycerol stock. Single colonies were then inoculated into 50 ml of the above mentioned medium amended with either 0.5 mM sodium nitrate or 0.5 mM ammonium chloride. The cultures were transferred three times in either the medium with nitrate or ammonium before the experiment began.

Experimental design

Experiments were conducted in 160 ml glass serum bottles with 50 ml of medium amended with either 0.5 mM sodium nitrate or 0.5 mM ammonium chloride. Biotic treatments were inoculated with 2.5 ml (5% of the total volume) of a two days old culture of *M. hydrocarbonoclasticus* SP17. Bottles were sealed with rubber stoppers and aluminium rings and the aerated bottles had a sterile needle penetrated through a rubber stopper

connecting the outside air with the headspace of the bottle through a 0.2 µm filter. The head space of the sealed bottles was flushed with N_2 for 5 minutes in order to lower the initial oxygen level. There were ten different treatments (Table S1), each treatment with five replicates. The bottles were incubated at 25^{o}C with 100 rpm shaking for 6 weeks.

Metal coupons

The metal samples used were round (diameter of 10 mm and thickness of 1 mm) 1018 carbon steel coupons (Alabama Specialty Products, Inc., Munford, AL). The coupons were cleaned prior to use in the experiment as previously described (Liang *et al*., 2014). In brief, coupons were sonicated in water individually for 15 minutes, dipped briefly in acetone and then in methanol before drying using N_2 gas. The coupons were weighed, placed in sealed serum bottles under N_2 and were autoclaved.

After the experiment ended all coupons were cleaned following ASTM standard protocol (ASTM G1-03, 2011). Coupons were dipped in coupon cleaning solution (3.5 g/l of hexamethylenetetramine (100-97-0 Sigma-Aldrich, St. Louis, MO) in 6M HCl) for 5 minutes and then in acetone and methanol. Subsequently, they were dried using N_2 gas and were weighed.

Data collection

Treatments 1 - 9 (Table S1) were sampled weekly and at the end of study after the six weeks. In order to maintain substantial volume of medium in each treatment, three replicates (a, b, c) from each treatment were sampled weekly for viable counts and, nitrate depletion measurements. The other two replicates (d, e) of each treatment were sampled weekly for dissolved oxygen and dissolved Fe (II) measurements. The replicates a, b, c of treatments 5, 6 and 9 (Table S1) were sampled for optical density (OD) measurements every week. The treatments with coupons were not sampled for OD since the corrosion products interfered with the measurements. All five replicates were sampled for nitrate depletion and coupon weight loss at the end of the study. The data of one replicate was removed from final analysis due to contamination of an abiotic bottle (Treatment 8, replicate a, contamination seen at week 5). Only weight loss data was collected for treatment 10.

Growth of *Marinobacter* during the experiment was monitored by optical density at 600nm and viable plate counts of planktonic cells. A 1:10 dilution series were made for three replicates (a, b, c) of each treatment and 100 µl were plated on tryptic soy agar (TSA). The dissolved oxygen concentration of one milliliter samples removed from each bottle was measured using the FireStingO2 fiberoptic oxygen meter (PyroScience GmbH, Aachen, Germany). Dissolved ferrous ion was measured by ferrozine assay based on a protocol previously described (Liang and Suflita, 2015). To summarize, 0.5 ml of the sample from replicates d and e were acidified with 10 µl of 37% HCl and left for 15 minutes. An aliquot (0.1 ml) of the mixture was added to 5 ml of ferrozine reagent. Ferrozine reagent consists of 1 g of (3-(2-Pyridyl)-5, 6-diphenyl-1, 2, 4-triazine-p, p'-disulfonic acid monosodium salt hydrate) in 1 L of 50mM HEPES, pH = 7.0. Nitrate depletion was analyzed on an ion chromatograph (model ICS-1100, Dionex Corp., Sunnyvale, CA) equipped with an ion-exchange column system (IonPac® AS23 4X250 mm analytical column and an IonPac® AG23 4X50 mm guard column)-(Dionex Corp., Sunnyvale, CA). The entire biofilm on replicates a, b, c coupons was scrapped into 1 ml of Widdel's aerobic medium each using a sterile flathead wooden toothpick and used for viable plate counts at the end of the study. Coupons a, b, c were then cleaned as described above.

Statistical analysis

Mean, standard deviation, variance were calculated using Microsoft Excel version 2013. Also, T test, one-way ANOVA, 2-way ANOVA, and Tukey HSD (Honestly Significant Difference) were used to analyze the data in Microsoft Excel version 2013.

Results

Growth and nitrate consumption of *M. hydrocarbonoclasticus* SP 17

Based on optical density measurements and viable plate counts of the planktonic cells, the organism reached the highest density at 7 days when grown under aerated conditions in Widdel's medium with either 0.5 mM nitrate or ammonium (Figures S1 and S2). While the numbers show a gradual decrease with time, the viable cell density remained above 10^7 CFU/ml after 6 weeks (Figure S2). The attached cell population (e.g. "biofilm", as determined by viable counts) showed no significant difference between sealed vs unsealed/aerated

(nitrate-amended) conditions (n=3, p-value = 0.78). Biofilm cover of ammonium-amended condition had a high variance between replicates (Figure S3).

The nitrate amounts in the treatments containing *Marinobacter* showed a steep decline in the first week, with treatments containing coupons at a higher nitrate level than those without coupons, and were close to the limit of detection of the instrument (30 μM) for all treatments with *Marinobacter* by the fourth week (Figure 1). The values in abiotic treatments showed some fluctuation but did not show a significant loss of nitrate.

Dissolved oxygen measurements

Dissolved oxygen in the medium of aerated treatments maintained original ambient levels with some fluctuations (Figure 2). The oxygen in sealed-abiotic treatment decreased from around 9.5 mg/l to 6.87 mg/l in 6 weeks. In contrast, the sealed treatments with cells had much greater decrease of dissolved oxygen with values reaching around 3 mg/l by the end of 6 weeks.

Coupon weight loss

The weight loss of coupons with cells was lower than without cells regardless of the nitrogen source or aeration (Figure 3). The five coupons incubated under nitrate-amended and aerated treatment with cells showed more than a seven-fold decrease in weight loss compared to that of nitrate-amended and aerated without cells. However, two coupons under these conditions gained weight (187 mg and 2 mg). The oxygen-limited treatments (sealed) showed less weight loss compared to the aerated treatments either with or without cells. A two way ANOVA was performed to determine the effect of oxygen limitation and the presence of *Marinobacter* cells on coupon weight loss (Table S2). There was a statistically significant interaction between the effect of oxygen limitation and presence of cells on coupon weight loss, ($F_{(1, 8)} = 265.006$, $p = 2.04 \times 10^{-7}$). The least weight loss was observed in the sealed (limited dissolved oxygen) treatments with cells under nitrate-amended conditions. The coupon weight loss was significantly higher with aerated treatments than sealed ones irrespective of the presence of cells (between treatments with cells: p = 0.006, between treatments without cells: p = 0.00004). As far as the effect of different nitrogen sources (e.g. nitrate, ammonium, no additional nitrogen source) are considered, for aerated

abiotic controls (Figure 4), there was no statistically significant difference among the groups as determined by one-way ANOVA ($F_{(2,6)} = 1.50$, $p = 0.27$, Table S3).

Dissolved ferrous ion measurements

The amount of dissolved ferrous ion at the end of the experiment showed similar trends to coupon weight loss data (Figure 5). The amount of dissolved ferrous ion was lower in the presence of cells compared to the abiotic control treatment regardless of the nitrogen source or dissolved oxygen status. The quantity was six-fold less in the presence of cells under nitrate-amended aerated conditions whereas it was three-fold less under sealed conditions. In the ammonium-amended aerated treatments, the amount of dissolved ferrous ion was 2.5-fold less in the presence of cells compared to the treatment without cells.

Discussion

According to phenomenological model of marine corrosion by R.E. Melchers, dissolved inorganic nitrogen (DIN) is thought to contribute to microbially induced corrosion through stimulation of growth/activity of microorganisms (Melchers, 2007; Melchers and Jeffrey, 2011; Melchers, 2014b). The objective of this experiment was to investigate the effect of *Marinobacter* biofilm/activity on corrosion of 1018 carbon steel under elevated levels of nitrate. Our results demonstrate that the presence of *Marinobacter* cells reduced or inhibited the corrosion of 1018 carbon steel. Further, there was no statistically significant difference in weight loss between coupons exposed to nitrate compared to ammonium under abiotic conditions.

Based on the coupon weight loss data as well as dissolved ferrous ion data, the presence of *Marinobacter* cells in the medium reduced/inhibited the corrosion of 1018 carbon steel. Furthermore, the corrosion of coupons was much lower in sealed treatments in which dissolved oxygen concentration was limited illustrating the well-known positive effect of oxygen on corrosion. Interestingly, statistical analysis of weight loss data shows an interaction between the presence of *Marinobacter* cells and the limited oxygen concentration. Based on the electrochemistry of metal corrosion, oxygen reduction coupled with elemental iron oxidation is the most common mechanism of corrosion under aerobic conditions (Zuo, 2007).

Oxygen is considered one of the most corrosive agents and the removal of oxygen could therefore reduce/inhibit corrosion. The collective effect of oxygen and *Marinobacter* cells (possibly in the form of biofilm) is likely due to the cells respiring oxygen in addition to the abiotic oxygen reduction with elemental iron oxidation.

Removal of corrosive substances through bacterial activity/metabolism (i.e. mainly oxygen under aerobic conditions) is one of the proposed mechanisms by which biofilms inhibit metal corrosion (reviewed in Zuo, 2007; Kip & Veen, 2015). Research on corrosion inhibition by biofilms of a close relative of *Marinobacter*, *Pseudomonas* spp., provide evidence of protecting metal surfaces such as 1018 carbon steel, steel, unalloyed copper and aluminium alloy 2024 under aerobic conditions (reviewed in Kip and Veen, 2015). The proposed protection mechanisms are oxygen removal through metabolic activity/respiration (Jayraman *et al*., 1997a; Jayraman *et al.,* 1999a) and production of a phosphate precipitation layer (Gunasekaran *et.al.,* 2004; Chondgar *et al*., 2005). In the current study, two coupons incubated with nitrate and cells showed a gain in weight, but no precipitation layer was noted upon visual examination after the coupons were cleaned and weighed.

Previous research (Pedersen and Hermansson, 1991; Jayraman *et al*., 1997a; Jayraman *et al.,* 1999a; Ismail *et al*, 2002) investigated oxygen removal as a possible cause of inhibition of corrosion, but could not directly demonstrate a relationship between oxygen removal and corrosion inhibition. However, the studies showed that the inhibition is a consequence of a living biofilm. Thus some cellular activity is involved in the process (Pedersen and Hermansson, 1991; Ismail *et. al*, 2002). Dubiel and group (2002) investigated corrosion inhibition of iron-respiring *Shewanella oneidensis* strain MR-1 by comparing the wild type to its non-biofilm-forming and/or non-iron-respiring mutants. The results suggested that the corrosion inhibition was due to the consumption of oxygen by the Fe (II) ions that are produced by the reduction of Fe (III) to Fe (II) by the iron reducing biofilm (Dubiel *et al.,* 2002). The authors further suggest that Fe (II) by scavenging oxygen acts as a barrier and prevents the oxygen from attacking the metal (Dubiel *et al.,* 2002).

Other literature shows that the effect of cellular activity may not be limited to oxygen scavenging. Removal of oxygen by flowing nitrogen through the medium was found to be less effective than the presence of living cells of *Pseudomonas fragi* strain K in corrosion inhibition

(Ismail *et al.,* 2002). Hence Ismail *et al*. concluded that bacterial activity beyond the mere consumption of oxygen contributed to the overall diminution of corrosion. A more recent study on corrosion inhibition using *Marinobacter aquaeolei* found that the presence of the organism was associated with high corrosion resistance in X80 pipeline steel (Khan *et al.,* 2019). Open circuit potential and linear polarization resistance electrochemistry was used to monitor the system and scanning electron microscopy (SEM) and, confocal laser scanning microscopy were used to study the biofilm and X-ray photoelectron spectroscopy (XPS) was utilized to identify corrosion products on metal surface (Khan *et.al.,* 2019). X-ray photoelectron spectroscopy (XPS) revealed the presence of iron oxide, iron phosphate as well as iron-EPS complexes (organic ligands, nitrosyl ligands, phenyl/benzyl and carbonyl ligands in complexes with iron). The authors suggest that the *Marinobacter* biofilm protected the metal by minimizing the amount of oxygen from reaching the metal surface while the associated EPS created a protective layer on the surface (Khan *et al.,* 2019).

In the current study there was no statistically significant difference in weight loss measured between the abiotic controls with nitrate, ammonium and without a nitrogen source (Figure 4). This contradicts the observations of Pillay and Lin (2013) where the addition of 5 mM $NaNO_3$ or NH_4NO_3 to deionized water in aerated flasks increased corrosion (no mechanism was proposed by the authors). The current study was performed using a synthetic medium that more closely mimicked the high chloride chemical composition of sea water (Widdel aerobic medium) and maybe the difference in results lies in the chemistry of the medium.

In the oil and gas sector, the application of nitrate or nitrite to restrict sulfide formation and thereby minimize corrosion and reservoir souring is becoming more common (Voordouw, 2003; Dunsmore *et al.,* 2006; Hidaka *et al.,* 2018). The principal objective is to inhibit sulfide production by sulfate reducing bacteria (SRBs) through the provision of a thermodynamically preferred electron acceptor like the nitrogen oxyanions. Numerous studies have been done investigating the effectiveness of the practice and also the multiple underlying mechanisms involved. A few main points have been highlighted in these studies (Dunsmore *et al.,* 2006; Gao *et al.,* 2014; Pillay and Lin, 2013; Schwermer *et al.,* 2008): Upon addition of NO_3^- (1) The community is shifted from sulfate-reducing to nitrate reducing, (2) The community is shifted from high diversity community to low diversity community

dominated by nitrate reducing bacteria, (3) General corrosion was reduced. Marques and group studied the effect of nitrate treatment on carbon steel corrosion using a complex microbial community found in production water (Marques *et al.,* 2012). Coupons from all experiments with a nitrate treatment (continuous injections of 180 mg/L of sodium nitrate solution in a rate of 0.5 ml/min) showed slightly higher weight loss. It should be noted that *Marinobacter* species have been found to positively respond to high levels of nitrate via increases in cell numbers in multiple studies (Dunsmore *et al.,* 2006; Marques *et al.,* 2012; Pillay and Lin, 2014). Thus, it appears that utilizing an organism such as *Marinobacter* would certainly help in understanding the effect of nitrate in MIC. However, contrary to observations of the present study, Marques and colleagues (2012) as well as Pillay and Lin (2014) found an increase in corrosion with high levels of nitrate, indicating that any inhibition of corrosion by *Marinobacter* could be overwhelmed by the effects of nitrate on other members of the community.

While appreciating the insights gained via single species studies, it is absolutely vital to investigate the mechanisms of MIC with multi-species communities. A biofilm on metal surface has various microhabitats facilitating the presence of aerobes such as *Marinobacter* as well as anaerobes such as SRBs which are known to cause MIC (Beech and Sunner, 2004; Dall'Agnol and Moura, 2014). *Marinobacter* sequences have been found in biofilms that caused severe corrosion (Vigneron *et al.,* 2016). The influence of microbial activity on a metal surface can be thought of as the combined effect of complementary, antagonistic or parallel microbial pathways present in the biofilm (Vigneron *et al.,* 2018).

With the existing need of environmentally friendly corrosion mitigation techniques, studies of the mechanisms involved in enhancing or inhibiting MIC have gained much more attention. The current study investigated the effect of elevated nitrate on carbon steel corrosion in the presence of *Marinobacter hydrocarbonoclasticus* cells. The observations support the hypothesis that *Marinobacter* biofilm protects 1018 carbon steel under aerobic conditions. The most likely mechanism of corrosion inhibition by the organism appears to be oxygen respiration by the organism that ultimately reduces the ability of oxygen to react with the metal surface. The observations of the current study do not support the hypothesis of enhanced corrosion in abiotic systems due to the presence of elevated levels of nitrate compared to ammonium.

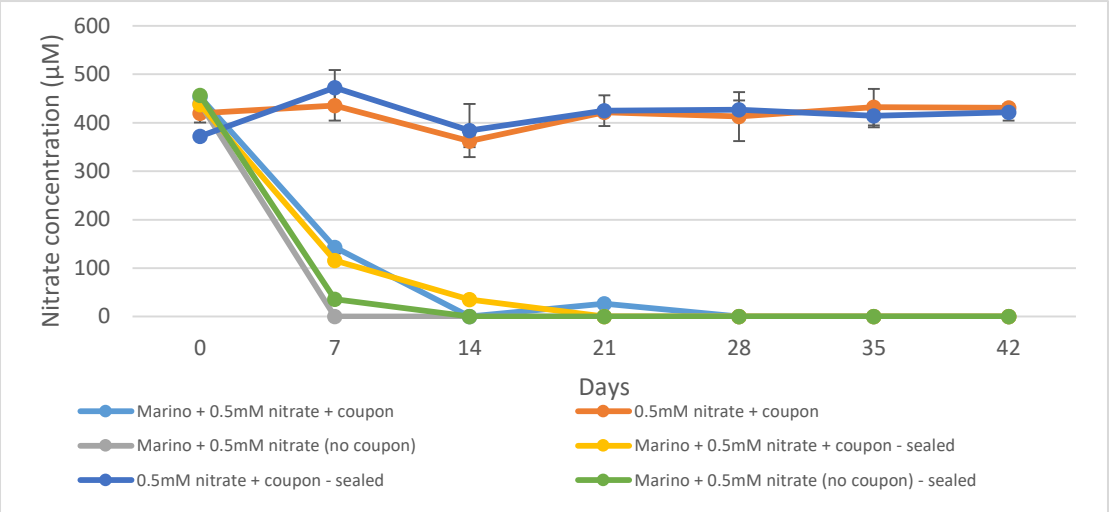

Figure 1. Nitrate depletion of nitrate-amended treatments as determined by ion chromatography (n = 3). "Marino" treatments were inoculated with *Marinobacter* cells. Points represent average values with error bars (+/- STD). Marino + 0.5mM nitrate + coupon: Treatment 1, 0.5mM nitrate + coupon: Treatment 2, Marino + 0.5mM nitrate (no coupon): Treatment 5, Marino + 0.5mM nitrate + coupon (sealed): Treatment 7, 0.5mM nitrate + coupon: Treatment 8 and Marino + 0.5mM nitrate (no coupon): Treatment 9. Treatments are listed in Table S1.

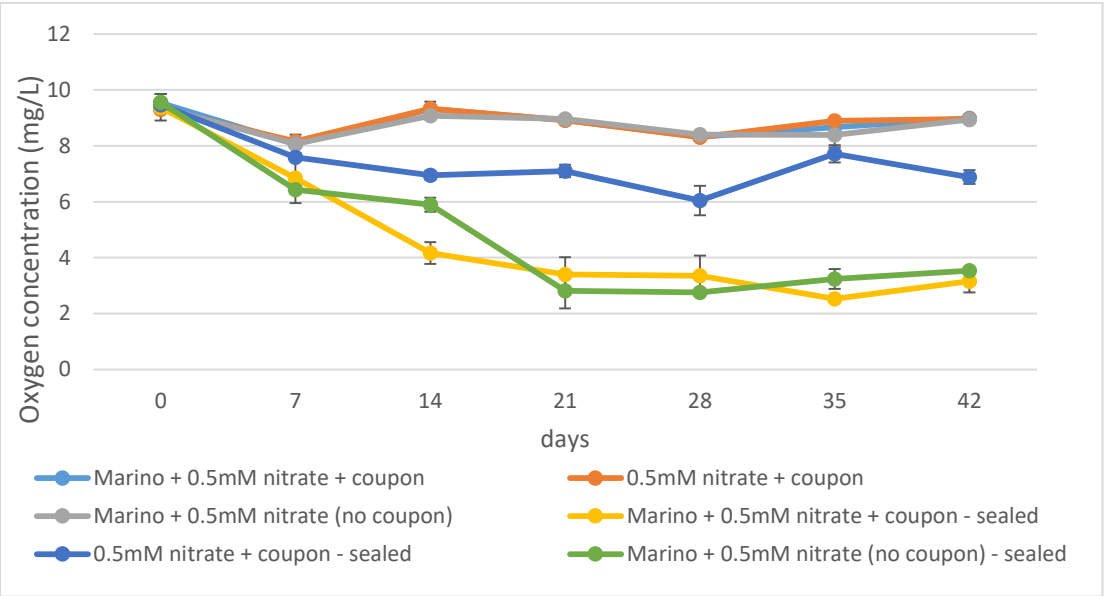

Figure 2. The dissolved oxygen level in the medium (n = 2). "Marino" treatments were inoculated with *Marinobacter* cells. Points represent average values with error bars (+/- STD). Marino + 0.5mM nitrate + coupon: Treatment 1, 0.5mM nitrate + coupon: Treatment 2, Marino + 0.5mM nitrate (no coupon): Treatment 5, Marino + 0.5mM nitrate + coupon (sealed): Treatment 7, 0.5mM nitrate + coupon: Treatment 8 and Marino + 0.5mM nitrate (no coupon): Treatment 9. Treatments are listed in Table S1.

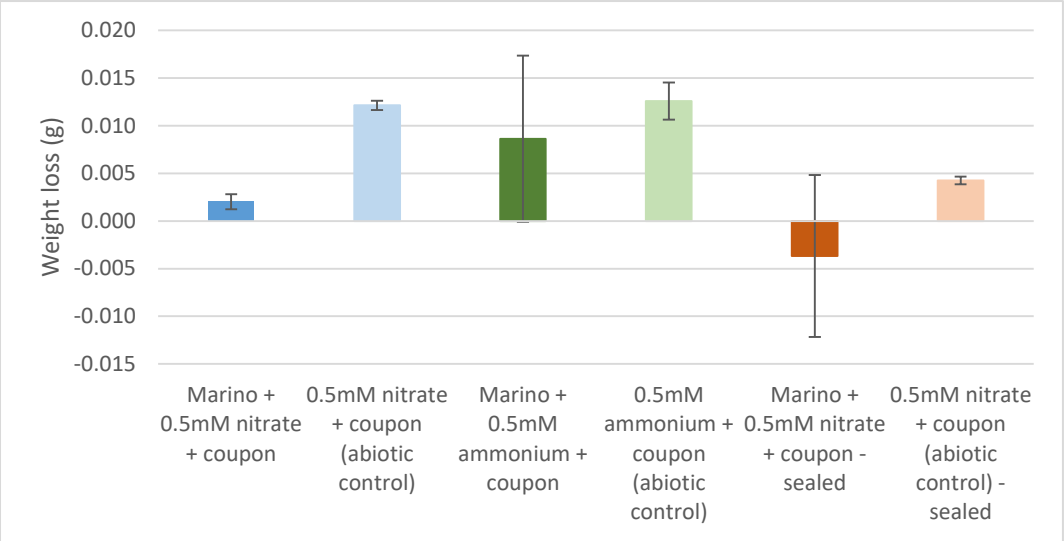

Figure 3. Weight loss of 1018 carbon steel coupons after 6 weeks of exposure (n = 5 except where noted). "Marino" treatments were inoculated with *Marinobacter* cells. Bars represent average values with error bars (+/- 1 STD). Marino + 0.5mM nitrate + coupon: Treatment 1, 0.5mM nitrate + coupon: Treatment 2, Marino + 0.5mM ammonium + coupon: Treatment 3, 0.5mM ammonium + coupon: Treatment 4, Marino + 0.5mM nitrate + coupon (sealed): Treatment 7, 0.5mM nitrate + coupon: Treatment 8. Treatments are listed in Table S1. The data of one coupon of the treatment 8 was removed from the analysis due to contamination (n=4 for Treatment group 8). There was a net loss of weight for Treatment 7 when all 5 coupons were included, as three coupons lost weight and two coupons gained weight.

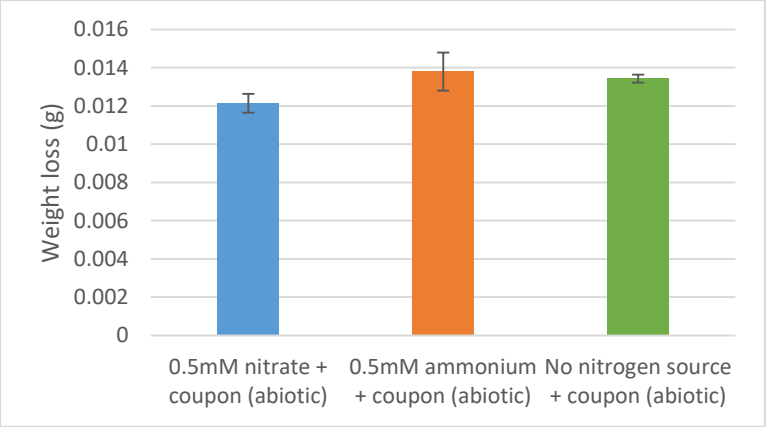

Figure 4. Comparison of effect of nitrogen source on weight loss of 1018 carbon steel coupons in aerated incubations without cells. Coupons were exposed for 6 weeks. Bars represent average values with error bars (+/- 1 STD). Statistical analysis was performed using unequal sample sizes (0.5mM nitrate + coupon, n=5; 0.5mM ammonium + coupon, n = 5; no nitrogen source, n = 4). There was no statistically significant difference between the groups as determined by one-way ANOVA ($F_{(2, 9)} = 1.50$, $p = 0.27$). 0.5 mM nitrate + coupon: Treatment 2, 0.5 mM ammonium + coupon: Treatment 4, no nitrate + coupon: Treatment 10. Treatments are listed in Table S1.

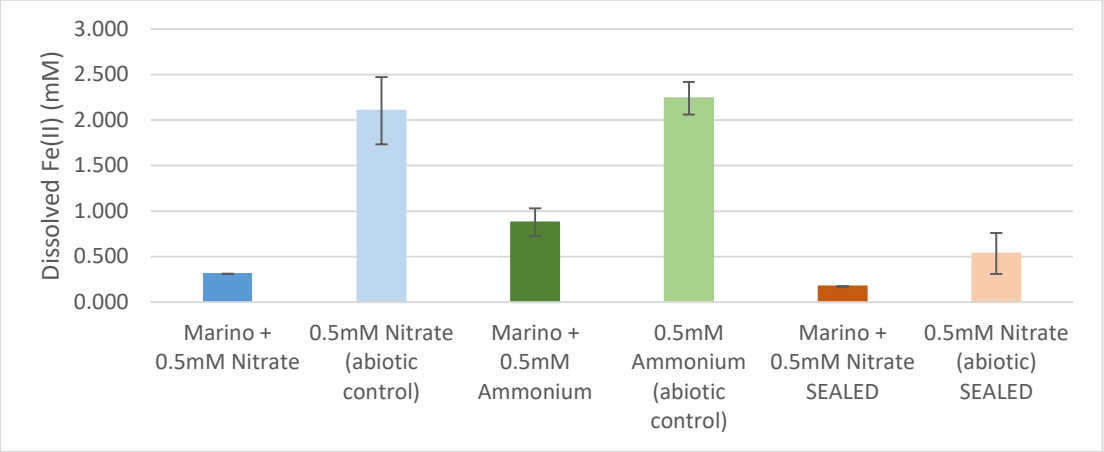

Figure 5. Amount of dissolved Fe (II) determined by ferrozine assay after 6 weeks of incubation (n=2). "Marino" treatments were inoculated with *Marinobacter* cells. Bars represent average values with error bars (+/- STD). Marino + 0.5mM nitrate + coupon: Treatment 1, 0.5mM nitrate + coupon: Treatment 2, Marino + 0.5mM ammonium + coupon: Treatment 3, 0.5mM ammonium + coupon: Treatment 4, Marino + 0.5mM nitrate + coupon (sealed): Treatment 7, 0.5mM nitrate + coupon: Treatment 8. Treatments are listed in Table S1.

Supplementary tables and figures.

TableS1. List of treatments. Each treatment had five replicates.

Treatment group	Nitrate	Ammonium	Marinobacter (5% v/total v)	1018 Coupons	Aerated/sealed
1	0.5mM	_	√	√	Aerated
2	0.5mM	_	_	√	Aerated
3	_	0.5mM	√	√	Aerated
4	_	0.5mM		√	Aerated
5	0.5mM	_	√	_	Aerated
6	_	0.5mM	√	_	Aerated
7	0.5mM	_	√	√	sealed
8	0.5mM	_	_	√	sealed
9	0.5mM	_	√	_	sealed
10	_	_	_	√	Aerated

Table S2. Results of the two-way ANOVA on effect of dissolved oxygen and presence of *Marinobacter* cells on coupon weight loss. Treatments 1 (with *Marinobacter*, aerated) 2 (without *Marinobacter*, aerated), 7 (with *Marinobacter*, sealed) and 8 (without *Marinobacter*, sealed) were compared. Three replicates (uncontaminated) were chosen from each treatment for analysis since the analysis needed equal sample sizes. (F critical = 5.32)

ANOVA

Source of Variation	*SS*	*df*	*MS*	*F*	*P-value*
Sample	1.46×10^{-4}	1	1.46×10^{-4}	1.05×10^{3}	9.14×10^{-10}
Columns	5.68×10^{-5}	1	5.68×10^{-5}	4.05×10^{2}	3.86×10^{-8}
Interaction	3.71×10^{-5}	1	3.71×10^{-5}	2.65×10^{2}	2.04×10^{-7}
Within	1.12×10^{-6}	8	1.4×10^{-7}		
Total	2.41×10^{-4}	11			

Table S3. Results of the one-way ANOVA on effect of nitrogen source on coupon weight loss of abiotic treatments under aerated conditions. Treatments 2 (0.5 mM nitrate + coupon, n=5), 4 (0.5 mM ammonium + coupon, n=5) and 10 (no nitrogen source + coupon, n=4) were used for the analysis. (F critical = 4.26).

ANOVA

Source of Variation	*SS*	*df*	*MS*	*F*	*P-value*
Between Groups	6.08×10^{-6}	2	3.04×10^{-6}	1.50	0.27
Within Groups	1.83×10^{-5}	9	2.03×10^{-6}		
Total	2.44×10^{-5}	11			

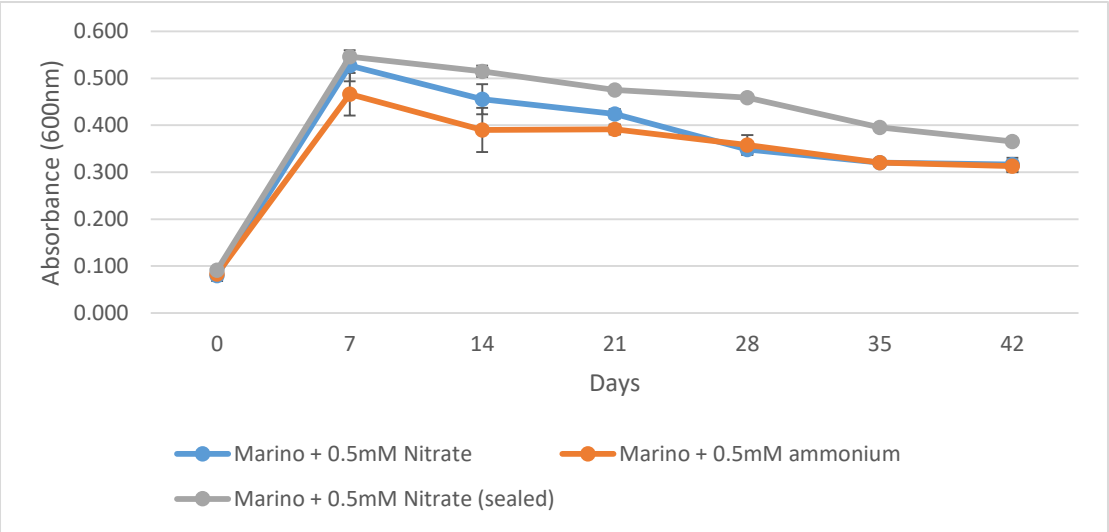

Figure S1. Optical density/OD (at 600nm) of the planktonic phase of treatments with *M. hydrocarbonoclasticus* and without coupons (n=3). "Marino" treatments were inoculated with *Marinobacter* cells. Points represent average values with error bars (+/- 1 STD). OD was measured only in treatments that did not have coupons. In treatments with coupons, corrosion products interfered with the OD measurements. Marino + 0.5 mM nitrate: Treatment 5, Marino + 0.5 mM ammonium: Treatment 6 and Marino + 0.5 mM nitrate (sealed): Treatment 9. Treatments are listed in Table S1.

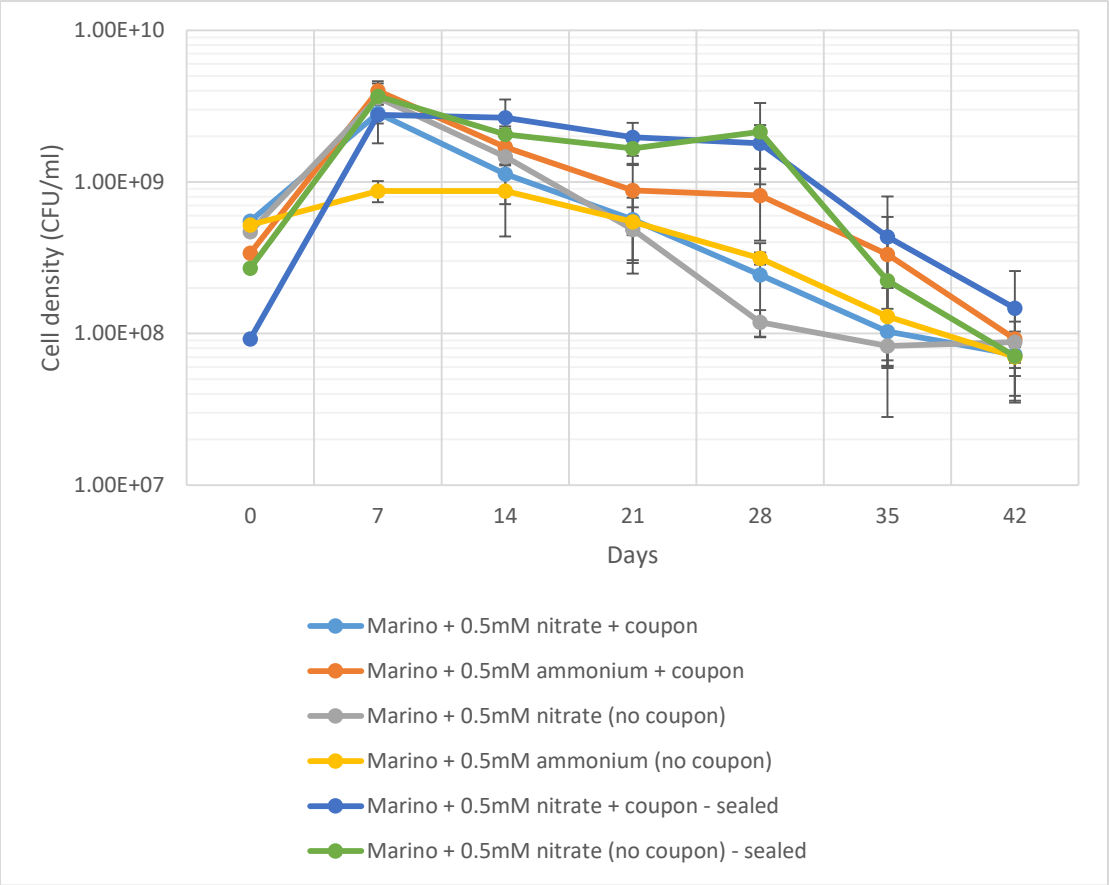

Figure S2. Viable cell counts of the planktonic phase of treatments with *Marinobacter hydrocarbonoclasticus* (n=3). "Marino" treatments were inoculated with *Marinobacter* cells. Points represent average values with error bars (+/- 1 STD). Marino + 0.5mM nitrate + coupon: Treatment 1, Marino + 0.5mM ammonium + coupon: Treatment 3, Marino + 0.5mM nitrate (no coupon): Treatment 5, Marino + 0.5mM ammonium (no coupon): Treatment 6, Marino + 0.5mM nitrate + coupon (sealed): Treatment 7, Marino + 0.5mM nitrate (no coupon): Treatment 9. Treatments are listed in Table S1.

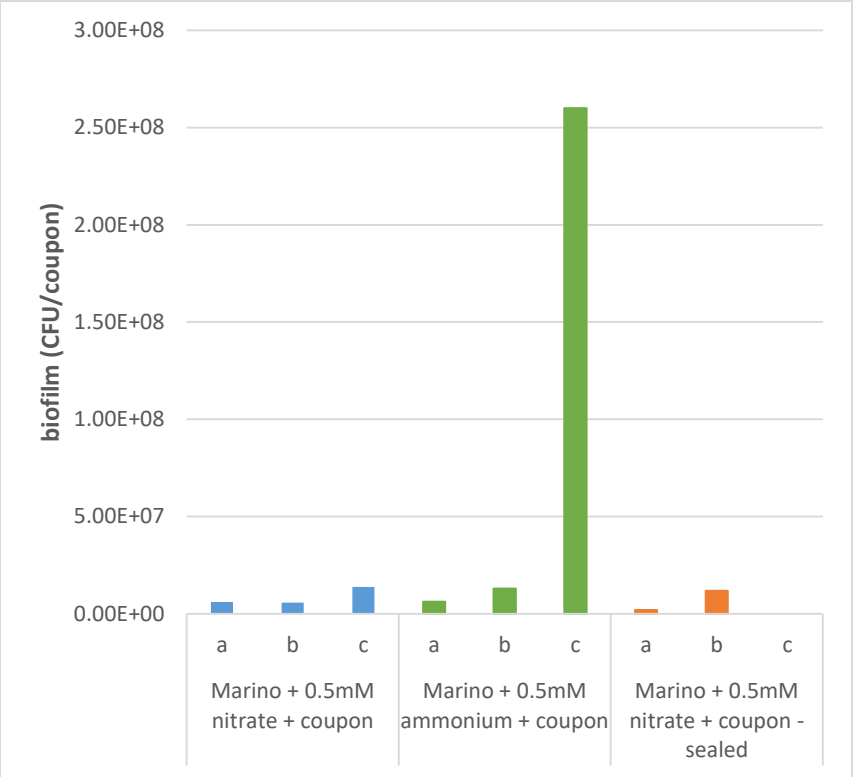

Figure S3. *Marinobacter hydrocarbonoclasticus* biofilm determined by viable cell counts (n=3). "Marino" treatments were inoculated with *Marinobacter* cells. Marino + 0.5mM nitrate + coupon: Treatment 1, Marino + 0.5mM ammonium + coupon: Treatment 3, Marino + 0.5mM nitrate + coupon (sealed): Treatment 7. Treatments are listed in Table S1.

References

American Society for Testing and Materials (Philadelphia, Pennsylvania). (2004). ASTM G1-03: Standard Practice for Preparing, Cleaning, and Evaluating Corrosion Test Specimens. ASTM.

Beech, I. B. Sunner, J. (2004). Biocorrosion: towards understanding interactions between biofilms and metals. *Current Opinion in Biotechnology*, *15*(3), 181-186.

Beech, I. B., and Sunner, J. (2004). Biocorrosion: towards understanding interactions between biofilms and metals. *Current Opinion in Biotechnology*, *15*(3), 181-186.

Bødtker, G., Thorstenson, T., Lillebø, B. L. P., Thorbjørnsen, B. E., Ulvøen, R. H., Sunde, E., Torsvik, T. (2008). The effect of long-term nitrate treatment on SRB activity, corrosion rate and bacterial community composition in offshore water injection systems. *Journal of Industrial Microbiology & Biotechnology*, *35*(12), 1625-1636.

Chongdar, S., Gunasekaran, G., Kumar, P. (2005). Corrosion inhibition of mild steel by aerobic biofilm. *Electrochimica Acta*, *50*(24), 4655-4665.

Dall'Agnol, L. T., & Moura, J. J. G. (2014). Sulphate-reducing bacteria (SRB) and biocorrosion. *Understanding Biocorrosion: Fundamentals and Applications*, 77.

Dall'Agnol, L. T., and Moura, J. J. G. (2014). Sulphate-reducing bacteria (SRB) and biocorrosion. *Understanding Biocorrosion: Fundamentals and Applications*, 77.

Dubiel, M., C. H. Hsu, C. C. Chien, F. Mansfeld, D. K. Newman. (2002) Microbial iron respiration can protect steel from corrosion. *Applied and Environmental Microbiology* 68, no.3: 1440-1445.

Dunsmore, B., Youldon, J., Thrasher, D. R., Vance, I. (2006). Effects of nitrate treatment on a mixed species, oil field microbial biofilm. *Journal of Industrial Microbiology and Biotechnology*, *33*(6), 454-462.

Fontaine, E., Rosen, J., Potts, A., Ma, K. T., Melchers, R. (2014). SCORCH JIP-Feedback on MIC and pitting corrosion from field recovered mooring chain links. In *Offshore Technology Conference*. Offshore Technology Conference.

Gao, P. K., Li, G. Q., Zhao, L. X., Dai, X. C., Tian, H. M., Dai, L. B., ... Ma, T. (2014). Dynamic processes of indigenous microorganisms from a low-temperature petroleum reservoir during nutrient stimulation. *Journal of Bioscience and Bioengineering*, *117*(2), 215-221.

Garcia, H. E., R. A. Locarnini, T. P. Boyer, J. I. Antonov, O.K. Baranova, M.M. Zweng, J.R. Reagan, D.R. Johnson, 2014. World Ocean Atlas 2013, Volume 4: Dissolved Inorganic Nutrients (phosphate, nitrate, silicate). S. Levitus, Ed., A. Mishonov Technical Ed.; NOAA Atlas NESDIS 76, 25 pp.

Gauthier, M. J., Lafay, B., Christen, R., Fernandez, L., Acquaviva, M., Bonin, P., Bertrand, J. C. (1992). *Marinobacter hydrocarbonoclasticus gen. nov., sp. nov.,* a new, extremely halotolerant, hydrocarbon-degrading marine bacterium. *International Journal of Systematic and Evolutionary Microbiology*, *42*(4), 568-576.

Gunasekaran, G., Chongdar, S., Gaonkar, S. N., Kumar, P. (2004). Influence of bacteria on film formation inhibiting corrosion. *Corrosion Science*, *46*(8), 1953-1967.

Handley, K. M., Lloyd, J. R. (2013). Biogeochemical implications of the ubiquitous colonization of marine habitats and redox gradients by *Marinobacter* species. *Frontiers in Microbiology*, *4*, 136.

Hidaka, K., Miyanaga, K., Tanji, Y. (2018). The presence of nitrate-and sulfate-reducing bacteria contributes to ineffectiveness souring control by nitrate injection. *International Biodeterioration & Biodegradation*, *129*, 81-88.

Ismail, K. M., Gehrig, T., Jayaraman, A., Wood, T. K., Trandem, K., Arps, P. J., Earthman, J. C. (2002). Corrosion control of mild steel by aerobic bacteria under continuous flow conditions. *Corrosion*, *58*(5), 417-423.

Jayaraman, A., Cheng, E. T., Earthman, J. C., Wood, T. K. (1997a). Axenic aerobic biofilms inhibit corrosion of SAE 1018 steel through oxygen depletion. *Applied Microbiology and Biotechnology*, *48*(1), 11-17.

Jayaraman, A., Earthman, J. C., Wood, T. K. (1997b). Corrosion inhibition by aerobic biofilms on SAE 1018 steel. *Applied Microbiology and Biotechnology*, *47*(1), 62-68.

Jayaraman, A., Mansfeld, F. B., Wood, T. K. (1999b). Inhibiting sulfate-reducing bacteria in biofilms by expressing the antimicrobial peptides indolicidin and bactenecin. *Journal of Industrial Microbiology and Biotechnology*, *22*(3), 167-175.

Jayaraman, A., Ornek, D., Duarte, D. A., Lee, C. C., Mansfeld, F. B., Wood, T. K. (1999a). Axenic aerobic biofilms inhibit corrosion of copper and aluminum. *Applied Microbiology and Biotechnology*, *52*(6), 787-790.

Jiang, X., Dang, H., Jiao, N. (2015). Ubiquity and diversity of heterotrophic bacterial *nasA* genes in diverse marine environments. *PloS One*, *10*(2), e0117473.

Jigletsova, S. K., Rodin, V. B., Kholodenko, V. P., Zhirkova, N. A., Alexandrova, N. V. (2004, January). Influence of nutrient medium composition on the direction of microbiologically induced corrosion. In *CORROSION 2004*. NACE International.

Khan, M. S., Xu, D., Liu, D., Lekbach, Y., Yang, K., Yang, C. Corrosion inhibition of X80 steel in simulated marine environment with *Marinobacter aquaeolei*. *Acta Metallurgica Sinica (English Letters)*, 1-12.

Kilbane, J. I., Bogan, B., Lamb, B. (2005, January). Quantifying the contribution of various bacterial groups to microbiologically influenced corrosion. In *CORROSION 2005*. NACE International.

Kip, N., Van Veen, J. A. (2015). The dual role of microbes in corrosion. *The ISME Journal*, *9*(3), 542.

Lee, W., Lewandowski, Z., Nielsen, P. H., Hamilton, W. A. (1995). Role of sulfate-reducing bacteria in corrosion of mild steel: a review. *Biofouling*, *8*(3), 165-194.

Liang, R., Grizzle, R. S., Duncan, K. E., McInerney, M. J., Suflita, J. M. (2014). Roles of thermophilic thiosulfate-reducing bacteria and methanogenic archaea in the biocorrosion of oil pipelines. *Frontiers in Microbiology*, *5*, 89.

Liang, R., Suflita, J. M. (2015). Protocol for evaluating the biological stability of fuel formulations and their relationship to carbon steel biocorrosion. In *Hydrocarbon and Lipid Microbiology Protocols* (pp. 211-226). Springer, Berlin, Heidelberg.

Little, B. J. (2003). A perspective on the use of anion ratios to predict corrosion in Yucca mountain. *Corrosion*, *59*(8), 701-704.

Little, B. J., Lee, J. S. (2014). Microbiologically influenced corrosion: an update. *International Materials Reviews*, *59*(7), 384-393.

Mand, J., Park, H. S., Jack, T. R., Voordouw, G. (2014). The role of acetogens in microbially influenced corrosion of steel. *Frontiers in Microbiology*, *5*, 268.

Marques, J. M., de Almeida, F. P., Lins, U., Seldin, L., Korenblum, E. (2012). Nitrate treatment effects on bacterial community biofilm formed on carbon steel in produced water stirred tank bioreactor. *World Journal of Microbiology and Biotechnology*, *28*(6), 2355-2363.

Melchers, R. (2014a). Modelling long term corrosion of steel infrastructure in natural marine environments. *Understanding Biocorrosion: Fundamentals and Applications*, *66*, 213.

Melchers, R. E. "Predicting long-term corrosion of metal alloys in physical infrastructure." *npj Materials Degradation* 3, no. 1 (2019): 4.

Melchers, R. E. (2003). Modeling of marine immersion corrosion for mild and low-alloy steels—Part 1: Phenomenological model. *Corrosion*, *59*(4), 319-334.

Melchers, R. E. (2010). Transient early and longer term influence of bacteria on marine corrosion of steel. *Corrosion Engineering, Science and Technology*, *45*(4), 257-261.

Melchers, R. E. (2012). Influence of dissolved inorganic nitrogen on accelerated low water corrosion of marine steel piling. *Corrosion*, *69*(1), 95-103.

Melchers, R. E. (2014b). Long-term immersion corrosion of steels in seawaters with elevated nutrient concentration. *Corrosion Science*, *81*, 110-116.

Melchers, R. E., Jeffrey, R. (2011). Bacteria have transient influences on marine corrosion of steel.

Melchers, R. E., Jeffrey, R. (2012). Corrosion of long vertical steel strips in the marine tidal zone and implications for ALWC. *Corrosion Science*, *65*, 26-36.

Ngatia, L., Grace III, J. M., Moriasi, D., Taylor, R. (2019). Nitrogen and phosphorus eutrophication in marine ecosystems. In *Monitoring of Marine Pollution*. IntechOpen.

Nguyen, C. K., Stone, K. R., Edwards, M. A. (2011). Nitrate accelerated corrosion of lead solder in potable water systems. *Corrosion Science*, *53*(3), 1044-1049.

Pedersen, A., Hermansson, M. (1991). Inhibition of metal corrosion by bacteria. *Biofouling*, *3*(1), 1-11.

Pillay, C., Lin, J. (2013). Metal corrosion by aerobic bacteria isolated from stimulated corrosion systems: Effects of additional nitrate sources. *International Biodeterioration & Biodegradation*, *83*, 158-165.

Pillay, C., Lin, J. (2014). The impact of additional nitrates in mild steel corrosion in a seawater/sediment system. *Corrosion Science*, *80*, 416-426.

Rajasekar, A., Ting, Y. P. (2011). Role of inorganic and organic medium in the corrosion behavior of *Bacillus megaterium* and *Pseudomonas* sp. in stainless steel SS 304. *Industrial & Engineering Chemistry Research*, *50*(22), 12534-12541.

Rodin, V. B., Jigletsova, S. K., Kobelev, V. S., Akimova, N. A., Aleksandrova, N. V., Rasulova, G. E., Kholodenko, V. P. (2000). Development of biological methods for controlling the aerobic microorganism–induced corrosion of carbon steel. *Applied Biochemistry and Microbiology*, *36*(6), 589-593.

Schwermer, C. U., Lavik, G., Abed, R. M., Dunsmore, B., Ferdelman, T. G., Stoodley, P., De Beer, D. (2008). Impact of nitrate on the structure and function of bacterial biofilm communities in pipelines used for injection of seawater into oil fields. *Appl. Environ. Microbiol. 74*(9), 2841-2851.

Soracco, R. J., Pope, D. H., Eggers, J. M., Effinger, T. N. (1988). *Microbiologically influenced corrosion investigations in electric power generating stations* (No. CONF-880314--). Houston, TX; National Assoc. of Corrosion Engineers.

Stadler, R., Fuerbeth, W., Harneit, K., Grooters, M., Woellbrink, M., Sand, W. (2008). First evaluation of the applicability of microbial extracellular polymeric substances for corrosion protection of metal substrates. *Electrochimica Acta*, *54*(1), 91-99.

Stadler, R., Wei, L., Fürbeth, W., Grooters, M., Kuklinski, A. (2010). Influence of bacterial exopolymers on cell adhesion of *Desulfovibrio vulgaris* on high alloyed steel: corrosion inhibition by extracellular polymeric substances (EPS). *Materials and Corrosion*, *61*(12), 1008-1016.

Suflita, J. M., Phelps, T. J., Little, B. (2008). Carbon dioxide corrosion and acetate: a hypothesis on the influence of microorganisms. *Corrosion*, *64*(11), 854-859.

Tanner, R. S. (1989). Monitoring sulfate-reducing bacteria: comparison of enumeration media. *Journal of Microbiological Methods*, *10*(2), 83-90.

Videla, H. A., Herrera, L. K. (2005). Microbiologically influenced corrosion: looking to the future. *International Microbiology*, *8*(3), 169.

Vigneron, A., Alsop, E. B., Chambers, B., Lomans, B. P., Head, I. M., & Tsesmetzis, N. (2016). Complementary microorganisms in highly corrosive biofilms from an offshore oil production facility. *Appl. Environ. Microbiol.*, *82*(8), 2545-2554.

Vigneron, A., Head, I. M., & Tsesmetzis, N. (2018). Damage to offshore production facilities by corrosive microbial biofilms. *Applied Microbiology and Biotechnology*, *102*(6), 2525-2533.

Voordouw, G. (2003). Oil field biotechnology: Should we use nitrate or nitrite to remediate souring. In *Canadian International Petroleum Conference*. Petroleum Society of Canada.

Zuo, R. (2007). Biofilms: strategies for metal corrosion inhibition employing microorganisms. *Applied Microbiology and Biotechnology*, *76*(6), 1245-1253.

Appendix

Transcriptomic response of *Marinobacter hydrocarbonoclasticus* SP17 biofilms to elevated levels of nitrate in the environment

Abstract

The phenomenological model of corrosion of steel in sea water by Dr. R. E. Melchers and group has two phases during which bacterial activity dominates corrosion. The rate of corrosion during these phases depends on bacterial metabolism, thus becomes a function of nutrient supply. The major limiting nutrient for bacterial activity in sea water is dissolved inorganic nitrogen which is mainly nitrate in oxygenated water. The current study investigated the effect of elevated levels of nitrate in the environment on *Marinobacter hydrocarbonoclasticus* SP17 biofilm at the level of transcription. It was hypothesized that genes for assimilatory and/or dissimilatory nitrate reduction in *Marinobacter* biofilms would be differentially expressed in the presence of elevated levels of inorganic nitrogen (nitrate vs. ammonium). The biofilm was grown aerobically on an inert surface (glass), RNA was extracted and a microarray containing 3697 Open Reading Frames (ORFs) was performed comparing biofilm cells as well as planktonic phase under nitrate-amended vs. ammonium-amended conditions. Only 4 transcripts showed upregulation (i.e. $\log_2 R \geq 2$) under nitrate amended biofilm conditions compared to ammonium amended biofilm conditions and 1086 showed downregulation (i.e. $\log_2 R \leq -2$). Contrary to expectations, the majority of genes in dissimilatory nitrate reduction were to be found downregulated in biofilm under nitrate-amended conditions. Among other genes downregulated were *glnG, glnL* (two-component nitrogen regulatory system) and genes coding for nitrogen/nitrate transport systems/transporters. Seven of the genes coding for subunits of cytochrome c oxidases were found downregulated in nitrate-amended compared to ammonium-amended conditions in biofilm as well as planktonic phase. The shutting down of nitrate/nitrogen metabolism perhaps is due to the excessive amounts of nitrate. The downregulation of cytochromes is indicative of the culture reaching anaerobic conditions, as has been seen for *Pseudomonas aeruginosa*.

Introduction

Aggregates of microorganisms in which cells are frequently embedded within a self-produced matrix of extracellular polymeric substance (EPS) that are adhere to each other and/or to a surface (IUPAC recommendations, Vert *et al.,* 2012) are called biofilms. A biofilm is an essential part of natural environment, with both beneficial as well as detrimental aspects. A biofilm community functions very differently than the cells in a free-living community (Flemming *et al.,* 2016). Many different factors, including nutrient availability or limitation can influence the growth, function and metabolism of a biofilm. Furthermore, these factors can differentially affect the biofilm during different phases of its development.

As far as the marine environment is concerned, dissolved inorganic nitrogen (DIN) is critical for bacterial growth and/or activity since it is limited in the ocean compared to other nutrients. The different forms of dissolved inorganic nitrogen in sea water include nitrate, nitrite and ammonium. Many harbors around the world which are polluted with industrial, agricultural as well as urban runoff have shown increased levels of DIN. Based on field data analysis and modeling, Rob Melchers and group was able to demonstrate a positive correlation between elevated levels of annual average DIN in sea water (7 - 70 µmol/L) and accelerated low water corrosion (ALWC) of steel piling (Melchers, 2012; Melchers, 2014; Melchers and Jeffrey, 2012). Bacterial growth and/or activity is known to be influenced by the availability of nutrients (Little and Lee, 2014 and references there in). In the relationship between ALWC and DIN proposed by Melchers', DIN appears to be mainly nitrate, on the basis that oxygenated sea water has very low concentrations of nitrite and ammonium (Melchers, 2012).

Addition of NO_3^- or NO_2^- to injection water of oil and gas fields has been practiced for quite a long time. The principal objective is to inhibit the activity of sulfate reducing bacteria (SRBs) and other corrosion-inducing microorganisms. In most of these studies, these main points have been highlighted (Dunsmore *et al.*, 2006; Gao *et al.*, 2014; Pillay and Lin, 2013; Schwermer *et al*., 2008) : Upon addition of NO_3^- (1) the community shifted from sulfate-reducing to nitrate reducing, (2) The community shifted from high diversity community to low diversity nitrate reducing bacteria dominating community, (3) General corrosion was reduced. However, these environments differ from ALWC in that they are typically anaerobic, higher temperature, and have abundant hydrocarbons.

The effect of presence of high levels of nitrate in the marine environment were mostly studied and explained in terms of microbial community diversity, biofilm architecture, the extent of corrosion and acquisition of nitrate. However, the effect at the cellular level is yet to be elucidated. The behavior and function of marine biofilms/biofilm cells exposed to elevated levels of nitrate should be understood in order to explain the outcomes observed in the literature mentioned above.

The objective of current study was to investigate the effect of elevated levels of nitrate in the environment on marine biofilms at transcription level. We employed *Marinobacter hydrocarbonoclasticus* SP17 (Gauthier *et.al*, 1992), which is commonly found in marine biofilms as the model organism. It is capable of utilizing nitrate under anaerobic conditions as an electron acceptor. *Marinobacter* biofilms were grown aerobically on an inert surface (glass slides) and were exposed to elevated levels of either nitrate or ammonium (acting as the control state). It was hypothesized that genes for assimilatory and/or dissimilatory nitrate reduction in *Marinobacter* biofilms will be differentially expressed in the presence of elevated levels of inorganic nitrogen (nitrate vs. ammonium).

Materials and Methods

Cultivation of *M. hydrocarbonoclasticus* SP17, experimental design and sample collection

M. hydrocarbonoclasticus SP 17 obtained from glycerol stocks were grown in modified artificial sea water (ASW) medium (Lindell *et.al.*, 1998) with 0.01 % (w/v) lactate as the sole carbon source, amended with either 0.5mM sodium nitrate or 0.5mM of ammonium chloride. The cultures were incubated under aerobic conditions at 25℃ with shaking (100 rpm) and the growth was monitored by standard plate counts using tryptic soy agar (TSA)

Exponentially grown cells in ASW were harvested by centrifugation at 6000x g 10 min at room temperature, washed three times (by repeating centrifugation at 6000x g for 5 min and suspending in fresh media). The cells were resuspended to a final OD_{600nm} of 0.06 (10%) in ASW with 0.01% (w/v) lactate and amended with either 0.5mM sodium nitrate or 0.5mM ammonium chloride.

Clear, glass microscope slides (75 X 25 X 1 mm, VWR, Radnor, PA) horizontally immersed in 50 ml of culture in polystyrene petri dishes (100 X 20 mm)-(VWR, Radnor, PA) were used as the substratum for biofilm growth. The petri dishes were incubated at 25℃ on a rocking

platform shaker (VWR, Radnor, PA) at speed 4 and the growth was monitored using OD at 600nm. Nitrate depletion was monitored using an ion chromatograph (IonPac® AS23 4X250mm analytical column and an IonPac® AG23 4X50mm guard column)-(Dionex Corp., Sunnyvale, CA) and a conductivity detector.

The biofilm and planktonic samples were collected at the mid exponential phase after seven days of incubation. The culture medium with planktonic cells were carefully extracted using a micropipette and collected into sterile 50ml centrifuge tubes. Glass slides were briefly dipped in sterile fresh medium to remove any non-attached cells. Then, the biofilm on the glass was scraped into sterile 50ml centrifuge tubes using Teflon spatulas. Both planktonic and biofilm sample tubes were centrifuged at 6000x g for 5 minutes, cell pellets were resuspended in 2ml of sterile, fresh medium and transferred to 2ml screw cap tubes. The screw cap tubes were stored at -80℃ until used for RNA extraction.

Total RNA extraction, cDNA synthesis and cDNA labeling

Extraction of total RNA was performed using Nucleospin® extraction kit (Macherey-Nagel Inc, Bethlehem, PA) following manufacturer's instructions. Contaminating DNA was removed with RQ1 RNase-free DNase (Promega, Madison, WI). The absence of DNA contamination was confirmed via PCR amplification using the 16S universal primers 27F (5' AGAGTTTGATCMTGGCTCAG3') and 519R (5'GWATTACCGCGGCKGCTG3') (Lane, 1991). Total RNA in each sample was quantified using a Qubit® 2.0 Fluorometer and the Qubit® RNA BR assay (Life Technologies, Grand Island, NY) according to manufacturer's instructions.

For each RNA sample, 800ng of total RNA, 3.3 µl of random primers (3 µg/µl stock) were added to each tube and nuclease free water was added to bring the final volume to 16.5µl. The tubes were incubated at 70℃ for 10 min in a thermocycler. After transferring the tubes to ice, 6 µl of 5X buffer, 0.1M DTT, 1.5 µl of dNTP mix, 1 µl of RNase inhibitor and 1 µl of 1mM Cy3 dUTP dye were added to each tube. The tubes were incubated at room temperature for 10 minutes. Then, 1 µl of Reverse Transcriptase was added and each tube was incubated at 42℃ for 3 hours and then 98℃ for 2 minutes to terminate the reaction. The tubes were then transferred to ice. The labeled cDNA samples were purified using Spinsmart nucleic acid purification columns (Denville scientific, Holliston, MA) following the manufacturer's instructions. Labelling efficiency was measured Nanodrop 2000 spectrophotometer (Thermo Fisher

Scientific Inc., Wilmington, DE) and the nucleic acid pellet was dried in a Savant DNA Speed Vac (Thermo Fisher Scientific Inc., Wilmington, DE).

Genomic DNA extraction and labeling

M. hydrocarbonoclasticus genomic DNA was extracted using Maxwell® 16 Tissue LEV Total RNA purification kit AS1220 with the Maxwell® 16 instrument (Promega Corp, Madison, WI) with modifications as described in Oldham et al. (2012). Two ml of broth culture were centrifuged at 6000 xg for 5 min, 500 µl of 10mM Tris:1mM EDTA (pH=8) were added to the cell pellet, vortexed briefly to resuspend the pellet. RNA lysis buffer (RLA, 250 µl) and RNA dilution buffer (RDB, 250 µl) were added and the sample was processed using DNA/FFPE program in Maxwell® 16 instrument. DNA was quantified using a Qubit® 2.0 Fluorometer and the Qubit® dS DNA HS assay (Life Technologies, Grand Island, NY) according to manufacturer's instructions.

The dNTP mix for gDNA labeling was prepared by adding 5 µl of each dA/G/CTP, 2.5 µl of dTTP and 82.5 µl of DEPC treated water to a tube. For the random primer mix, 5.5 µl of random primer (Life Technologies, 3 ng/µl stock), 29.5 µl of gDNA were added to a tube, mixed and incubated at 99℃ for 5 minutes in a thermocycler and transferred immediately to ice. The labeling mix was prepared by adding 5 µl of 10X buffer, 2.5 µl of dNTP mix, 0.5 µl of Cy5 dye (25 nM stock) and water to make total volume of 15 µl. The 15 µl of labeling mix was transferred to the DNA/random primer mix and was mixed well. The reaction was incubated at 37℃ for 4 hours. The tubes were then incubated at 95℃ for 3 minutes to inactivate the reaction then at 4℃ until used. These incubation steps were done using a thermocycler. The labelled gDNA was purified using Qiagen QIAquick nucleic acid purification kit following manufacturer's instructions. Labelling efficiency was measured with the Nanodrop 2000 spectrophotometer (Thermo Fisher Scientific Inc., Wilmington, DE) and the nucleic acid pellet was dried in a Savant DNA Speed Vac (Thermo Fisher Scientific Inc., Wilmington, DE).

Microarray hybridization and scanning

The cDNA samples and gDNA sample were rehydrated by adding 6 µl and 54 µl of water, respectively. The gDNA was mixed with hybridization solution (247.5 µl of 2X HI-RPM hybridization buffer, 49.5 µl of 10X aCGH blocking agent, 49.5 µl of 40% formamide and 41.4 µl of water). 49.1 µl of the mix were added to each cDNA sample tube. The samples were

denatured at 95 ℃ for 3 minutes and were immediately transferred to 37 ℃ and, incubated for 30 min. 48 µl of each sample were loaded into the array and hybridized overnight at 67 ℃ (MAUI Hybridization Station, BioMicro systems Inc., Salt Lake City, UT). The disassembly of the slide was done in wash buffer 1 (Agilent Gene Expression wash buffers, Agilent Technologies, Santa Clara, CA). The microarray slide was washed using wash buffer 1 for 5 minutes and then with wash buffer 2 for 1 minute following manufacturer's instructions. The arrays were scanned for Cy3 and Cy5 fluorophores using ScanArray Express microarray scanner (Perkin Elmer, Boston, MA).

Microarray design and analysis

Custom DNA microarray was designed by Agilent based on the complete genome sequence of *Marinobacter hydrocarbonoclasticus* SP17 (GenBank Accession#: NC_017067). A total of 3697 ORFs were targeted using up to six 50-mer oligonucleotide probes for each ORF. All probes were represented in triplicate in the array.

Scanned images were processed and analyzed using Agilent Feature Extraction Software v10.7 (Agilent Technologies, Santa Clara, CA). After quantifying the spot signal intensity and background signals, signal-to-noise ratios (SNR) were calculated for each spot using the following formula: SNR = (spot signal-background signal)/standard deviation of background signal. Spots with SNR < 2 or without enough replicates were eliminated whereas spots with SNR > 2 were considered positive and were included in the analysis. The difference in gene expression between biofilm samples were determined by calculating the log ratio according to a previously published formula (Mukhopadhyay *et al.*, 2006):

$Log_2R = \log_2 (treatment) - \log_2 (control)$

The significance of the normalized log ratios was evaluated based on the Z-score calculated as previously described (Mukhopadhyay *et al.*, 2006):

$$Z = \frac{\log_2 (treatment/control)}{\sqrt{0.25 + \sum variance}}$$

Results

Nitrate-amended biofilm vs. ammonium-amended biofilm

Most (2173) of the 3697 ORFs used for the microarray did not show differential expression (i.e. 2 > log2R > -2) between the biofilm cells exposed to nitrate and biofilm cells exposed to ammonium. Interestingly, only 4 transcripts showed upregulation (i.e. $\log_2 R \geq 2$) under nitrate amended conditions compared to ammonium amended conditions. A total of 1086 genes were downregulated (i.e. $\log_2 R \leq -2$) in nitrate amended biofilm compared to ammonium amended biofilm.

Nitrogen metabolism: In the dissimilatory nitrate reduction pathway of *M. hydrocarbonoclasticus* SP17, the genes coding for respiratory nitrate reductase subunits *narJ* and *narH* were downregulated in biofilm exposed to nitrate compared to ammonia. However, the gene *narG* (codes for the alpha subunit) had a $\log_2 R$ value of only -1.66, e.g. close to but not quite at the level of significance. *nasA*, which codes for the alpha subunit of assimilatory nitrate reductase did not show a significant up or down regulation under nitrate-amended conditions compared to ammonium amended conditions. The nitrite reductase coding genes, *nirS* and *nirB* were downregulated in nitrate-amended biofilm cells but *nirD* was not differentially expressed. The two genes coding for a subunits of nitric oxide reductase (*norB, norC*) were found to be downregulated. Furthermore, the genes involved in dissimilatory periplasmic nitrate reduction pathway were downregulated under nitrate-amended conditions compared to ammonium amended conditions: ubiquinol-cytochrome c reductase iron-sulfur subunit-*petA*, ubiquinol-cytochrome c reductase, cytochrome B-*petB* and Ubiquinol-cytochrome c reductase, cytochrome c1 – *petC.* Several genes associated with nitrate and nitrite transport were downregulated in biofilm cells exposed to nitrate compared to that exposed to ammonia: putative nitrate-and nitrite-responsive positive regulator (MARHY0169), ATP-binding nitrate transport protein (MARHY0170), nitrate transporter (MARHY0171), ABC-type nitrate/sulfonate/bicarbonate transport system, periplasmic component precursor (MARHY0172). Moreover, two component nitrogen regulatory system *glnG* and *glnL* had $\log_2 R$ values below -2.

Iron metabolism: Among the upregulated in cells exposed to nitrate (compared to ammonium) was *irgB*, which is a transcriptional regulator for iron-regulation proteins. There

are two gene clusters located immediately upstream and downstream of this gene. The genes of both of these operons are involved in iron-homeostasis. The upstream gene cluster has a putative siderophore uptake periplasmic binding protein (MARHY3134) and *cirA*, ferric iron-catecholate outer membrane transporter (MARHY3135) and the downstream gene cluster has *fecB*, an iron complex transport system protein and ferric-enterobactin transport protein components *fepD, fepG* and *fepC*. Interestingly, none of these showed differential expression between the two treatments.

Other important genes with differential expression: Almost all of the genes coding for subunits of cytochrome c oxidases were found downregulated under nitrate-amended conditions compared to ammonium amended conditions. Among them are cytochrome c oxidase subunit II (MARHY0048), cytochrome c oxidase assembly protein coxG (MARHY0050), cytochrome c oxidase subunit III (MARHY0051), *ctaD* - cytochrome c oxidase, subunit I, *ccoP* - cytochrome c oxidase cbb3-type, diheme subunit, cytochrome c oxidase cbb3-type subunit II, cytochrome c oxidase cbb3-type subunit I and cytochrome c oxidase cbb3-type CcoQ subunit.

Nitrate-amended biofilm cells vs planktonic cells

Only 16 transcripts showed upregulation (i.e. $\log_2 R \geq 2$) and 13 transcripts showed downregulation (i.e. $\log_2 R \leq -2$) in biofilm cells compared to planktonic cells. The upregulated genes were mostly membrane transporters. Among them were Putative Na+/H+ antiporter NhaD (MARHY1846), potB, spermidine/putrescine transport protein (ABC superfamily, membrane), putative NADH dehydrogenase, precursor (MARHY2024), conserved hypothetical protein, putative S-adenosyl-L-methionine-dependent methyltransferases super family (MARHY2892). The downregulated genes included exaC, a dependent acetaldehyde dehydrogenase, exaB, a Cytochrome c550, precursor and putative dioxygenase (LigB family enzyme, MARHY0129) and some membrane proteins (e.g. conserved hypothetical protein, putative membrane protein, putative EAL domain, MARHY3509).

Ammonium-amended biofilm cells vs planktonic cells

More genes (195) showed upregulation than downregulation (37) in biofilm cells compared to planktonic cells. There were few nitrate metabolism and transport proteins upregulated in biofilm cells: (narJ, nitrate reductase delta subunit, narV, nitrate reductase gamma subunit,

ATP-binding nitrate transport protein (MARHY0170), narH, nitrate reductase beta (Fe-S) subunit). The upregulated transcripts were mainly membrane proteins including transporters. Among them were tricarboxylate transport proteins (putative membrane protein TctB (MARHY2791), putative Membrane protein TctA (MARHY2790)), several ABC family proteins/transporters (e.g., transporter permease protein membrane component (MARHY3815), putative branched-chain amino acid transport protein (MARHY3816) and the ATP-binding domains of transporters (eg. livG, a leucine/isoleucine/valine transporter subunit ATP-binding, cysA, a sulfate/thiosulfate transporter subunit; ATP-binding component, MARHY3810, Putative ATP-dependent protease ATP-binding subunit).

Nitrate-amended vs. ammonium amended planktonic cells

Sixteen transcripts showed upregulation (i.e. $\log_2 R \geq 2$) and 319 transcripts showed downregulation (i.e. $\log_2 R \leq -2$) in nitrate-amended compared to ammonium-amended planktonic cells. Some cytochrome-c-oxidases were found downregulated (MARHY0051, Cytochrome c oxidase subunit III, MARHY0050, Cytochrome c oxidase assembly protein coxG, MARHY0053, Putative transmembrane cytochrome oxidase complex biogenesis factor, ccoP, Cytochrome c oxidase cbb3-type, diheme subunit, MARHY0048, Cytochrome c oxidase, subunit II, MARHY1521, Cytochrome c oxidase, cbb3-type, subunit I, MARHY0369, putative Cytochrome c5, MARHY1519, cytochrome c oxidase, cbb3-type, CcoQ subunit).

Discussion

The transcriptomic response of *M.hydrocarbonoclasticus* SP 17 biofilms on glass to elevated levels of nitrate in the environment compared to elevated levels of ammonium was investigated using a microarray. Contrary to expectations, most of the genes involved in nitrate, nitrite and urea metabolism were found to be downregulated under nitrate amended conditions. Additionally, cytochrome c oxidase coding genes also were downregulated under nitrate-amended conditions. It appears that the biofilm is approaching an anaerobic environment under nitrate-amended conditions. However, the downregulation of dissimilatory nitrate reduction pathway genes does not support the hypothesis that the organism was using nitrate as an electron acceptor under these conditions. Given the limited number of transcriptomic studies done with marine biofilms on solid substrata, further

investigation is needed to discover the pathways of *Marinobacter* involved in energy production as well as understand the behavior under elevated nitrate levels.

The microarray data clearly demonstrated the downregulation of dissimilatory as well as periplasmic nitrate reduction pathways in biofilms under nitrate-amended conditions. It may be the high levels of nitrate in the medium were shutting down nitrate utilization. Marine waters typically have very low levels of nitrate (0.01mg/L, Melchers and Jeffrey, 2012) and most marine organisms including *Marinobacter* are accustomed to limited nitrate conditions. However, biofilm communities extracted from 1018 carbon steel coupons exposed to marine coastal waters polluted with fertilizer (0.1-0.9 mg/L of dissolved inorganic nitrogen, assuming most is nitrate) were found dominated by *Marinobacter* spp. (Beech, unpublished data). This observation suggests that *Marinobacter* is surviving as well as successful under high levels of nitrate in the environment.

The downregulation of cytochrome c oxidase coding genes in nitrate-amended biofilm compared to that of ammonium, is an indication of experiencing anaerobic conditions. Downregulation of cytochrome c oxidase coding genes has been observed in biofilms of *Pseudomonas aeruginosa* clones isolated from Cystic fibrosis (CF) patients (Manos *et al.,* 2008). The same research and that of others showed upregulation of genes involved in anaerobic respiration with nitrate in CF biofilms (For example - Manos *et al.,* 2008; Palmer *et al.,* 2007; Van *et al.,* 2007). The nitrate level commonly found in CF sputum is 0.4mM (Palmer *et al.,* 2007). However, gene expression studies using microarray have often chosen 0.1mM of nitrate since it provides ample electron acceptor for growth (For example - Palmer *et al.,* 2007 and references therein). Based on this information, it is possible that 0.5 mM nitrate used in the current study is above the amount needed for *Marinobacter* growth.

The upregulation of membrane proteins/transporters in biofilms of both nitrate and ammonium amended conditions compared to their planktonic forms is an interesting observation. Membrane proteins and transporters play a critical role in homeostasis. The differential expression (upregulation) of the transcripts coding for these proteins could be due to unavailability or inaccessibility of nutrients/molecules needed for growth and/or metabolism.

The transcriptomic profile provides some information on the relative role of elevated levels of nitrate in the marine biofilms. However, the data from a single time point will only reveal part of the response since a biofilm has different stages of development and its transcriptome is expected to vary with stage. Therefore, data from several time points will be useful in obtaining a full picture on the response of marine organisms to exposure of high levels of nitrate. Moreover, metabolomic analysis and gene-deletion analysis will go hand in hand with the current study in providing valuable information of which pathways are truly induced in marine biofilms with high nitrate levels in the environment.

References

Allan, V. J., Callow, M. E., Macaskie, L. E., Paterson-Beedle, M. (2002). Effect of nutrient limitation on biofilm formation and phosphatase activity of a *Citrobacter* sp. *Microbiology*, *148*(1), 277-288.

Castaneda, H., Benetton, X. D. (2008). SRB-biofilm influence in active corrosion sites formed at the steel-electrolyte interface when exposed to artificial seawater conditions. *Corrosion Science*, *50*(4), 1169-1183.

Chen, G., Walker, S. L. (2007). Role of solution chemistry and ion valence on the adhesion kinetics of groundwater and marine bacteria. *Langmuir*, *23*(13), 7162-7169.

Dunsmore, B., Youldon, J., Thrasher, D. R., Vance, I. (2006). Effects of nitrate treatment on a mixed species, oil field microbial biofilm. *Journal of Industrial Microbiology and Biotechnology*, *33*(6), 454-462.

Flemming, H. C., Wingender, J., Szewzyk, U., Steinberg, P., Rice, S. A., Kjelleberg, S. (2016). Biofilms: an emergent form of bacterial life. *Nature Reviews Microbiology*, *14*(9), 563.

Gao, P. K., Li, G. Q., Zhao, L. X., Dai, X. C., Tian, H. M., Dai, L. B., ... Ma, T. (2014). Dynamic processes of indigenous microorganisms from a low-temperature petroleum reservoir during nutrient stimulation. *Journal of Bioscience and Bioengineering*, *117*(2), 215-221.

Hunt, S. M., Werner, E. M., Huang, B., Hamilton, M. A., Stewart, P. S. (2004). Hypothesis for the role of nutrient starvation in biofilm detachment. *Applied and Environmental Microbiology*, *70*(12), 7418-7425.

Jia, R., Yang, D., Xu, J., Xu, D., Gu, T. (2017). Microbiologically influenced corrosion of C1018 carbon steel by nitrate reducing *Pseudomonas aeruginosa* biofilm under organic carbon starvation. *Corrosion Science*, *127*, 1-9.

Kjellerup, B. B., Kjeldsen, K. U., Lopes, F., Abildgaard, L., Ingvorsen, K., Frølund, B., ...Nielsen, P. H. (2009). Biocorrosion and biofilm formation in a nutrient limited heating system subjected to alternating microaerophilic conditions. *Biofouling*, *25*(8), 727-737.

Lewandowski, Z., Stoodley, P., Altobelli, S. (1995). Experimental and conceptual studies on mass transport in biofilms. *Water Science and Technology*, *31*(1), 153-162.

Lin, J., Madida, B. B. (2015). Biofilms affecting progression of mild steel corrosion by Gram positive *Bacillus* sp. *Journal of Basic microbiology*, *55*(10), 1168-1178.

Lindell, D., Padan, E., Post, A. F. (1998). Regulation of ntcA expression and nitrite uptake in the marine *Synechococcus* sp. strain WH 7803. *Journal of Bacteriology*, *180*(7), 1878-1886.

Little, B. J., Lee, J. S. (2014). Microbiologically influenced corrosion: an update. *International Materials Reviews*, *59*(7), 384-393.

Manos, J., Arthur, J., Rose, B., Tingpej, P., Fung, C., Curtis, M., ... Bye, P. (2008). Transcriptome analyses and biofilm-forming characteristics of a clonal *Pseudomonas aeruginosa* from the cystic fibrosis lung. *Journal of Medical Microbiology*, *57*(12), 1454-1465.

Marques, J. M., de Almeida, F. P., Lins, U., Seldin, L., Korenblum, E. (2012). Nitrate treatment effects on bacterial community biofilm formed on carbon steel in produced water stirred tank bioreactor. *World Journal of Microbiology and Biotechnology*, *28*(6), 2355-2363.

Melchers, R. E. (2012). Influence of dissolved inorganic nitrogen on accelerated low water corrosion of marine steel piling. *Corrosion*, *69*(1), 95-103.

Melchers, R. E. (2014). Long-term immersion corrosion of steels in seawaters with elevated nutrient concentration. *Corrosion Science*, *81*, 110-116.

Melchers, R. E., Jeffrey, R. (2012). Corrosion of long vertical steel strips in the marine tidal zone and implications for ALWC. *Corrosion Science*, *65*, 26-36.

Mukhopadhyay, A., He, Z., Alm, E. J., Arkin, A. P., Baidoo, E. E., Borglin, S. C., ... Huang, K. (2006). Salt stress in *Desulfovibrio vulgaris* Hildenborough: an integrated genomics approach. *Journal of Bacteriology*, *188*(11), 4068-4078.

Oldham A.L., Drilling H.S., Stamps B.W., Stevenson B.S., Duncan K. E. (2012). Automated DNA extraction platforms offer solutions to challenges of assessing microbial biofouling in oil production facilities. *Applied Microbiology and Biotechnology Express*.2:60 doi:10.1186/2191-0855-2-60

Palmer, K. L., Brown, S. A., Whiteley, M. (2007). Membrane-bound nitrate reductase is required for anaerobic growth in cystic fibrosis sputum. *Journal of Bacteriology*, *189*(12), 4449-4455.

Picioreanu, C., Van Loosdrecht, M. C., Heijnen, J. J. (2001). Two-dimensional model of biofilm detachment caused by internal stress from liquid flow. *Biotechnology & Bioengineering*, *72*(2), 205-218.

Pillay, C., Lin, J. (2013). Metal corrosion by aerobic bacteria isolated from stimulated corrosion systems: Effects of additional nitrate sources. *International Biodeterioration & Biodegradation*, *83*, 158-165.

Rice, S. A., Koh, K. S., Queck, S. Y., Labbate, M., Lam, K. W., Kjelleberg, S. (2005). Biofilm formation and sloughing in *Serratia marcescens* are controlled by quorum sensing and nutrient cues. *Journal of Bacteriology*, *187*(10), 3477-3485.

Schwermer, C. U., Lavik, G., Abed, R. M., Dunsmore, B., Ferdelman, T. G., Stoodley, P., …de Beer, D. (2008). Impact of nitrate on the structure and function of bacterial biofilm communities in pipelines used for injection of seawater into oil fields. *Applied and Environmental Microbiology*, *74*(9), 2841-2851.

Sheng, X., Ting, Y. P., Pehkonen, S. O. (2008). The influence of ionic strength, nutrients and pH on bacterial adhesion to metals. *Journal of Colloid and Interface Science*, *321*(2), 256-264.

Van Alst, N. E., Picardo, K. F., Iglewski, B. H., Haidaris, C. G. (2007). Nitrate sensing and metabolism modulate motility, biofilm formation, and virulence in Pseudomonas aeruginosa. *Infection and immunity*, *75*(8), 3780-3790.

Vert, M., Doi, Y., Hellwich, K. H., Hess, M., Hodge, P., Kubisa, P., ... Schué, F. (2012). Terminology for biorelated polymers and applications (IUPAC Recommendations 2012). *Pure and Applied Chemistry*, *84*(2), 377-410.

Zhou, G., Li, L. J., Shi, Q. S., Ouyang, Y. S., Chen, Y. B., Hu, W. F. (2013). Effects of nutritional and environmental conditions on planktonic growth and biofilm formation of *Citrobacter werkmanii* BF-6. *Journal of Microbiology and Biotechnol*ogy, *23*(12), 1673-1682.